[redacted]

CENTRAL RESEARCH LIBRARY
DOCUMENT COLLECTION

MARTIN MARIETTA ENERGY SYSTEMS LIBRARIES
3 4456 0360630 0

ORNL-1432
Progress

LABORATORY RECORDS
1954

CHEMISTRY DIVISION

QUARTERLY PROGRESS REPORT

FOR PERIOD ENDING SEPTEMBER 30, 1952

CENTRAL RESEARCH LIBRARY
DOCUMENT COLLECTION

LIBRARY LOAN COPY

DO NOT TRANSFER TO ANOTHER PERSON

If you wish someone else to see this document, send in name with document and the library will arrange a loan.

OAK RIDGE NATIONAL LABORATORY
OPERATED BY
CARBIDE AND CARBON CHEMICALS COMPANY
A DIVISION OF UNION CARBIDE AND CARBON CORPORATION
UCC
POST OFFICE BOX P
OAK RIDGE, TENNESSEE

[redacted]

[redacted]

[redacted]

DECLASSIFIED

CLASSIFICATION CHANGED TO

BY AUTHORITY OF TID-1148

BY R. Morrison 7/26/57

ORNL-1432

This document consists of 73 pages

Copy 4 of 136 copies Series A

Contract No W-7405-eng-26

CHEMISTRY DIVISION

QUARTERLY PROGRESS REPORT

for Period Ending September 30, 1952

S. C. Lind, Acting Director
G. E. Boyd, M. A. Bredig, Associate Directors

DATE ISSUED

FEB 11 1956

OAK RIDGE NATIONAL LABORATORY
Operated by
CARBIDE AND CARBON CHEMICALS COMPANY
A Division of Union Carbide and Carbon Corporation
Post Office Box P
Oak Ridge, Tennessee

[redacted]

[redacted]

MARTIN MARIETTA ENERGY SYSTEMS LIBRARIES

3 4456 0360630 0

[redacted]

INTERNAL DISTRIBUTION

1. G. T. Felbeck (C&CCC)
2. Biology Library
3. Health Physics Library
4-5. Central Research Library
6-13. Central Files
14. Reactor Experimental Engineering Library
15. C. E. Center
16. C. E. Larson
17. W. B. Humes (K-25)
18. L. B. Emlet (K-12)
19. A. M. Weinberg
20. E. H. Taylor
21. E. J. Murphy
22. E. D. Shipley
23. S. C. Lind
24. F. C. VonderLage
25. R. C. Briant
26. J. A. Swartout
27. F. L. Steahly
28. A. H. Snell
29. A. Hollaender
30. M. T. Kelley
31. G. H. Clewett
32. K. Z. Morgan
33. J. S. Felton
34. A. S. Householder
35. C. S. Harrill
36. C. E. Winters
37. D. W. Cardwell
38. E. M. King
39. J. A. Wethington
40. G. E. Boyd
41. M. A. Bredig
42. R. W. Stoughton
43. R. B. Briggs
44. G. W. Parker
45. C. J. Borkowski
46. G. H. Jenks
47. K. A. Kraus
48. H. A. Levy
49. R. S. Livingston
50. T. E. Willmarth
51. C. H. Secoy
52. C. J. Hochanadel
53. W. H. Baldwin
54. A. R. Brosi
55. R. N. Lyon
56. S. A. Reynolds
57. P. F. Thomason
58. E. G. Bohlmann
59. C. P. Keim
60. C. D. Susano
61. D. D. Cowen
62. M. Reyling
63. R. Livingston
64. G. H. Cartledge
65. E. R. Gilliland
66. S. D. Schlosman (K-25)
67. E. P. Wigner (Consultant)
68. G. C. Williams

[redacted]

[redacted]

[redacted]

EXTERNAL DISTRIBUTION

69. Argonne National Laboratory
77-84. Atomic Energy Commission, Washington
85-88. Brookhaven National Laboratory
89-92. Carbide and Carbon Chemicals Company (Y-12 Plant)
93-96. E. I. du Pont de Nemours and Company
97-98. Knolls Atomic Power Laboratory
99-104. General Electric Company, Richland
105. Idaho Operations Office (Phillips Petroleum Co.)
106-109. Los Alamos
110. Mound Laboratory
111-113. New York Operations Office
114. Patent Branch, Washington
115. Savannah River Operations Office, Wilmington
116-130. Technical Information Service, Oak Ridge
131-134. University of California Radiation Laboratory
135-136. Westinghouse Electric Corporation

[redacted]

[redacted]

Chemistry Division quarterly progress reports previously issued in this series are as follows

ORNL-65	March, April, May, 1948
ORNL-176	June, July, August, 1948
ORNL-229	September, October, November, 1948
ORNL-336	December, 1948, January and February, 1949
ORNL-286	Period Ending June 30, 1949
ORNL-499	Period Ending September 30, 1949
ORNL-607	Period Ending December 31, 1949
ORNL-685	Period Ending March 31, 1950
ORNL-795	Period Ending June 30, 1950
ORNL-870	Period Ending September 30, 1950
ORNL-1036	Period Ending December 31, 1950
ORNL-1053	Period Ending March 31, 1951
ORNL-1116	Period Ending June 30, 1951
ORNL-1153	Period Ending September 30, 1951
ORNL-1260	Period Ending December 31, 1951
ORNL-1285	Period Ending March 31, 1952
ORNL-1344	Period Ending June 30, 1952

[redacted]

[redacted]

CONTENTS

PAGE

ABSTRACT 1

INORGANIC AND PHYSICAL CHEMISTRY 4
- Density of Uranyl Fluoride Solutions 4
- Anion Exchange Studies in Sulfate Media 7
- Thermodynamics of Complex Ions 12
- Chemistry of Corrosion 13
- Chemistry of Fused Salts 14
- Metal-Metal Halide Systems 15

NUCLEAR CHEMISTRY 17
- Growth of the Radium E Beta Spectrum into Radium D 17
- Cerium-144-Praseodymium-144 Decay Schemes 17
- Neutron-Capture Cross Section of Protactinium-233 17
- Radiation Characteristics of Samarium-145 and Promethium-145 18

RADIO-ORGANIC CHEMISTRY 22
- Radiation and Analytical Organic Chemistry 22
- Isotope Effect Studies 22
  - Examination of the bromine addition to carbon-14-labeled methyl cinnamate for an isotope effect 22
  - Specific activity relationships in reactions having isotope effect 23
  - Studies of carbon-14 isotope effects in the saponification of carboxyl-labeled esters at 25°C 23
  - Isotope effect in the dehydration of formic-C^{14} acid 24
  - Isotope effect studies in the acid hydrolysis of hydrocyanic acid 24
- Studies of Solution Scintillation Counting of Radioisotopic Organic Compounds 26
- Organic Reaction Mechanism Studies 26
  - Wagner rearrangement of 7-phenylacenapthenol-8-C^{14} 26
  - Wagner rearrangement of 3-methyl-9-fluorenyl(carbinol-C^{14}) 29
  - Thermal rearrangement of amine nitrites 29

CHEMISTRY OF SEPARATION PROCESSES 31
- Organic Chemistry of Solvents 31
- Study of the Electrodeposition of Ruthenium from Very Dilute Solutions 32
- Ion-exchange Studies 32
  - The osmotic free energy of ion exchangers 32

[redacted]

[redacted]

[redacted]

PAGE

Electrochemical properties of ion exchange materials 34
Self-diffusion of sodium ion in linear sodium polystyrenesulfonate solutions 38
Donnan partition coefficients at low external electrolyte concentrations 39

CHEMICAL PHYSICS 40
Radio-Frequency Spectroscopy 40
Neutron Diffraction Studies 41

RADIATION CHEMISTRY 45
Nucleation of Bubbles in Superheated Solutions by Fission Recoils . . 45
Oxidation of Uranium(IV) by Gamma Rays 46
Gamma-ray Effects in Ice 47
Gamma Irradiation of Aqueous Benzene Solutions 48
Reduction of Cerium(IV) by Gamma Radiation 49

INSTRUMENTATION 50

REACTOR CHEMISTRY 51
Solubility of UO_3 in Aqueous UO_2SO_4 and UO_2F_2 at 175 and 250°C 51
Extension of the Study of the Two-Liquid-Phase Region of the System UO_2SO_4-H_2SO_4- H_2O 53
Conductivity Measurements of Aqueous Solutions of Uranyl Sulfate and Uranyl Fluoride 57
Vapor Pressures of Aqueous Uranyl Sulfate Solutions 61
Conductometric Method for Studying the Kinetics of Peroxide Decomposition in Uranyl Sulfate Solutions 62
Alternate Fuel Media and Possible Corrosion Inhibitors 64
HRP Radiation Chemistry 66

[redacted]

[redacted]

CHEMISTRY DIVISION QUARTERLY PROGRESS REPORT

SUMMARY

INORGANIC AND PHYSICAL CHEMISTRY

The density of uranyl fluoride solutions has been redetermined. It appears that density measurements can be used for rapid and accurate determination of the concentration of uranyl fluoride solutions, particularly at high concentrations. The apparent molal volumes and partial molal volumes of UO_2F_2 have been evaluated from the densities.

Various anion-exchange studies in sulfate media were carried out. Iron(III) is readily adsorbed by the quarternary-amine anion-exchange resin Dowex-1 from dilute, less than 0.1 *m*, sulfuric acid solutions and from both dilute and concentrated ammonium sulfate solutions. The distribution coefficients appear to be independent of the iron(III) concentration of the solution.

Experiments demonstrating the separation of nonadsorbable aluminum from iron(III) in sulfate solutions are considered to be typical of the separation of nonadsorbable ions from iron.

Dowex-1, in its sulfate form, adsorbs sulfuric and other acids according to the reaction

$$R_2SO_4 + HX \longrightarrow RHSO_4 + RX \ .$$

Therefore the resin can be used to separate sulfuric acid from nonadsorbable or weakly adsorbable metal sulfates, for example, copper sulfate.

The transition elements Co, Ni, and Cu were found to be not adsorbed in 1.0 and 3.5 *M* sulfuric acid solutions and only weakly adsorbed in ammonium sulfate solutions with similar concentrations.

As a contribution to the understanding of the heat and entropy effects in the formation of complex aqueous ions, the equilibrium between the bis- and tris-malonato manganese(III) has been measured and compared with similar equilibriums in the oxalato and pentanedione systems.

In connection with corrosion studies, experiments are in progress to determine the variation of the electrode potential of stainless steel and its separate components as a function of temperature.

Apparatus has been assembled and put into partial operation for the measurement of electrical conductivities, densities, transport numbers, and heats of compound formation in molten-salt mixtures.

The solubility of potassium metal in the ternary molten eutectic of LiF, NaF, and KF has been determined to be 3.7 ± 0.5 mole % at 920°C by an improved technique.

NUCLEAR CHEMISTRY

It was demonstrated that the unusual shape of the radium E beta spectrum is not due to the presence of an isomer of half life very different from the well-known value.

The unique shape of one of the gamma-coincident beta-ray spectra of Pr^{144}, measured with a thin magnetic lens spectrometer, makes it possible to assign a definite spin to the transition. A decay scheme for Pr^{144} can now be written with some confidence.

Work on the determination of an effective capture cross section of Pa^{233} for reactor neutrons has continued. A preliminary value is 130 ± 30 barns.

Samarium-145, prepared by a long neutron irradiation of 200 mg of enriched Sm^{144}, was found to decay by orbital-electron capture with a half life of approximately 400 days, in verification of earlier results. The Pm^{145} produced emitted *K* and *L* x rays of neodymium and decayed with a

half life of at least 30 years. Gamma rays of energies 80, 460, and 750 kev were also observed and may indicate the presence of another promethium isotope. A cross section of 0.03 barn is estimated for Sm^{144} activation.

RADIO-ORGANIC CHEMISTRY

The study of the products formed by the action of gamma radiation from Co^{60} on dilute aqueous solutions of aliphatic acids has continued. An analytical method for the identification of small quantities of acidic substances has been developed. Of the major nonvolatile constituents of the irradiation product from acetic acid solutions, succinic acid, tricarboxylic acid, and the two forms of butane-1,2,3,4-tetracarboxylic acid have been positively identified.

The addition of bromine to methyl cinnamate-α-C^{14} has been shown to proceed without an isotope effect. Changing the nature of the solvent and the concentration of the solute in the alkaline hydrolyses of ethyl benzoate (carboxy-C^{14}) has been found to have no influence on the extent of the isotope effect. A new technique has been applied to the kinetic study of the decomposition of formic-C^{14} acid. This technique involves a determination of the specific activity of the unreacted formic acid as a function of time.

A terphenyl scintillation counter has been constructed for use in the determination of solution radioactivities containing weak beta-emitters.

During a general study of the dehydration-rearrangement of 7-phenylacenaphthenol-8-C^{14}, an isotope effect was demonstrated in the permanganate oxidation of this compound to 8-benzoylnaphthoic (carboxy-C^{14}) acid.

3-Methyl-9-fluorenyl (carbinol-C^{14}) has been subjected to the conditions of the Wagner rearrangement. The electrical effect of the 3-methyl group has been found to favor migration of the substituted benzo-moiety of this carbinol in the ratio of 73 27.

The effect has been studied for several different variations of environment upon the rates of decomposition of 2-phenyl-2-(*p*-tolyl)ethyl-1-C^{14} nitrite and 2-phenyl-2-(3,4-dimethylphenyl-1)ethyl-1-C^{14} ammonium nitrite, and upon the migration ratios thus obtained.

CHEMISTRY OF SEPARATION PROCESSES

Equivalent weights of inorganic and organic salts were determined within 1% accuracy by means of the anion-exchange resin Dowex-1 by using potassium phthalate as a salt standard.

The solubility in various organic solvents of sodium di-*n*-butyl phosphate, reaction product of the purification of tributyl phosphate with NaOH, was determined.

Phosphorus-32 labeled $POCl_3$ and di(2-ethyl hexyl)phosphinic acid were prepared for a study of the distribution of the latter between organic and aqueous solvents.

Isopiestic measurements of the osmotic free energy in various salt-forms of a strong-base type of anion exchanger are reported. As with the cation exchanger, the swelling pressure is independent of the salt form and depends only on the volume.

The effects of increasing amounts of gamma radiation on both cation- and anion-exchange membranes may be summarized (1) the exchange capacity decreases uniformly, (2) the moisture content uniformly increases, (3) the electrical conductivity either remains almost constant (coherent membranes) or decreases markedly (heterogeneous membranes), and (4) the permselectivity decreases but slightly.

The self-diffusion of sodium ion in linear sodium polystyrenesulfonate solutions was measured in a wide range

of concentrations, with 2.6 y Na^{22} as a radiotracer.

Attempts were made to measure Donnan-equilibrium partition coefficients at low external-electrolyte concentrations by equilibration through the vapor phase.

CHEMICAL PHYSICS

Work on the determination of the nuclear moments of I^{131} by microwave technique has been largely concerned with chemical purification.

Line width and frequency were measured for Cl^{35} in ethylene chloride at temperatures between -253 and -173.2°C. The line becomes too broad to be measurable at -100°C, which is the temperature of a specific heat anomaly assumed to involve considerable motion in the C-Cl bond and drop in the quadrupole coupling.

Neutron diffraction data on the sodium chloride type of modification of deutero-ammonium bromide and iodide permit the free rotation of the deutero-ammonium ion to be ruled out and suggest one model, or a combination of three other models that involve a single, a double, or a triple approach between deuterium atoms and bromine ions. Theoretical calculations show the triple-approach model to represent a stable potential minimum, whereas the double- and single-approach models represent saddle points of decreasing stability.

RADIATION CHEMISTRY

The probability of bubble formation in superheated uranyl sulfate solutions, when nucleated by fission recoil tracks, was found to be unity. This probability drops rapidly at lower temperatures. Bubble formation in superheated ether was also observed in irradiation with 50 kv x rays and with fast neutrons.

The effect of several variables, such as concentration, pH, and the presence of hydrogen peroxide, oxygen, and hydrogen, on the rate of oxidation of uranium(IV) in dilute sulfuric acid solutions have been studied.

From irradiations of ice, pure(degassed) or containing helium, hydrogen, oxygen, or potassium bromide, it is concluded that little, if any, reaction occurs between molecular oxygen and the products formed by the radiation at -196°C. At higher temperatures, reactions in the ice of the primary decomposition products with normally stable molecules H_2, H_2O_2, and O_2 are possible.

Experiments on the pH-dependence of the reduction of cerium(IV) solutions by gamma radiation indicate that in solutions containing oxygen, reduction may take place through the intermediate formation of hydrogen peroxide and not by reaction with the HO_2 or with OH radicals. Oxygen seems to prevent reduction of cerium(IV) by H through formation of HO_2.

The formation of phenol and hydrogen peroxide in oxygenated aqueous benzene solutions irradiated with cobalt gamma rays was studied.

INSTRUMENTATION

The development of the circuit of a new linear amplifier having greatly increased overload capacity and counting rate for a given energy resolution degradation has been completed.

The circuit for a scintillation-counter-regulated high-voltage supply that uses a r-f oscillator for the source of voltage was developed.

The alpha energy analyzer has been greatly improved.

Excellent stability has been obtained with the multichannel analyzer that uses 10 channels and incorporates a Hathaway galvanometer.

A 404-A tube tester and ager that can handle 11 tubes simultaneously was designed and constructed.

REACTOR CHEMISTRY

Measurements of the solubility of UO_3 in aqueous solutions of uranyl sulfate and fluoride at elevated temperatures, up to 250°C, were continued.

An improved and simplified apparatus for the determination of two-liquid-phase equilibria in uranyl sulfate solutions has been constructed. Data obtained with the apparatus, covering SO_4-to-U ratios from 1.000 to 2.955, can be applied directly to a selection of reactor-fuel media. Because of phase stability at lower SO_4-to-U ratios, the sulfate system appears preferable to the phosphate system from the standpoint of corrosion.

An attempt to interpret, in terms of degree of dissociation, free energy, and entropy, some measurements of the electrical conductivity of uranyl sulfate and fluoride in aqueous solution as a function of temperature and concentration is reported. The interpretation is complicated by various factors such as the hydrolysis of the sulfate and the dimerization of the fluoride.

Vapor-pressure measurements of aqueous uranyl sulfate solutions, made with dibutylphthalate as the manometer fluid, require further improvement before activity coefficients can be calculated.

A conductometric method based on the presence of hydrogen ions according to the equation

$$UO_2^{++} + H_2O_2 \longrightarrow UO_4 + 2H^+$$

was developed for measuring the rate of peroxide decomposition in an aqueous uranyl sulfate solution.

An investigation of the possibility of complexing uranyl fluoride in aqueous solution with alkali and non-alkali metal fluorides and hydroxides, and the effect of complexing on corrosion behavior has been started.

Titanium was found to be far superior to type 347 stainless steel in tests concerned with the in-reactor corrosion by uranyl sulfate solutions at 250°C.

The first-order law for the homogeneous catalytic gas-recombination reaction seems to refer to cupric ion activity rather than concentration.

Studies of suspended heterogeneous catalysts of the platinum family have continued.

INORGANIC AND PHYSICAL CHEMISTRY

DENSITY OF URANYL FLUORIDE SOLUTIONS

J. S. Johnson K. A. Kraus

The interpretation of the ultracentrifugation measurements of uranyl fluoride necessitates a knowledge of the density of the solutions and of the partial specific volume ($\bar{v}_2$) of the solute. Some density measurements of uranyl fluoride solutions, particularly at high concentrations, have been reported by Dean[1] and by Marshall, Gill, and Secoy[2]. These measurements did not extend to sufficiently low concentration and, in addition, differed considerably from each other at the higher concentrations. Reinvestigation therefore seemed indicated.

Density were measured near 25 and some near 30°C, and all measurements corrected to 25 0 and 30 0°C by taking into consideration the observed expansibility. The measurements were in the concentration range 0.3 to

[1] G R Dean, *Properties of Uranyl Fluoride*, CC-2092, Sept 11, 1944

[2] W L Marshall, J S Gill, and C H Secoy, *Chem Quar Prog Rep June 30, 1950*, ORNL-795, p 22

4 3 *M* (*ca.* 2 5 to 61.5 wt %) by the use of a combination of pycnometric (25-cc samples) and gradient-tube[3,4] techniques. The uranium solutions were prepared from the samples of uranyl fluoride previously described.[5] The concentration of the solutions was obtained by analysis and by quantitative dilutions. For analysis, the solutions were dried under a heat lamp and ignited to U_3O_8 at 840 to 900°C. There was no significant weight change in this temperature range.

The results of the experiments are listed in Table 1, in which two values for the concentration of some of the solutions are given. The first column represents the values obtained from analysis, whereas the second column represents an average of the analysis of the solution and of computed values based on analyses of aliquots from quantitatively diluted solutions. For purposes of computation, the latter values were used, and the analytical values are given mainly to indicate that the precision of the analyses cannot be considered to be better than 0 1%

It was found possible to represent the density data by the quadratic equation

$$\frac{1}{d} = \frac{1}{d_0} + aF_2 + bF_2^2 , \qquad (1)$$

where d is the density of the solution, d_0 the density of the pure solvent, and F_2 the weight fraction of UO_2F_2 At 25°C the empirical constants, a = −0 9126 and b = 0.0578, were obtained from the intercept and slope of a plot of $(1/d - 1/d_0)/F_2$ vs F_2. This plot, in agreement with Eq. 1, yields a straight line (Fig. 1). It should be pointed out that the

(3) K Linderstrom-Lang and H Lanz, *Compt Rend Trav Lab Carlsburg* **21**, 315 (1935)

(4) D W Wilson, A O C Nier, and S P Reimann, *Preparation and Measurement of Isotopic Tracers*, p 61, Edwards Bros , Ann Arbor, Mich , 1946

(5) J S Johnson and K A Kraus, *J Am Chem Soc* **74**, 4436 (1952)

TABLE 1. DENSITY OF URANYL FLUORIDE SOLUTIONS

CONCENTRATION OF UO_2F_2 (wt %)		MOLARITY	DENSITY		
Analytical	Average of Analyses[a]		25°C (exp)	25°C (calc)	30°C
	2 495	0 0826	1 0202[b]	1 0203	
4 999	4 985	0 1690	1 0443	1 0444	1 0429
	5 025	0 1704	1 0448	1 0448	
10 20	10 20	0 3637	1 0983	1 0984	1 0967
20 08	20 09	0 7934	1 2164	1 2167	1 2146
20 46	20 48	0 8123	1 2219[b]	1 2219	
30 09	30 10	1 332	1 3632	1 3635	
30 14	30 18	1 337	1 3632	1 3646	1 3607
	40 30	2 030	1 5509	1 5516	1 5481
50 27	50 27	2 921	1 7893	1 7899	1 7859
61 50	61 63	4 326	2 1627	2 1622	2 1589

(a) Values obtained by considering all analyses in a series of dilutions Since some dilutions were used only for measurements of refractive index, not all analyses are indicated Calculated values based on average concentrations

(b) Measured by gradient tube technique

experimental points fall considerably closer to the straight line of Fig. 1 than might have been expected from the precision of the analyses. It is very interesting that, as also shown in Fig 1, the densities determined by Dean[1] are in excellent agreement with those determined here. Therefore it appears that there is no systematic error in the analyses, which limit the precision of the measurements. The data of Marshall, Gill, and Secoy[2] show considerably wider scatter. The density of uranyl fluoride solutions at 25 °C apparently can be satisfactorily described by the equation

$$\frac{1}{d} = 1\ 0029 - 0\ 9126F_2 + 0\ 0578F_2^2$$

from very low concentrations to the saturated solution

By assuming that the density of the uranyl fluoride solutions follows Eq 1, the apparent molal volume, ϕ_v, at 25 °C can be computed by

$$\phi_v = M_2\left(\frac{1}{d_0} + a + bF_2\right)$$

$$= 308.08(0.0903 + 0.0578F_2)$$

$$= 27\ 8 + 17\ 8\ F_2\ , \quad (2)$$

where M_2 = 308.08 is the molecular weight of uranyl fluoride.

Equation 2 can be derived from the expression of the apparent molal volume as given in Harned and Owen [6]

$$\phi_v = \frac{1000}{mdd_0}(d_0 - d) + \frac{M_2}{d}\ ,$$

[6] H S Harned and B B Owen, *The Physical Chemistry of Electrolytic Solutions*, 2d ed , p. 250, Reinhold, New York, 1950

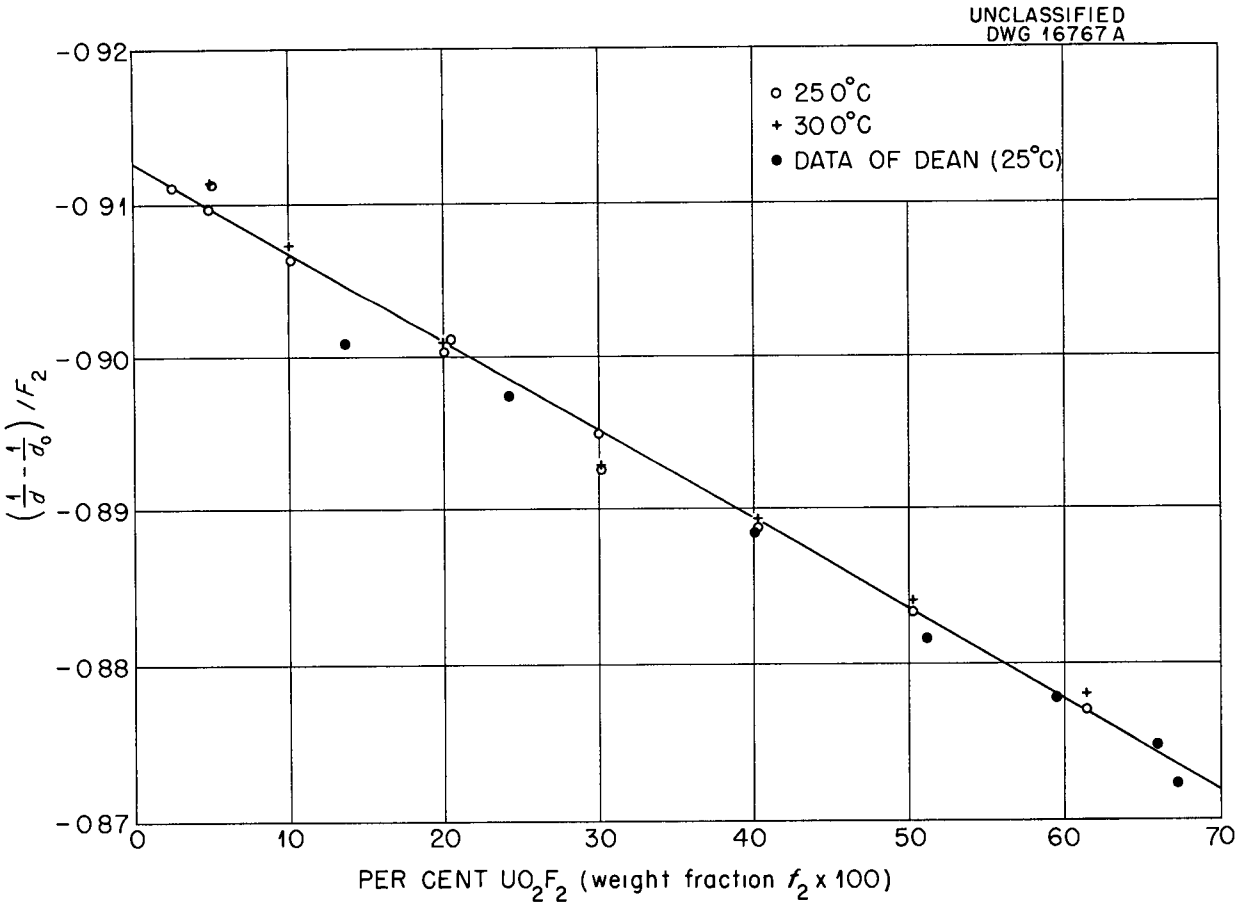

Fig. 1. Change of Density of Uranyl Fluoride Solutions with Concentration

remembering that the molality m is given by

$$m = \frac{1000F_2}{(1 - F_2)M_2}.$$

It is interesting that the apparent molal volume, ϕ_v, varies linearly with F_2. This, at first glance, is similar to the equation expected for nonelectrolytes,[7] in which case ϕ_v varies linearly with c (molarity). For electrolytes, ϕ_v is expected to vary linearly with $\sqrt{c}$. However, a plot of ϕ_v for UO_2F_2 vs molarity is found to be not linear with c but approximately linear with $\sqrt{c}$. Since it has been shown that uranyl fluoride is essentially undissociated[2] into ions, a linear variation of ϕ_v with c might have been expected.

Since the partial molal volume, $\bar{V}_2$, is related to the apparent molal volume, ϕ_v, by

$$\bar{V}_2 = \phi_v + n_2\left(\frac{\partial\phi_v}{\partial n_2}\right)_{n_1},$$

where n_1 and n_2 are the number of moles of solvent and solute, respectively, the expression

$$\bar{V}_2 = M_2\left(\frac{1}{d_0} + a + 2bF_2 - bF_2^2\right)$$
$$= 27\ 8 + 35\ 6F_2 - 17\ 8F_2^2 \quad (3)$$

can be derived from Eq 2. Extrapolation of Eqs 2 and 3 to $F_2 = 0$ yields $\phi_v^0 = \bar{V}_2^0 = 27\ 8$ cc It should be remembered that, because of low dissociation of UO_2F_2 at moderate concentrations, this value probably refers to the unassociated monomer rather than the completely dissociated salt Extrapolation to $F_2 = 1$ yields $\phi_v = \bar{V}_2 = 45\ 7$ cc This may be compared with the calculated molal volume for solid UO_2F_2, which is found to be 48 3 on the basis of the crystallographic value for the density ($\rho = 6\ 38$)[8]

(7) *Ibid*, p 260

(8) W H Zachariasen, *Acta Cryst* **1**, 277 (1948)

ANION-EXCHANGE STUDIES IN SULFATE MEDIA

K. A. Kraus F. Nelson
J. F. Baxter[9]

Adsorbability of Fe(III) from Sulfuric Acid Solutions. The adsorbability of Fe(III) from various sulfuric acid solutions and from ammonium sulfate solution (containing *ca* 0 01 *M* H_2SO_4) was studied in a series of experiments with the sulfate form of the quaternary-amine anion-exchange resin Dowex-1 This resin was prepared from the chloride form by washing with 1 to 2 *M* sulfuric acid until free of chloride, followed by washing with water until the pH of the wash was greater than 5. As shown in Tables 2 and 3, iron can be adsorbed readily from dilute sulfuric acid solutions (M H_2SO_4 < 0.1) and from both dilute and concentrated ammonium sulfate solutions. The distribution coefficients are apparently independent of the Fe(III) concentration of the solution (Table 3).

The adsorbed Fe(III) complex in the resin phase has an intense red-brown color. The nature of the species is not known. It should be pointed out that the data in Tables 2 and 3 cannot be interpretated readily in terms of the species adsorbed because some acid is also adsorbed (see section "Adsorption of Sulfuric Acid by Dowex-1 in the Sulfate Form") and the initial sulfuric acid concentration given in the tables may be considerably larger than that occurring at equilibrium. A detailed interpretation of the adsorption equilibrium can be expected only after an intensive study of the reaction.

Separation of Fe(III) and Al(III) in Sulfate Solution. In the previous section it was shown that Fe(III) can be adsorbed from sulfate solutions and some dilute sulfuric acid solutions by the sulfate form of Dowex-1.

(9) Summer participant, 1951 Some work done more than one year ago is included for the sake of completeness

Preliminary experiments indicate that Al(III) shows only negligible adsorption under these conditions. The difference in the adsorbability can be used to separate the two elements by anion exchange. The following experiments, which can be considered typical for the separation of nonadsorbable ions from Fe(III) in sulfate media, illustrate the separation.

TABLE 2. ADSORPTION OF Fe(III) ON DOWEX-1 FROM SULFATE SOLUTIONS

Shaking time 1 to 2 hr
Resin Dowex-1, $SO_4^=$ form, 250 to 500 mesh
Temperature 25°C

M $(NH_4)_2SO_4$	M H_2SO_4 (initial)	M Fe(III) x 10^3 (initial)	FRACTION OF Fe(III) ADSORBED	WT RESIN[b] (mg)	VOLUME (ml)	D[a]
-	0 001	0 4	0 52	69 4	5 00	108
-	0 005	0 4	0 30	85 7	5 00	35
-	0 01	1 0	0 30	96 9	5 00	31
-	0 025	0 4	0 31	82 8	5 00	37
-	0 05	0 4	0 17	153 5	5 00	9
-	0 10	1 0	low	46 5	5 00	low
-	1 0	1 0	negl	52 0	5 00	negl
-	4 2	1 0	negl	51 7	5 00	negl
0 01	0 01	1 0	0 24	62 7	5 00	negl
0 1	0 01	1 0	0 22	61 2	5 00	32
1 0	0 01	1 0	0 11	61 9	5 00	14
4 0	0 01	1 0	0 09	63 2	5 00	11

[a] $D = \frac{\text{amount of Fe(III) per gram of oven-dried resin}}{\text{amount of Fe(III) per milliliter of solution}}$

[b] Weight of air dried resin (% water = 27 6)

TABLE 3. ADSORBABILITY OF Fe(III) ON DOWEX-1

Solvent 0.010 M H_2SO_4
Shaking time 1 to 2 hr
Resin Dowex-1, $SO_4^=$ form, 250 to 500 mesh
Temperature 25°C

M Fe(III) x 10^4 (initial)	FRACTION Fe(III) ADSORBED	WT RESIN (mg)	VOLUME (ml)	D[a]
0.1	0.24	66.7	5.00	33
0.2	0.20	59.5	5.00	29
0.3	0.23	82.1	5.00	25
0.5	0.28	88.9	5.00	30
1.0	0.28	95 7	5.00	28
10.0	0.30	96.9	5.00	30

[a] $D = \frac{\text{amount of Fe(III) per gram of oven-dried resin}}{\text{amount of Fe(III) per milliliter of solution}}$

A column of Dowex-1, 0.187 cm^2 by 9.3 cm, in the sulfate form was equilibrated with 0.01 *M* H_2SO_4. A 0.5-ml sample of a solution containing 5×10^{-3} *M* Fe(III) and 5×10^{-3} *M* Al(III) in 0.01 *M* H_2SO_4 was added to the column, and elution was started with 0.01 *M* H_2SO_4. The effluent was tested qualitatively for Al(III) with alizarin and for Fe(III) with KSCN. In addition, the Fe(III) fractions were analyzed spectrophotometrically by measuring the optical density of aliquots in 6 *M* HCl. Figures 2*a* and 2*b* show that Al(III) appeared in the first few fractions, as was expected for a nonadsorbable species. The Al fraction, as well as the other fractions between the Al and Fe bands, gave a negative test for Fe(III). Elution of the adsorbed Fe(III) was accomplished by increasing the sulfuric acid concentration in the eluent to 0.1 or 1 *M* H_2SO_4. Comparison of Figs. 2*a* and 2*b* shows that the iron band appears more rapidly with the more concentrated sulfuric acid solution. The long-delayed appearance of the Fe(III) band in the 0.1 *M* H_2SO_4 solution is probably connected with the resin adsorbing sulfuric acid and thereby being converted to the bisulfate form. This adsorption considerably decreases the sulfuric acid concentration of the effluent until the column has been equilibrated with the new medium, after which the elution of the Fe(III) band becomes rapid. In both experiments the Fe(III) band was fairly narrow and showed little tailing.

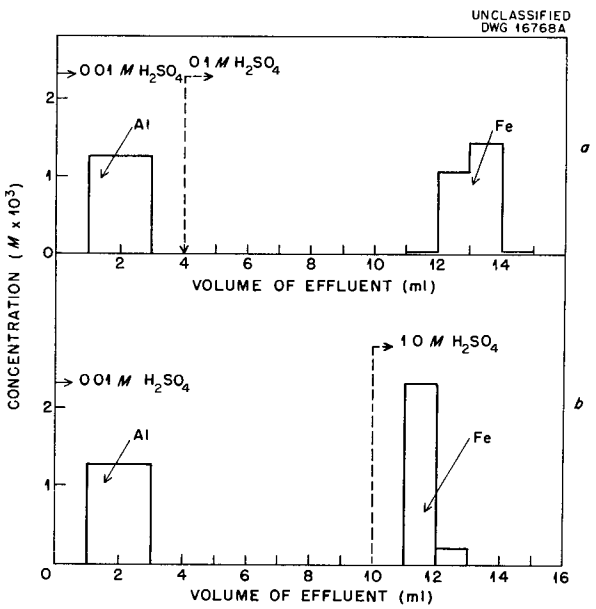

Fig. 2. Separation of Al(III) and Fe(III) by Anion Exchange in Sulfate Solutions. Column Dowex-1, 0.187 cm^2 by 9.3 cm.

Adsorption of Sulfuric Acid by Dowex-1 in the Sulfate Form. The sulfate form of Dowex-1 can be considered as a base that can react with hydrogen ions to form the bisulfate form of the resin. At the same time, of course, an equivalent number of negative ions must enter the resin. The resin apparently adsorbs acids according to the reaction

$$R_2SO_4 + HX \longrightarrow RHSO_4 + RX \ .$$

In the case of sulfuric acid, the reaction would become

$$R_2SO_4 + H_2SO_4 \rightleftharpoons 2RHSO_4 \ .$$

The adsorption of sulfuric acid was demonstrated by passing 0.5 *M* H_2SO_4 into a 0.042-cm^2 by 37.5-cm (1.58 cc) column of well-washed Dowex-1 in the sulfate form. Approximately 1 mmole of sulfuric acid was adsorbed, and the effluent had a pH of 4 or higher.

A series of equilibration experiments was conducted in which samples of the resin were shaken with 10^{-1} to 10^{-3} *M* sulfuric acid solutions. The sulfuric acid adsorbed by the resin was determined conductimetrically by the use of appropriate calibration curves. The concentration of sulfuric acid in the resin was computed from the change in sulfuric acid concentration of the solution after the addition of the resin and from the known weights and volumes of the resin and solution. The results of

some of the preliminary experiments are shown in Table 4.

Attempts have been made to interpret the results according to the equilibrium

$$R_2SO_4 + H_3O^+ + HSO_4^- \rightleftharpoons 2RHSO_4 + H_2O ,$$

or the equivalent reaction

$$R_2SO_4 + 2HSO_4^- \rightleftharpoons 2RHSO_4 + SO_4^{--} .$$

However, no consistent constant was obtained. The apparent equilibrium constants increased strongly with decreasing initial sulfuric acid concentration. The results are now being rechecked to see whether this pronounced drift in the constant is due to an impurity in the resin. Therefore the data in Table 4 should be taken only as indicating that sulfuric acid can be adsorbed by the resin and should not be used as a quantitative expression of the adsorbability until they are further verified.

TABLE 4. ADSORPTION OF SULFURIC ACID BY DOWEX-1*

MOLARITY H_2SO_4		RATIO OF RESIN (mg) TO SOLUTION (cc)	D**	EQUILIBRATION TIME (hr)
Initial	Final			
1.00×10^{-3}	9.26×10^{-4}	0.184	430	50
	9.38×10^{-4}	0.432	150	50
	9.15×10^{-4}	0.872	106	50
	8.92×10^{-4}	1.56	78	50
	7.74×10^{-4}	7.64	38	50
1.00×10^{-2}	9.90×10^{-3}	0.228	41	39
	9.86×10^{-3}	0.396	36	39
	9.78×10^{-3}	0.732	31	39
	9.65×10^{-3}	1.23	29	39
	9.46×10^{-3}	1.93	30	39
	9.23×10^{-3}	2.93	29	39
	8.91×10^{-3}	4.34	28	39
	8.41×10^{-3}	6.12	31	39
1.00×10^{-1}	9.84×10^{-2}	2.02	0.80	17
	9.71×10^{-2}	3.98	0.75	17
	9.49×10^{-2}	7.26	0.74	17
	8.93×10^{-2}	14.6	0.83	17
	8.13×10^{-2}	25.4	1.47	17
	6.16×10^{-2}	77.4	8.1	17

*Preliminary results.

$$**D = \frac{\text{Moles of } H_2SO_4 \text{ per kg of resin}}{\text{Moles of } H_2SO_4 \text{ per l of solution}} .$$

Separation of Sulfuric Acid from the Metal Sulfates The adsorption of sulfuric acid by Dowex-1, as described in the previous section, implies that the resins can be used to separate sulfuric acid from nonadsorbable or weakly adsorbable metal sulfates. This method of separation is demonstrated by the use of a mixture of copper sulfate and sulfuric acid.

One-milliliter portions of copper sulfate in sulfuric acid were placed on a 0.187-cm^2 by 9.3-cm column (bed volume of 1.74 cc) filled with well-washed Dowex-1 in the sulfate form. The column was then eluted with distilled water. Approximately 1-ml fractions of the eluate were collected and tested for copper and sulfuric acid. The copper concentration was determined spectrophotometrically after making aliquots 0 5 *M* in NH_3. The sulfuric acid concentration was determined either by pH measurements combined with a calibration curve, or by titration. The results of two experiments using 0.1 *M* $CuSO_4$ in 0.1 *M* H_2SO_4 and 0.1 *M* $CuSO_4$ in 0.5 *M* H_2SO_4 are shown in Fig. 3. Good separation of copper sulfate from the acid was obtained in both experiments with the copper-containing eluate having a pH > 4.5.

The volume of eluate that is collected before the appearance of acid depends on the amount of sulfuric acid initially passed into the column ("loading" with respect to sulfuric acid) because the acid has to be moved through the remaining part of the sulfate column. In the experiment with 0.1 *M* H_2SO_4, acid appeared after about eight column volumes of water had been used, whereas in the experiment with 0 5 *M* H_2SO_4, acid appeared after two column volumes. In these experiments about 7 5 and 38%, respectively, of the adsorptive capacity of the column for H_2SO_4 were utilized.

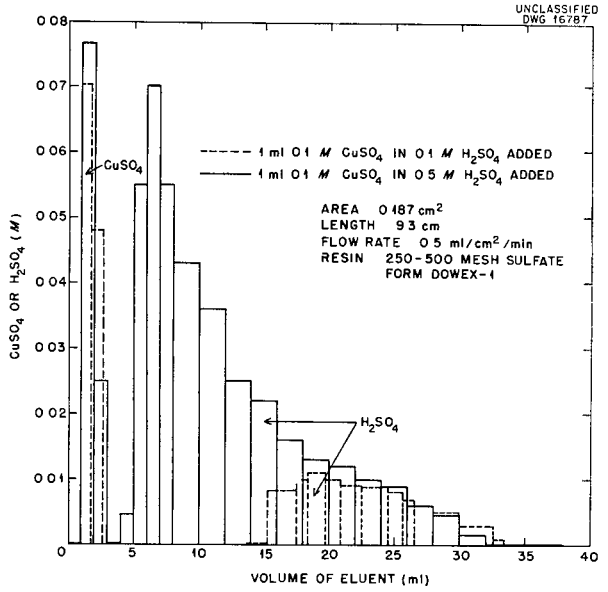

Fig. 3. Anion-exchange Separation of $CuSO_4$ and H_2SO_4 by Elution with Water at 25°C.

Although the removal of sulfuric acid from the $CuSO_4$ solution was quite satisfactory, the regeneration of the resin (removal of H_2SO_4 from resin) using only water takes place slowly, as is shown in Fig. 3. About 22 column volumes of water were necessary before the pH of the eluate rose to around 4.5.

In an attempt to increase the efficiency of the regeneration process, an experiment was carried out at 60°C because it was believed that slow rates of equilibration might be partly responsible for the trailing edge in the sulfuric acid elution. As shown in Fig. 4, operation at a higher temperature not only does not improve the regeneration but actually requires more water (about 32 column volumes) for the removal of H_2SO_4 than at a lower temperature, indicating that the tailing in the elution band is not due to slow rates of equilibration but probably arises from a pronounced nonlinearity of the adsorption isotherm. It is interesting to note that the copper band at 60°C definitely showed some adsorption, the apparent elution

constant being about 1 instead of the theoretical maximum of about 2.5. At the lower temperature, the copper band was less strongly adsorbed, although even then it did not travel with elution constant as large as 2.5.

Adsorption of Some Transition Elements from Sulfate Solutions The adsorbability of the transition elements Co, Ni, and Cu was tested in 1.0 and 3.5 *M* $(NH_4)_2SO_4$ and in 1.0 and 3.0 *M* H_2SO_4. As shown in Table 5, the elution constants $E = dA/V$, where d is the distance that an adsorption band moves on passage of V ml of eluent through a column of A cm^2 cross-sectional area, are about 2.4 for 1.0 and 3.0 *M* H_2SO_4, respectively. This is approximately the theoretical maximum[10] of E in the case of a non-adsorbable ion and suggests that under these conditions no adsorption of these three elements takes place. In 1.0 and 3.5 *M* $(NH_4)_2SO_4$, these elements show significantly smaller elution constants (1 4 to 1.8). Since E is still quite large, it appears that these elements are only weakly adsorbed under these conditions.

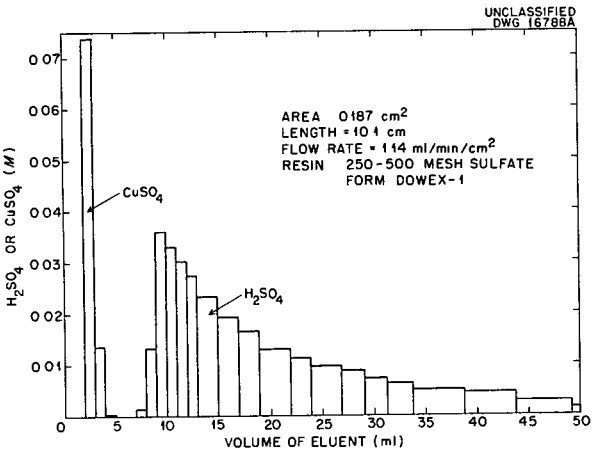

Fig. 4. Anion-exchange Separation of $CuSO_4$ and H_2SO_4 by Elution with Water at 61°C. Added 0.88 ml of 0.1 *M* $CuSO_4$ in 0.5 *M* H_2SO_4.

In this connection, it may be remembered that, as mentioned in the previous section, $CuSO_4$ is slightly adsorbed on a sulphate column in regions of low acidity, and this adsorbability increases markedly with temperature.

THERMODYNAMICS OF COMPLEX IONS

R. P. Yaffe G. H. Cartledge

Further work has been done as a contribution to the understanding of the heat and entropy effects in the formation of complex ions. Supplementing the work of Cartledge and Nichols[11] at 0°C, the equilibrium

[10] This is also the approximate value for the elution constant of tracer sodium ions (Na^{24}) in 1 0 and 3 5 *M* $(NH_4)_2SO_4$

[11] G H Cartledge and P M Nichols, *J Am Chem Soc* **62**, 3057 (1940)

TABLE 5. ELUTION CONSTANTS OF SOME TRANSITION ELEMENTS AND OF Na^+ IN SULFATE MEDIA

Dowex-1, sulfate form, room temperature, about 25°C

MEDIUM	ELUTION CONSTANTS			
	Co(II)	Ni(II)	Cu(II)	Na^+
1 0 *M* H_2SO_4	2 5	2 4	2 4	
3 0 *M* H_2SO_4	2 3	2.4	2 4	
1 0 *M* $(NH_4)_2SO_4$	1.7	1.8	1 5	2 7
3 5 *M* $(NH_4)_2SO_4$	1 7	1 8	1 4	2 4

between the bis- and tris-malonato manganese(III) complex ions has been investigated spectrophotometrically between 0 and 19.6°C. Instability of the system prevented the use of higher temperatures. The equilibrium constant is for the reaction

$$Mn(C_3H_2O_4)_3^{3-} + 2H_2O \rightleftharpoons Mn(C_3H_2O_4)_2^{-}(H_2O)_2 + C_3H_2O_4^{2-} .$$

When the method of least squares was applied to the numerous measurements, the graph of log K vs. $1/T$ was essentially linear over the temperature range that was covered. This led to the results shown in Table 6. These results may be compared with those previously obtained for the analogous complexing reactions of the oxalate and pentanedione anions.[12] If, as is likely, the entropy change in the oxalato system is about the same as in the malonato system, it is found that the energy for the bonding of the third anion is greatest for pentanedione and least for malonate. The heat changes (ΔH) for the pentanedione and oxalate systems are much closer together, however, than might be suspected from the comparative equilibrium constants alone, owing to the appreciable difference in the entropies associated with the different charge types.

(12) G H Cartledge, *J Am Chem Soc* **73**, 4416 (1951)

TABLE 6. THERMODYNAMIC CONSTANTS FOR EQUILIBRIUM BETWEEN BIS- AND TRIS-MALONATO MANGANESE(III) COMPLEX IONS

CONSTANT	AT 0°C	AT 25°C
K	0.057 ± 0.003*	0.0703**
$\Delta F°$	1550 cal	1560 cal
$\Delta H°$	1300 cal	1300 cal
$\Delta S°$	-0.8 e.u.	-0.8 e.u.

*Standard deviation.

**Extrapolated.

CHEMISTRY OF CORROSION

G H. Cartledge

Experiments have been in progress to determine the variation of the electrode potential of steel and its separate components as a function of temperature. The effect of various additions to the system is also under study in order to obtain a better understanding of the effects of local action in determining the actual potential of the system. The observed potentials are not necessarily thermodynamically reversible, the kinetic effects are the important considerations about which more information is desired

To date, experiments have been conducted in a simple system, open to the atmosphere, with vigorous agitation, and at temperatures up to 96°C. These orienting experiments were designed to disclose the peculiarities of the systems before beginning more careful studies from which quantitative kinetic indications might be obtained. The apparatus for these studies is being assembled.

Thus far, it has been observed that type 347 stainless steel, when immersed in 0.06 N sulfuric acid under the conditions of the experiments, becomes increasingly noble with time or upon successive treatments, although no visible film is formed. The electrode potential decreases almost linearly with rise in temperature, and the temperature coefficient is -2 to -4 mv/°C for electrodes with varying history. The potential of an electrode in stagnant electrolyte is 10 to 20 mv less noble than that of one in vigorously agitated solutions at temperatures above 50°C. Under similar conditions, the potential of a platinum-plated platinum electrode is approximately constant from about 40 to 80°C and about 900 mv more noble than the normal hydrogen electrode.

CHEMISTRY OF FUSED SALTS

A S Dworkin I S. Yaffe
D J Sasmor E. R Van Artsdalen

The major work on fused salts this quarter has involved assembling, testing, and calibrating several different types of apparatus and designing others Details of the methods and apparatus are not included in this report, although some preliminary results of electrical conductivity are reported

A Leeds and Northrup "Jones" conductivity bridge and auxiliary apparatus were assembled in preparation for determining conductivities of various molten salts and their mixtures, bridge balance is detected with an oscillograph Attempts were made to calibrate the bridge by comparison with National Bureau of Standards certified resistors according to the method recommended by Dike [13] However, values for the bridge resistors were obtained that were not self-consistent The inconsistency was finally traced to recent changes in the bridge circuit that were made by the manufacturer, which invalidated the *ratio-arm* method of Dike. The resistors of the bridge were finally calibrated against the NBS resistors by balancing the bridge with the R_2 slidewire instead of with the R_1 slidewire, then consistent results were obtained.

A preliminary check of the over-all method of measuring conductance was made with molten silver nitrate, which has been redetermined recently by Spooner and Wetmore.[14] The results were in quite satisfactory agreement

A rough determination of the conductance of molten lithium chloride was made, using the commercial c.p. salt Unfortunately, only four different temperatures between 640 and 717°C were investigated before the attack on the silica cell by the alkali halide became too great for further work. The density data for molten lithium chloride obtained by Biltz and Klemm[15] were used to calculate equivalent conductances, which were found to fit the equation

$$\Lambda = 161.8 + 0.193\ (t - 613)\ ,$$

where Λ is the equivalent conductance and t is the temperature in degrees centigrade. This may be compared with the equation given by Biltz and Klemm[15]

$$\Lambda = 166 + 0.170\ (t - 613)\ .$$

An apparent "activation energy" for electrical conductance may be calculated from these equations for the variation of equivalent conductance with temperature. The data obtained show an "activation energy" for the conduction process of 2.0 kcal/mole, whereas the data of Biltz and Klemm yield 1.7 kcal/mole.

An apparatus for measuring densities of molten salts has been constructed, and will be used in conjunction with the measurement of electrical conductivities The method chosen involves comparing the weights of a bob submerged alternately in the molten salt and in water

There has been some difficulty in obtaining satisfactory operation from the temperature-controlling equipment for the furnaces. However, operating experience should lessen this difficulty.

Apparatus has been constructed and preliminary experiments have been made in an attempt to determine the transport numbers of the ions present in binary mixtures of fused alkali halides. The principle of the method chosen involves measurement of the change in concentration of the two salts of a binary solution in both anode and

(13) P H Dike, *Rev Sci Instruments* **2**, 389 (1931)

(14) R C Spooner and F E W Wetmore, *Can J Chem* **20**, 777 (1951)

(15) W Biltz and W Klemm, *Z anorg Chem* **152**, 267 (1926)

cathode compartments after a known number of faradays of electricity has been passed through the melt. The current efficiency will be measured at the same time An incidental estimate of decomposition potential is also to be made

A Parr oxygen-combustion-bomb calorimeterhas been placedin operation to determine heats of combustion and formation. This calorimeter has been modified slightly to operate with an isothermal jacket rather than as an adiabatic instrument The temperature of the jacket is both controlled and recorded to ±0.001°C by a Speedomax recorder that operates in conjunction with a thermistor temperature-sensing element, a low-lag heater, and cooling water Only rarely do temperature fluctuations of the jacket exceed 0.001°C. Temperature in the calorimeter itself is measured to better than 0 001°C by means of a copper resistance thermometer, which was previously calibrated against a standardized platinum resistance thermometer, and a Mueller bridge. The calorimeter has been shown to operate satisfactorily in combustion calibrations made with NBS-certified benzoic acid At present, attempts are being made to measure the heat of combustion of boron nitride and several other boron compounds.

Frequently, complex salts are known to form when mixtures of molten salts are frozen. Knowledge of the heats of solution of the complex, as well as of the constituent salts under the same conditions, enables a computation of the heat of formation of the given complex salt Such information will be of considerable importance in interpreting the behavior of molten-salt solutions. In order to establish how elaborate measurements must be to give satisfactory data for present purposes, a simple calorimeter has been designed and built that will give a rough determination of the heats of solution of such complex salts The calorimeter is a silvered Dewar flask that contains a stirrer, a device for breaking ampoules containing the salts to be dissolved, a heater for adjusting the temperature and for calibrating purposes, and a thermistor with simple Wheatstone bridge for measuring temperature The thermistor was calibrated between 20 and 30°C against a standardized platinum resistance thermometer and will give temperature measurements to about 0.002°C The calorimeter has been calibrated electrically and gives a consistency of about 0 5% As a check on the calibration, the heat of solution of c p. potassium nitrate has been measured and found to agree with literature values to within about 1%

METAL-METAL HALIDE SYSTEMS

M. A Bredig H R. Bronstein
J W. Johnson W T. Smith[16]

Potassium Metal in Molten Potassium Chloride. Efforts have been continued to improve the experimental technique used to determine the solubility of an alkali metal in its molten salt. The simple stainless steel tubes that have been used thus far gave unsatisfactory analytical values for the potassium-metal content of the rapidly cooled salt ingot The values ranged from 26 mole % near the molten-metal surface to 7.5 mole % at the bottom of the salt ingot A cavity formed in the center of the salt phase on solidification This cavity connected with the molten-metal phase. The erroneous inclusion, in the analysis, of the metal in the cavity and the rejection into the cavity of molten metal dissolved in the molten salt are believed to be responsible for the high, and low values. A method of keeping the molten-salt and metal phases separated and equilibrating

[16] Consultant from University of Tennessee

through the medium of the metal vapor-phase has now been employed. Two preliminary tests, in which the molten salt was contained in a stainless steel crucible that was supported inside a closed stainless steel tube holding the metal phase at its bottom, gave solubilities greatly in excess of previous measurements by E. Mollwo,[17] who obtained a figure of approximately 2 mole %.

In the present technique, in which the heat flow was from the part of the tube containing the metal to the part containing the salt, the possibility that potassium metal in excess of the amount actually dissolved in the molten salt has distilled over to the salt portion cannot be entirely ruled out. An apparatus has now been constructed that permits the molten salt and the liquid metal to be independently heated. This is expected to give more quantitative data, including the effect of vapor pressure of the metal on its solubility.

An attempt to determine, by heating and cooling curves, the melting-point depression associated with saturation of the molten potassium chloride with potassium metal gave a value for ΔT of 12°C.

A possible relationship between molecular volume or structure of, and solubility of metal in, the molten salt was mentioned in the preceding progress report. In the sense of a modified Harker-Cubiciotti theory of such solutions, octahedral "holes" might be made available even in monohalides by transfer of part of the cations to fourfold coordinations (tetrahedral "holes"). A survey of the literature dealing with the molecular volume of solid and fused salts might, it is hoped, throw some light on the structure of the liquid phase. The results are being tabulated and will be discussed in succeeding reports.

Potassium Metal in Ternary Alkali Fluoride Eutectic. The need for better separation of the equilibrated liquid-salt and liquid-metal phases before quenching led to the design and construction of a capsule that incorporates a ball check valve as shown in the radiographic view in Fig. 5. During equilibration, with the capsule in a horizontal position, the ball rests in the side tube. After the two liquid phases are allowed to separate by holding the tube in a vertical position over a period of 1 hr, the tube is tilted before quenching to permit the ball to set on the constricted portion and thus separate the lowest part of the salt phase from the rest of the charge. This part is then analyzed for the alkali-metal content. In five tests at 920°C, a solubility in the ternary eutectic of LiF, NaF, and KF of 3.7 ± 0.5 mole % of metal, calculated as potassium, was obtained. Earlier values that ranged from 1.6 to 3.0 mole % for alcohol-leached samples and from 6.2 to 9.7 mole % for nonleached samples are believed to be too low because of loss of dissolved metal in the leaching process, and too high because of seepage of undissolved liquid metal into cracks of the solidified salt phase.

UNCLASSIFIED
DWG. 17398

Fig. 5. Equilibrium Capsule.

[17] E. Mollwo, *Physik. Zeitschr.* **36**, 740 (1935).

NUCLEAR CHEMISTRY

GROWTH OF THE RADIUM E BETA SPECTRUM INTO RADIUM D

R. R. Edwards B. H. Ketelle

Hot-atom chemical separations of bismuth from radium D at the University of Arkansas indicated the possibility that isomerism exists in radium E. Because of the interest in the shape of the radium E beta spectrum, the following study has been made.

The long-lived activity from a spent radon seed loaned by E. Rona was purified by dithizone extraction. The radium E was removed from the radium D by adsorption on a Dowex A-1 column, and a beta-ray spectrometer source of radium D was prepared as rapidly as possible. The growth of activity at 11 selected points that covered the spectrum from 60 to 912 kev was studied. At each energy, the data can be represented by the equations for the growth of a single daughter with a half life of 4.85 days. Therefore it is evident that the unusual shape of the radium E spectrum is not due to the presence of an isomer of half life very different from the well-known value.

CERIUM-144-PRASEODYNIUM-144 DECAY SCHEMES

B. H. Ketelle A. R. Brosi

Since 280-d Ce^{144} and its 17-m Pr^{144} daughter were thought to decay by beta emission only, high-intensity sources of Ce^{144} were once considered as possible energy sources that would require very little shielding. In some preliminary work, it was found that intense sources would require shielding because both Ce^{144} and Pr^{144} emit gamma radiation. This observation has been confirmed by several different authors who have published work on the two decay schemes. However, many uncertainties still existed with respect to these decay schemes, therefore further work was done by using a thin magnetic-lens beta spectrometer to measure electron-energy distributions coincident with particular gamma rays. Gamma-gamma coincidence measurements have also been made by using two scintillation spectrometers.

It has been found that one of the gamma-coincident beta spectra of Pr^{144} has a unique shape that makes it possible to assign a definite spin change to the transition. This work, together with previously published data, makes it possible to write a decay scheme for Pr^{144} with some confidence.

The Ce^{144} decay scheme appears to be much more complex. Since some of the transitions that have been attributed to this isotope may arise from impurities, a new high specific activity-high purity source is being prepared through the use of an ion-exchange column purification.

NEUTRON-CAPTURE CROSS SECTION OF PROTACTINIUM-233

J. Halperin R. W. Stoughton

Work on the determination of an effective capture cross section of Pa^{233} for reactor neutrons has continued.[1]

The program of neutron irradiation and subsequent processing of thorium slugs for the protactinium cross-section determination is now essentially complete. An evaluation of the data awaits only the mass spectrographic analyses that are being performed by the Y-12 Assay Laboratory. A preliminary value for an effective cross section of Pa^{233} for reactor neutrons is 130 ± 30 barns.

A total of 17 thorium slugs (about 1650 g per slug) has been irradiated

(1) J Halperin and R W Stoughton, *Chem Quar Prog Rep March 31, 1952*, ORNL-1285, p 30

in both the ORNL LITR and at Hanford. Twelve of the slugs were irradiated in a beryllium element of the lattice of the LITR. This beryllium assembly holds as many as four slugs at one time. Irradiations have been carried out over periods of time equivalent to ft values of 5×10^{18} to 1.5×10^{20} cm^{-2}. Average cooling periods of 4 to 5 months have been utilized to permit the Pa^{233} activity to fall to a level that could be handled in the Semi-Works equipment of the Chemical Technology Division.

RADIATION CHARACTERISTICS OF SAMARIUM-145 AND PROMETHIUM-145

G. W. Parker W. J. Martin

A number of authors[2,3] have pointed out reasons for the existence of a long-lived isotope of promethium at mass 145. In a recent paper,[4] F. D. S. Butement announced the discovery of the predicted isotope, which he obtained from neutron-irradiated samarium as a result of decay by orbital-electron capture in the 410-d Sm^{145}. At the same time, an approximate half life of 30 y for the promethium was determined by allowing it to grow for measured periods.

In the present investigation, the authors were fortunate in being able to obtain approximately 200 mg of calutron-enriched Sm^{144}, with which an extended irradiation in a high neutron flux had already been planned prior to the publication of Butement's work. Since the quantity of activity found by Butement was limited to a few hundred counts, an expanded scale of production was necessary to permit an extensive analysis of the characteristic radiations. An additional consideration of the production of fractional milligrams of Pm^{145} was the possible identification of Pm^{146}[5] by further neutron irradiation.

A much expanded preparation of Sm^{145}, by a long irradiation of enriched Sm^{144} from which the long-lived samarium and promethium activities are fractionated and then analyzed, clearly substantiates the conclusions of the earlier work. Samarium-145 was found to emit electromagnetic radiation that consists only of K and L x rays of promethium. The promethium gave off similar x rays that correspond to neodymium. In addition, three harder gamma rays were observed with energies of 80, 460, and 750 kev. These were not reported by Butement and may indicate the presence of another isotope of promethium.

The present observations verify a half life of about 400 d for the samarium and at least 30 y for the promethium. Separate decay has not been observed on the promethium gamma rays. Mass spectrometric and spectrographic determinations are in progress that will provide data for direct mass assignments. The cross section for Sm^{144} activation is estimated to be about 0.03 barn.

Experimental A sample of approximately 200 mg of enriched $Sm_2^{144}O_3$ was obtained from the stable-isotope production program with an analysis leading to the principal products shown in Table 7.

A 10-mg sample was retained for reference analyses, and the remainder (190 mg) was irradiated at Chalk River for a period of one year at an average flux of 3.6×10^{13} neutrons/sec. After a short cooling period, the highly activated sample (mainly Eu^{155} activity) was dissolved and adsorbed on a Dowex-50 ion-exchange column of sufficient capacity to allow chromatographic separation (Fig. 6) by citrate elution.

(2) N E Ballou, *Phys Rev* **75**, 1105 (1949)

(3) M G Ingraham, R J Hayden, and D C Hess, *Phys Rev* **71**, 643 (1947)

(4) F D S Butement, *Nature* **167**, 400 (1951)

(5) V Kistiakowsky, *Phys Rev* **87**, 859 (1952)

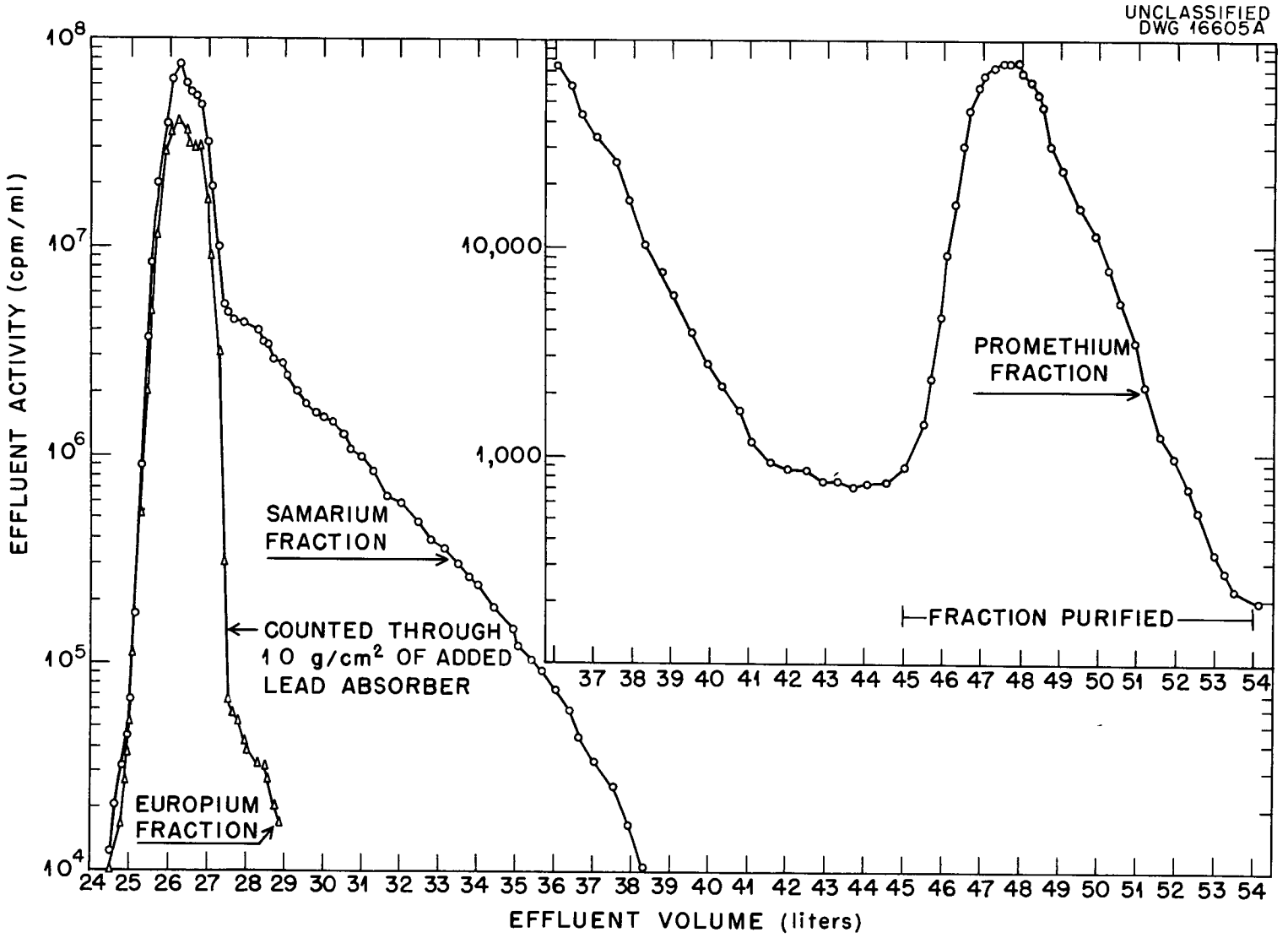

Fig. 6. Elution Curve of Activity in Irradiated Enriched Sm^{144} Observed on a Well-Type Sodium Iodide Scintillation Counter.

Samples from each fraction collected were counted for relative gamma activity in a high-efficiency sodium-iodide crystal scintillation counter that was especially well adapted for the detection of promethium x rays.

The typical elution curve showed the europium-samarium overlap (normal for the column efficiency employed) and a distinct lower order activity band of promethium (Fig. 6 inset).

The central portion of the promethium fraction was further purified by a second elution (Fig. 7), so that a limit of samarium contamination could be set at 0.01%.

Characteristic Radiations. Samples of the samarium and promethium were individually mounted for examination on both a scintillation and proportional spectrometer. The assistance of A. R. Brosi and C. J. Borkowski of the Chemistry Division is acknowledged. Figure 8 shows the expected minor difference in energy of the *K* x rays

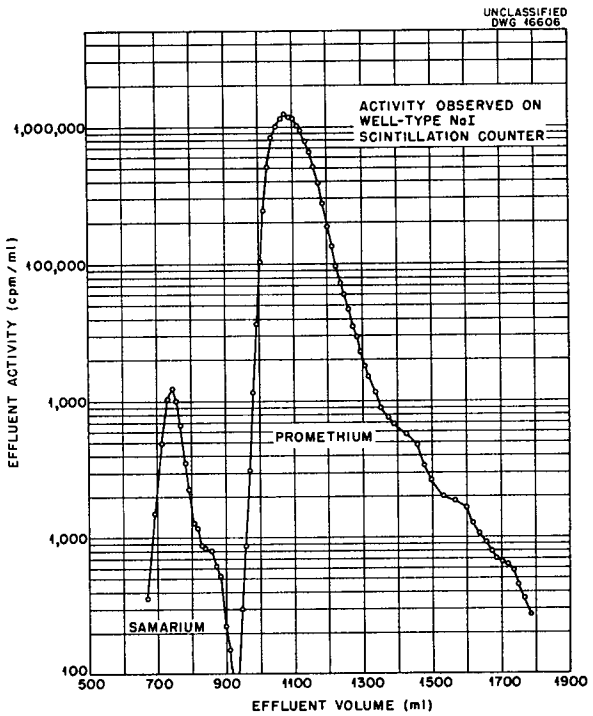

Fig. 7. Chromatogram of Purification of Promethium Fraction.

TABLE 7. ANALYSIS OF ENRICHED $Sm_2^{144}O_3$

ISOTOPE	ENRICHMENT (%)	CROSS SECTION (barns)	n,γ PRODUCTS
Sm^{144}	72 13	0 03*	Sm^{145} (410 d) $\xrightarrow{Oec^{**}}$ Pm^{145} (30 y)
Sm^{145}			
Sm^{146}			
Sm^{147}	7 69		Sm^{148}
Sm^{148}	4 40		Sm^{149}
Sm^{149}	4 41	~47,000	Sm^{150}
Sm^{150}	1 94		Sm^{151} (120 y)
Sm^{151}		7,200	
Sm^{152}	5 52	150*	Sm^{153} (47 h) $\xrightarrow{\beta^-}$ Eu^{153}
Sm^{153}			
Sm^{154}	3 91	5 5*	Sm^{155} (25 m) $\xrightarrow{\beta^-}$ Eu^{155} (2 y)
Eu	<0 15		

*Activation cross section

**Orbital electron capture

of each of the activities. Figure 9 indicates the presence of gamma rays in promethium at the energies 80, 460, and 750 kev.

Decay Characteristics. From a preliminary set of data, substantial decay in the samarium activity follows a half life of about 400 days. Conversely, the promethium shows no decay, indicating a rather long half life in numbers of years. In terms of relative intensity of activity, a promethium half life of about 40 times that of the samarium is estimated. Later growth studies will be used to better evaluate this half life.

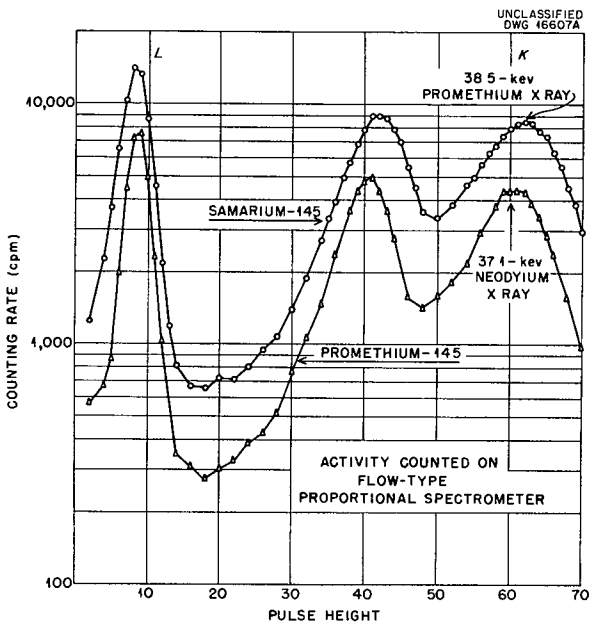

Fig. 8. Spectrograms of *K* and *L* X Rays in Sm^{145} and Pm^{145}. Krypton X-ray Counter.

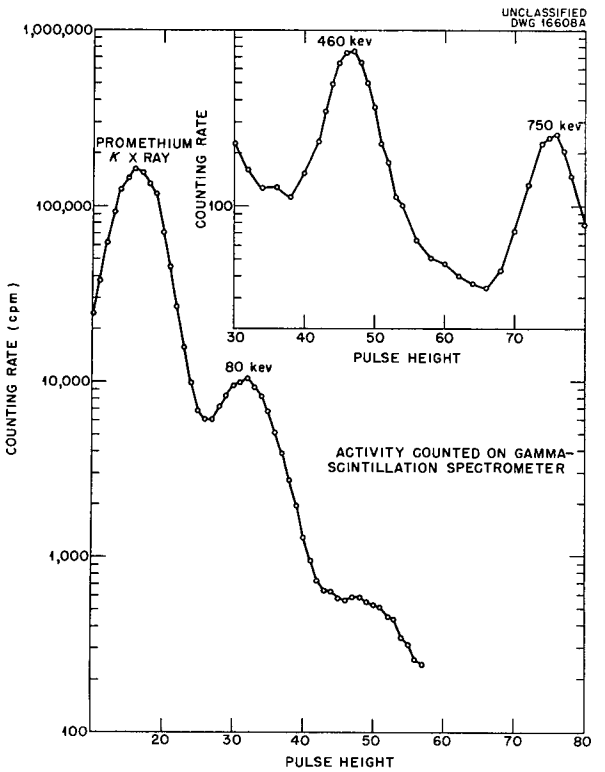

Fig. 9. Spectrograms of Gamma Rays in Pm^{145}.

RADIO-ORGANIC CHEMISTRY

C. J. Collins

RADIATION AND ANALYTICAL ORGANIC CHEMISTRY

A. R. Jones W. J. Skraba

The study of the products formed by the action of Co^{60} gamma radiation on dilute aqueous solutions of acetic acid has continued. The nonvolatile product was fractionated by partition chromatography, and tentative identification of the fractions was made by paper chromatography. Direct comparison with known compounds, by the use of different solvent combinations, indicated that the five major constituents were succinic, tricarbollylic, and citric acids and the two forms of butane-1,2,3,4-tetracarboxylic acid.

Positive characterization of these substances was difficult because of the impure condition of the fractions and the small amounts that were isolated. Although the pure substances are crystalline and have definite melting points, these products were gelatinous. For each substance, the melting point of the small amount of solid found corroborated the paper chromatographic results, however, they were too much below the melting points of the pure substances to allow mixture melting points to be taken. Infrared and ultraviolet absorption measurements and other common analytical techniques are of limited application for these compounds.

An analytical method was developed that makes use of a high-frequency grid-dip type of oscillator. By using this method, identification of small amounts of acidic substances was made possible by a comparison of the titration curves for equivalent quantities of the known and unknown compounds. The results are relatively independent of temperature, frequency, quantity, and the pressure on nonionic or weakly ionized impurities in the material.

Recently, several instruments that make use of high-frequency oscillators have been developed for the detection of endpoints in volumetric chemical reactions. For example, an acid-base titration yields a plot of oscillator grid current vs. milliliters of base that shows a sharp break in the curve (usually two intersecting straight lines) at the endpoint. A change in the form of the electrodes caused the instrument to produce curves that generally had no sharp break at the endpoint and were characteristic of individual acids.

Positive identification of succinic, tricarbollylic, and the two butane-1,2,3,4-tetracarboxylic acids was made by this method. The unknown substance, suspected to be citric acid, contained some sulfuric acid and is being purified.

ISOTOPE EFFECT STUDIES

Examination of the Bromine Addition to Carbon-14-Labeled Methyl Cinnamate for an Isotope Effect (V. F. Raaen, G. A. Ropp). It was shown in an earlier study[1] that very rapid additions of bromine to alpha and beta C^{14}-labeled styrene did not involve carbon isotope fractionation. As a continuation of this study, the much slower addition of bromine to methyl cinnamate-α-C^{14},

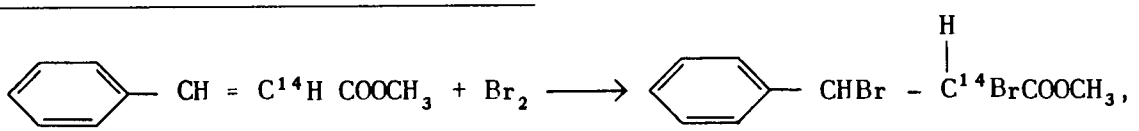

(1) V. F. Raaen and G. A. Ropp, *Chem. Quar. Rep. March 31, 1951*, ORNL-1053, p. 65

has been examined and has also been found not to show an isotope effect in carbon. At present, the corresponding reaction with methyl cinnamate-β-C^{14} is being investigated.

Methyl cinnamate-α-C^{14} (specific activity about 0.5 μc/mmole) was prepared from sodium acetate-2-C^{14} by means of the Perkin reaction. One sample of the labeled ester was brominated in carbon tetrachloride solution at 25°C with sufficient bromine to give 10% bromination, a second sample was brominated to 40%, and a third was completely brominated with excess bromine. The reaction to 10% bromination required 2 hours. As the assay values in Table 8 indicate, no isotope effect was found. The specific activities of the samples of dibrominated ester from the three reactions were essentially equal.

TABLE 8. SPECIFIC ACTIVITY OF METHYL CINNAMATE-α-C^{14} AFTER BROMINATION

BROMINATION (%)	ACTIVITY (μc/mmole)
10	0 449, 0 448, 0 441, 0 451 (avg 0 447)
40	0 4535, 0 4535 (avg 0 4535)
100	0 448, 0 451 (avg 0 450)

Specific Activity Relationships in Reactions Having Isotope Effects (G. A. Ropp). A series of curves (Figs. 10 and 11), based on modifications of an expression derived by Stevens and Attree[2] and Bigeleisen,[3] has been plotted. These curves show the values of S/S_{avg}, the ratio of the specific activity of accumulated product to the specific activity of the original reactant, at various percentages of reaction for a number of values of the isotope effect, k_{14}/k_{12}. A separate family of curves has been plotted for each of the values n = 1 and n = 2, where n is the number of molecules of labeled reactant that goes into the formation of a molecule of labeled product.

Studies of Carbon-14 Isotope Effects in the Saponification of Carboxyl-Labeled Esters at 25°C (V. F. Raaen, G. A. Ropp). The ratio k_{14}/k_{12} was measured for several saponifications by the method previously described.[4] As shown in Table 9, changing the solvent or the ester concentration did not appear to change the isotope effect at 25°C for the saponification of ethyl benzoate-α-C^{14}.

(2) W H Stevens and R W Attree, *Can J Res* **B27**, 807 (1949)

(3) J Bigeleisen, *Science* **110**, 14 (1949)

(4) G A Ropp and V F Raaen, *Chem Quar Prog Rep Dec 31, 1951*, ORNL-1260, p 47

TABLE 9. CARBON-14 ISOTOPE EFFECTS IN THE SAPONIFICATION OF CARBOXYL-LABELED ESTERS AT 25°C

ESTER SAPONIFIED	SOLVENT	APPROXIMATE ESTER CONCENTRATION (M)	k_{14}/k_{12}
Ethyl benzoate	90% ethanol	0.25	0.929
Ethyl benzoate	90% ethanol	1.25	0.926
Ethyl benzoate	56% acetone	0.25	0 928
t-Butyl benzoate	56% acetone	0 25	0.921*

*Preliminary value, subject to further checking.

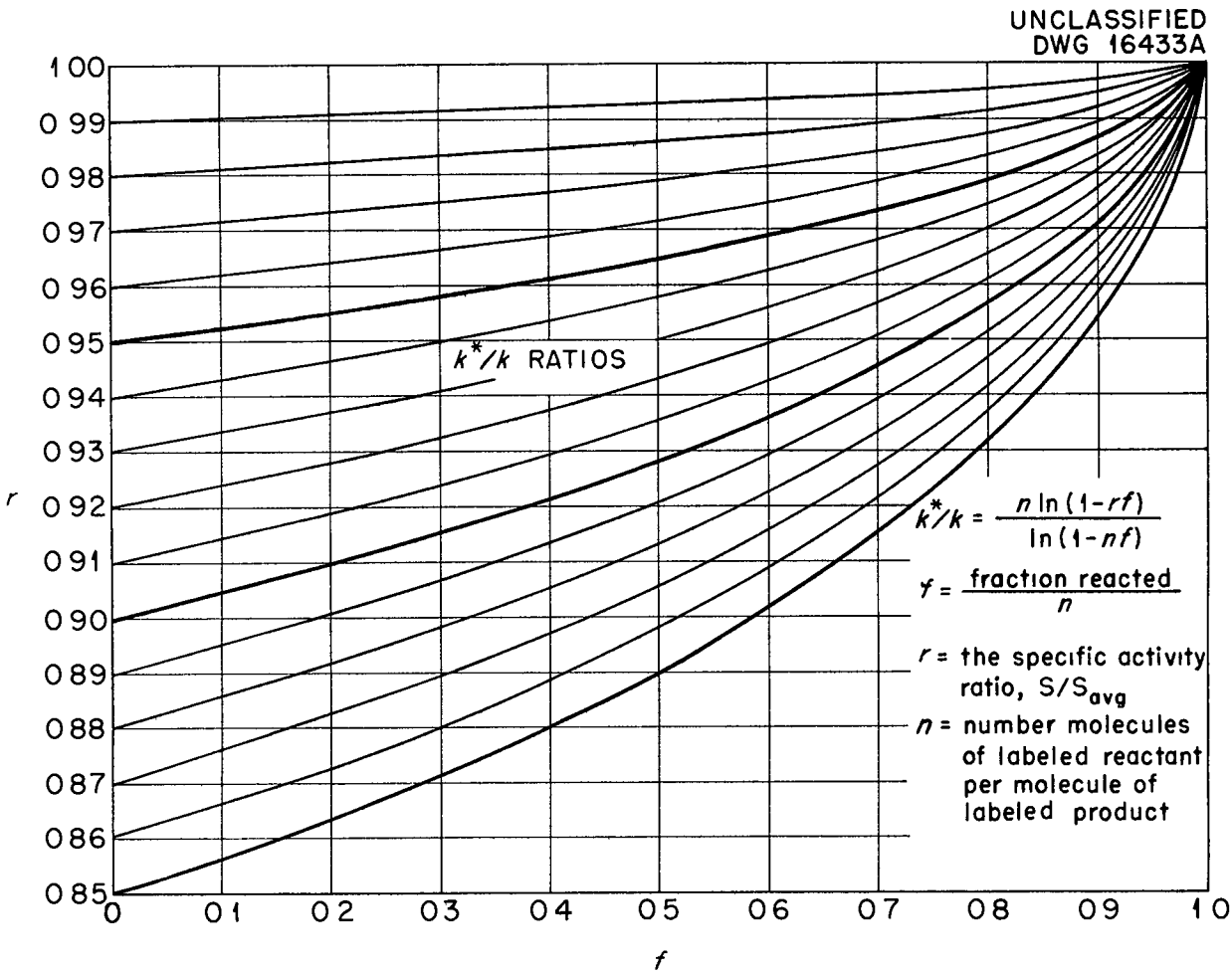

Fig. 10. Intermolecular Isotope-Effect Ratios at Various Percentages of Reaction for n = 1.

Isotope Effect in the Dehydration of Formic-C^{14} Acid (A. J. Weinberger, O. K. Neville, G. A. Ropp). The isotope effect[5] in the dehydration of C^{14}-labeled formic acid in 95% sulfuric acid is being studied by a new procedure that should eliminate some of the uncertainties connected with the method previously used. The new method is designed to avoid possible errors resulting from the unknown amount of internal mixing of the evolved carbon monoxide-C^{14} with carbon monoxide-C^{14} that is produced earlier in the reaction. The new procedure involves the determination of the specific activity of the unreacted formic acid as a function of time. The method was applied earlier in the study of the decarboxylation of malonic acids and is described in an earlier report.[6]

Isotope Effect Studies in the Acid Hydrolysis of Hydrocyanic Acid (G. A. Ropp, A. J. Weinberger, O. K. Neville). An aqueous solution (1 *M*) of hydrocyanic acid-C^{14} (3 μc/mmole) has been prepared. Studies are in progress to

[5] G A Ropp, A J Weinberger, and O K Neville, *J Am Chem Soc* **73**, 5573 (1951)

[6] G A Ropp and V F Raaen, *Chem Quar Prog Rep March 31, 1952*, ORNL-1285, p 43

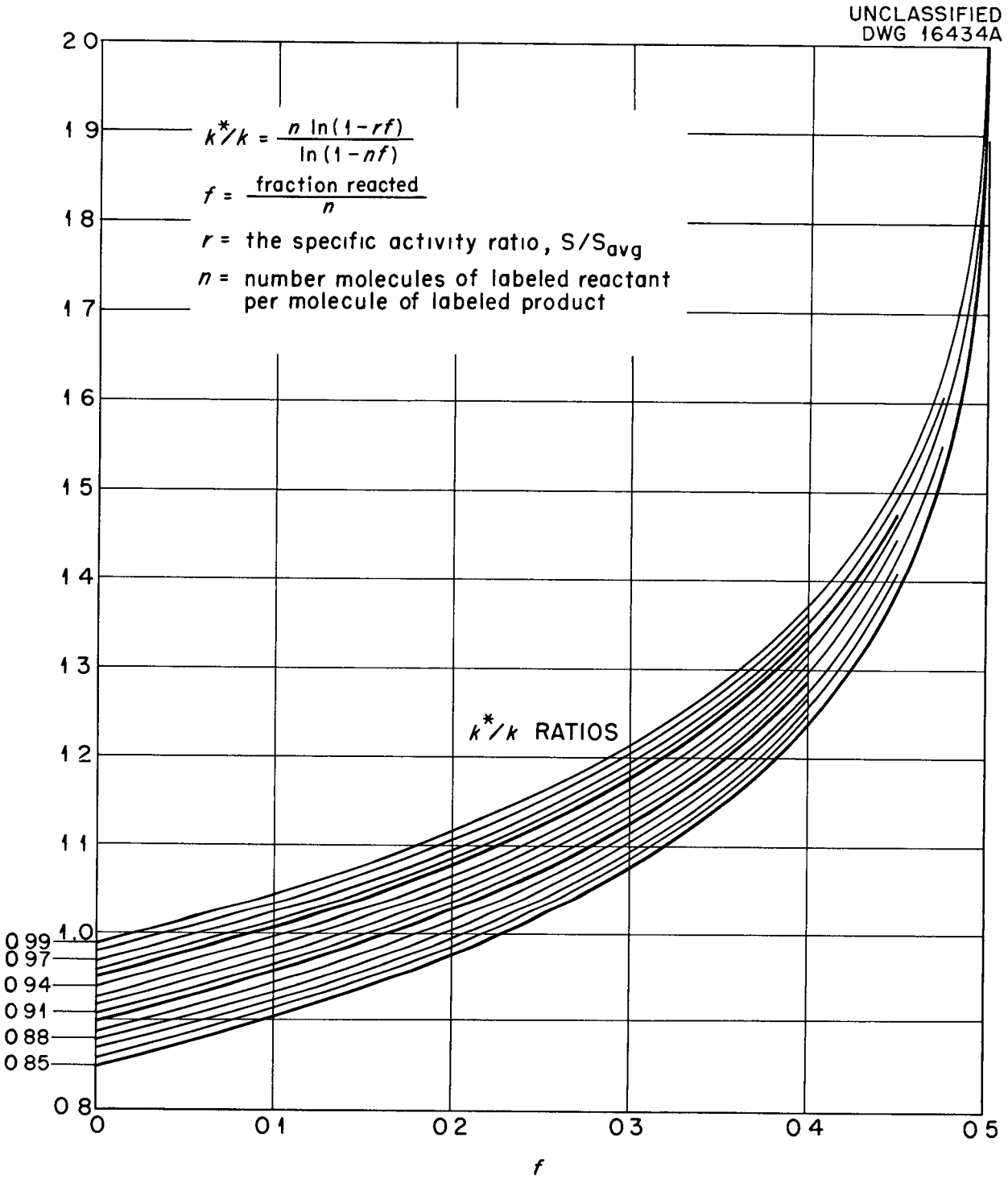

Fig. 11. Intermolecular Isotope-Effect Ratios at Various Percentages of Reaction for n = 2.

investigate the possibility of C^{14} and N^{15} isotope effects in the hydrolysis of hydrogen cyanide to ammonium formate in the presence of 5 to 7 *M* hydrochloric acid.[7]

STUDIES OF SOLUTION SCINTILLATION COUNTING OF RADIOISOTOPIC ORGANIC COMPOUNDS

G. A. Ropp J. Davidson[8]

A special instrument has been constructed, using a terphenyl scintillator,[9] to radioassay C^{14}-labeled, S^{35}-labeled, or other labeled organic compounds in solution in organic solvents. In the instrument, a standard solution and the sample solution are alternately moved into position before a photoelectric cell for a series of equal time intervals. The photoelectric cell is liquid-nitrogen cooled to reduce instrument noise. The radioactivity of the sample solution is indicated relative to the standard solution so that errors caused by instrument drift, etc. are eliminated. The instrument records the total counts for the standard solution and the total counts for the sample solution on two registers. It is hoped that this type of scintillation counter will give as precise assay data for some tracer studies as the more laborious procedures now in use, which require combustion of the organic compound. Figure 12 is a diagram of the instrument.

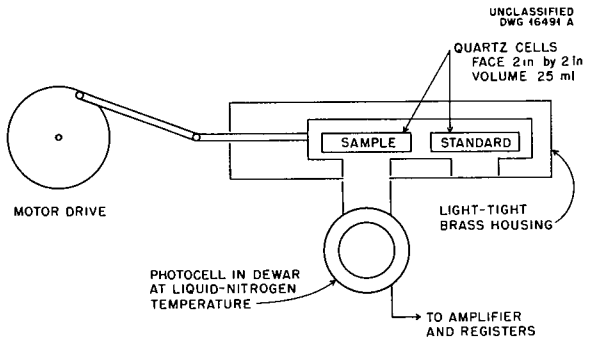

Fig. 12. Instrument for Use in Scintillation Counting of Organic Compounds in Solution.

ORGANIC REACTION MECHANISM STUDIES

Wagner Rearrangement of 7-Phenylacenaphthenol-8-C^{14} (W. A. Bonner, C. J. Collins). In the present problem, consideration is given to the stereochemical aspects of the Wagner rearrangement. The approach is designed to offer possibilities for establishing the existence or nonexistence of stereospecificity in hydrogen migration during such reactions. The compound, 7-phenylacenaphthenol-8-C^{14}, selected for the rearrangement study exists in isomeric *cis*- (I_c) and *trans*- (I_t) forms. The synthesis of both isomers was proposed in order to study any differences in the course of their migration rearrangements during dehydration to 7-phenylacenaphthylene (II).

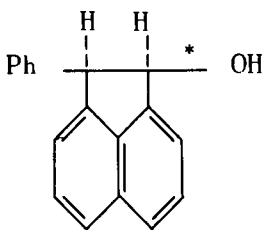

I_c

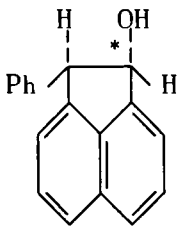

I_t

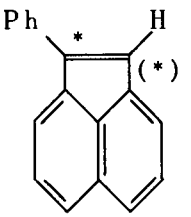

II

(7) V. K. Krieble and J. G. McNally, *J. Am. Chem. Soc.* **51**, 3368 (1929).

(8) Instrument Department.

(9) M. S. Raben and N. Bloembergen, *Science* **114**, 363 (1951).

The extent of migration during the dehydration of (I_c) and (I_t) can be established by a determination of the distribution of radioactivity in the product (II) by degradation. Two extreme cases illustrate the degradative sequence and the principles involved.

1. Assume (I) dehydrates to produce (II) without rearrangement. In this case the 8-benzoyl-1-naphthoic acid (III), produced on oxidation of (II), will have its radioactivity exclusively in the carboxyl group. Assay of the 1-benzoylnaphthalene (IV) and barium carbonate (V), obtained on decarboxylation of (III), will show no radioactivity in (IV) and 100% radioactivity in (V).

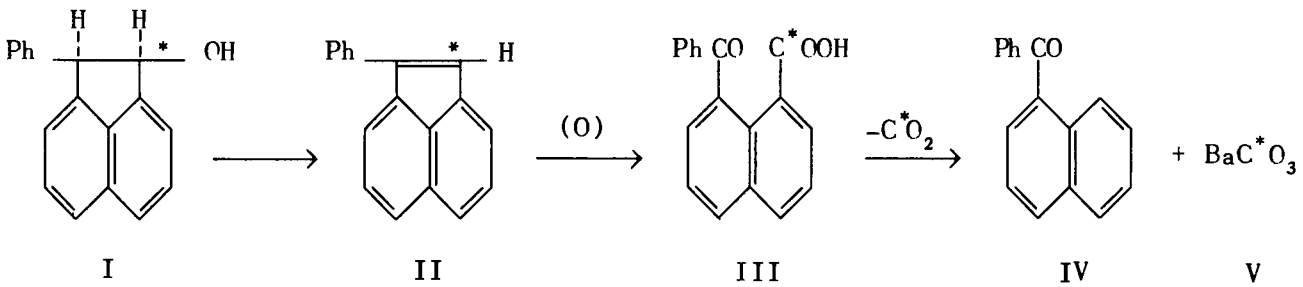

2. Assume (I) dehydrates with complete rearrangement. In this case radioactivity would be found in the degradation product (IV), but not in (V). Obviously, the extent of partial rearrangement in the transformation (I) ⟶ (II) may be established by determination of the distribution of radioactivity between the degradation products (IV) and (V).

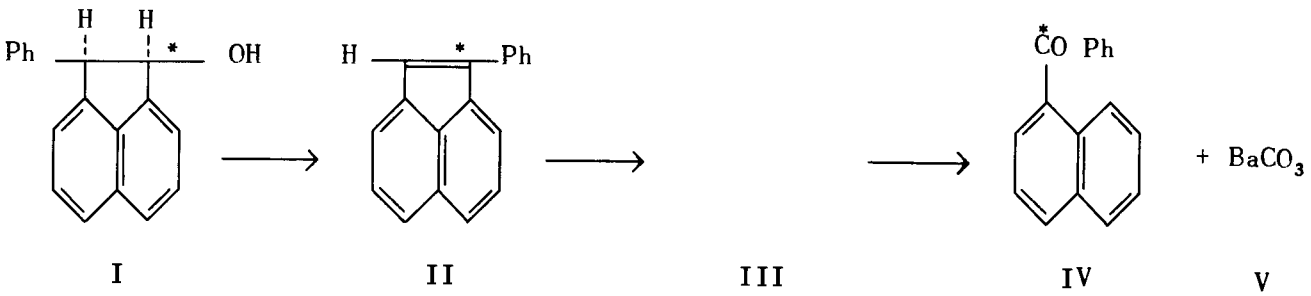

The 7-phenylacenaphthenol-8-C^{14} (I) was produced from 1-benzoylnaphthalene. The 1-benzoylnaphthalene was prepared by the Perrier modification of the Friedel-Crafts benzoylation of naphthalene according to the procedure of L. F. Fieser,[10] and (VI) could be oxidized conveniently and in good yield to 8-benzoyl-1-naphthoic-1-C^{14} acid (III) by aqueous potassium permanganate at room temperature.

Oxidation of 7-Phenylacenaphthenone-8-C^{14} (VI) Oxidation of (VI) (2.322 μc/mmole) with 12% excess permanganate in dilute acetone gave a 94% yield of the acid (III) of specific activity 2.341 μc/mmole.

Oxidation of 7-Phenylacenaphthenol-8-C^{14} (I) Oxidation of (I) (2.320 μc/mmole) with 12% excess permanganate in dilute acetone gave a 96% yield of the acid (III) with a specific activity of 2.234 μc/mmole. The latter assay is singificantly lower than that of the starting carbinol. After eliminating various technical causes for such a low assay, it was concluded that the

(10) L F Fieser, *Experiments in Organic Chemistry*, p 192, Heath and Co New York, 1941

discrepancy was due to an isotope effect prevailing during the oxidation of (I). This is discussed in detail in the following.

Decarboxylation of 8-Benzoyl-1-naphthoic-1-C^{14} Acid (III). The acid (III), of specific activity of 2.234 μc/mmole, was decarboxylated by refluxing in quinoline that contained a small quantity of copper chromite. The carbon dioxide was continuously swept into barium carbonate (V) with helium. The quinoline residue was processed to give a quantitative yield of 1-benzoylnaphthalene (IV). Assay showed the (IV) to be nonradioactive and the (V) to have a specific activity of 2.128 μc/mmole. This figure was low because of unavoidable contamination. These results establish the isotopic structures of the carbinol (I) and ketone (VI) and indicate the C^{14} to be exclusively in the 8-position in these molecules.

Isotope Effect in Carbinol Oxidations The anomalously low assay of the 8-benzoyl-1-naphthoic-1-C^{14} acid (III), resulting on oxidation of the carbinol (I), suggested the presence of an isotope effect during oxidation. Accordingly, experiments were undertaken to establish the presence or absence of such an isotope effect. The approach in these experiments was to conduct the oxidation with varying molar ratios of carbinol to oxidant (permanganate) and to examine the unoxidized carbinol and/or oxidation product, acid (III), as the basis of their comparative radioactive assays. The results are summarized in Table 10.

It is seen that the less oxidant employed (the less complete the oxidation), the lower the oxidation product assay. Similarly, the unoxidized carbinol is found to have a higher assay than the starting carbinol. These results establish an isotope effect during the oxidation of the carbinol (I) such that the $C^{12}HOH$ group oxidizes more readily than the $C^{14}HOH$ group. The isotope effect is characteristic of the oxidation, carbinol (I) $\longrightarrow$ ketone (VI), rather than the subsequent oxidation, ketone (VI) $\longrightarrow$ acid (III). This was shown by the assay of the acid (III), obtained on oxidation of ketone (VI), being identical with the assay of the ketone (VI), regardless of the quantity of oxidant employed.

Preliminary Wagner Rearrangement Experiments The Wagner rearrangement has received preliminary investigation. The action of P_2O_5 in xylene or benzene results in the immediate production of the olefin (II), as evidenced by formation of the known picrate of (II) by action of picric acid on the crude reaction mixture. In addition to (II), however, a higher melting substance appears to be formed that is also capable of picrate formation. This high-melting product may possibly be a polymerization product of (II).

TABLE 10. ISOTOPE EFFECT DURING OXIDATION OF 7-PHENYLACENAPHTHENOL-8-C^{14}

EQUIVALENTS OF CARBINOL (I)*	EQUIVALENTS OF $KMnO_4$	ACTIVITY OF ACID (III) (μc/mmole)	ACTIVITY OF UNOXIDIZED (I) (μc/mmole)
1 00	1 00	2 238	
1 00	1 10	2 230	
1 00	0 50	2 218	2 468
1 00	0 35	2 179	2 420
1 00	2 00	2 290	

*Specific activity 2 320 μc/mmole

Wagner Rearrangement of 3-Methyl-9-fluorenyl(Carbinol-C^{14}) (C. J. Collins). The dehydration-rearrangements of 1-methyl-9-fluorenyl(carbinol-C^{14}) and of 2-phenyl-2-(*o*-tolyl)ethanol-1-C^{14} were carried out by Benjamin and Collins.[11] Since the results were unexpected, it was important to compare them with the results of the dehydration-rearrangement of 3-methyl-9-fluorenyl(carbinol-C^{14}), (VI). The synthesis and rearrangement of the latter compound to labeled 3-methylphenanthrene have now been accomplished by experimental methods analogous to those described for the synthesis of phenanthrene-9-C^{14}.[12] The 3-methylphenanthrene-9, 10-C^{14} (VI) has been subjected to chemical degradation as indicated in the reaction series (VII) ⟶ (XI), inclusive. Radiochemical assays, as microcuries per millimole, for compounds (VIII)(6.580), (X)(6.714), and (XI)(1.771) are taken as evidence that the *p*-tolyl moiety of compound (VI) has migrated in preference to the phenyl moiety in the ratio of 73 27, thus demonstrating quantitatively the electrical effect of the 3-methyl group in the fluorene nucleus.

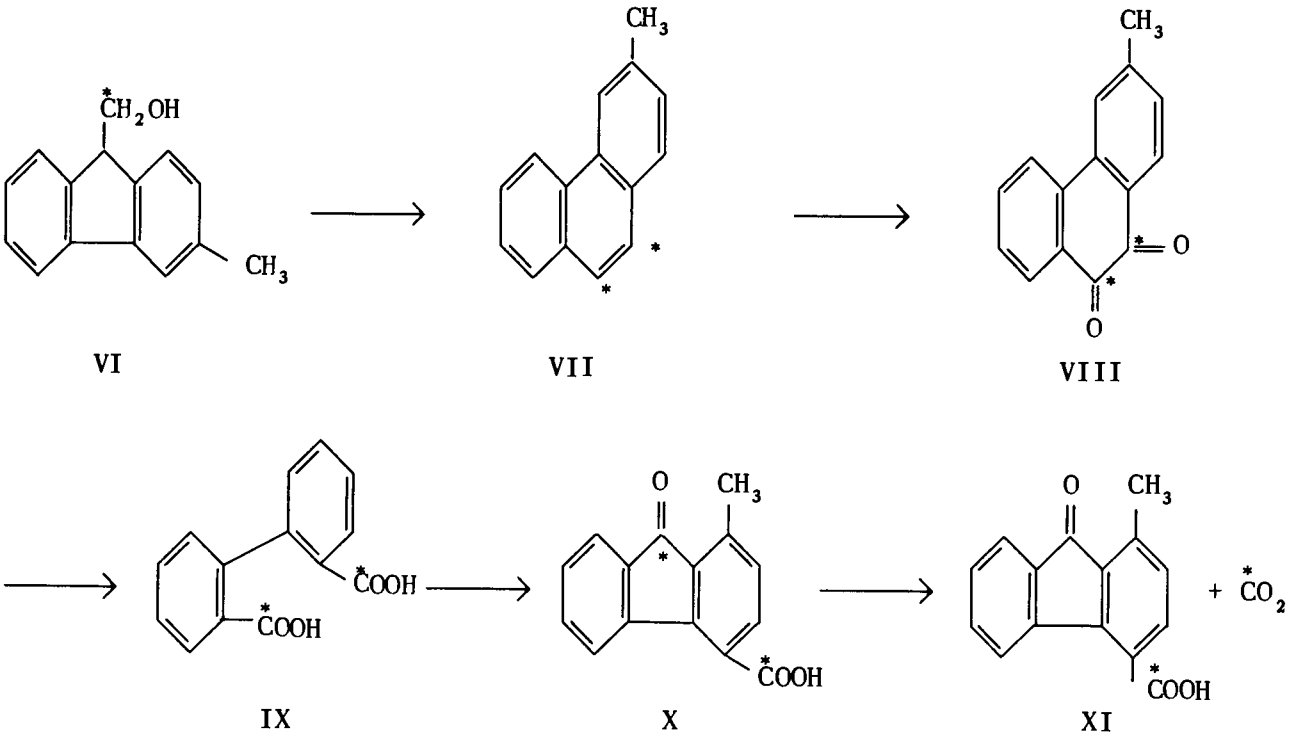

Thermal Rearrangement of Amine Nitrites (P. S. Bailey, J. G. Burr, Jr.). In a continuation of work reported previously,[13] the effect of several different variations of environment on the rate of decomposition of 2-phenyl-2-(*p*-tolyl)ethyl-1-C^{14} ammonium nitrite has been investigated. The effect on the migration ratio thus obtained has also been studied. The results are shown in Table 11.

(11) B M Benjamin and C J Collins, *op cit*, ORNL-1260, p 57

(12) C J Collins, *J Am Chem Soc* **70**, 2418 (1948)

(13) J G Burr, Jr and P S Bailey, Atlantic City Meeting of the American Chemical Society, September 14-19, 1952, *Abstracts of Papers*, p 39M, *Chem Quar Prog Rep June 30, 1952* (in press)

As can be seen from the experiments in A, B, and C, the migration ratios observed are not altered by excess nitrite ion or by the presence of hydrogen ion. The rates are similarly unaltered (the rate was not measured exactly in experiment C, but was roughly similar to the rates in experiments A and B). Parallel studies have been carried out upon 2-phenyl-2-(3,4-dimethylphenyl-1)ethyl-1-C^{14} ammonium nitrite (obtained as a crystalline salt, melting at 124°C, by the reaction of the corresponding amine hydrochloride with sodium nitrite solution). Rates were not measured upon this substance because the rate of decomposition at 70 to 100°C was inconveniently slow. Above 100°C, some alternate path of decomposition supervenes since the evolution of brown nitrous fumes was observed. The data obtained, with respect to migration ratios, are shown in Table 12. Again, the observed migration ratio is quite independent of the acidity of the medium.

TABLE 11. EFFECT OF EXPERIMENTAL CONDITIONS ON RATE OF DECOMPOSITION AND MIGRATION RATIO IN (*p*-TOLYL)ETHYL-1-C^{14} AMMONIUM NITRITE

EXPERIMENT	CONDITIONS	*k*	*p*-TOLYL MIGRATION (%)
A	Amine-nitrite in water at 70°C	0.0135	48
B	Amine-nitrite, 1 mole excess $NaNO_2$ in water at 70°C	0.0191	48
C	Amine-HCl, 1 mole $NaNO_2$ in 0.5 *N* HCl		48
D	Amine-HCl in water preheated to 70°C, then 1 mole $NaNO_2$ added	0 0948	56
E	Same as C, except amine-HCl solution preheated to 95°C		53

TABLE 12. EFFECT OF EXPERIMENTAL CONDITIONS ON MIGRATION IN 2-PHENYL-2-(3,4-DIMETHYL-1)ETHYL-1-C^{14} AMMONIUM NITRITE

CONDITIONS	DIMETHYLPHENYL MIGRATION (%)
Amine-hydrochloride and excess $NaNO_2$ in water at 95°C	49*
Amine-nitrite with 1 equivalent of 0.5 *N* HCl at 95°C	47**
Amine-nitrite and excess 1 0 *N* HCl at 95°C	49***

*Dimethylphenyl migration observed in the acid-catalyzed rearrangement of the correspondingly substituted ethanol-1-C^{14} was 66%.

**Reaction accompanied by a rapid evolution of nitrogen

***Evolution of nitrogen very slow.

CHEMISTRY OF SEPARATION PROCESSES

ORGANIC CHEMISTRY OF SOLVENTS

W. H. Baldwin C. E. Higgins

Determination of Equivalent Weight of Salts. The work reported earlier[1] has been extended by the use of anion-exchange resin. Weighed amounts (about 1 meq) of inorganic and organic salts were dissolved in water and passed through 5 meq of Dowex-1 in the hydroxide form. The basic effluent was collected in standard HCl and the amount determined by back titration with standard NaOH. The equivalent weights obtained are up to 4% high unless they are obtained empirically by first running a known such as potassium acid phthalate, in which case close agreement with theoretical is found (usually within 1%).

Preparation of Labeled Di-*n*-Butyl Phosphate-P^{32} For certain solubility tests, di-*n*-butyl phosphate-P^{32} (DBP*) was prepared with an 85% yield by the reaction of 2 8 mmole of dry sodium acetate with 20% excess tri-*n*-butyl phosphate-P^{32} at 200°C.[2]

Solubility of Sodium Di-*n*-Butyl Phosphate (NaDBP*) in Carbon Tetrachloride and Amsco 123-15. Since the method for purifying TBP involves the use of NaOH to wash out acids, it was of interest to determine the solubility of the sodium salt of DBP in CCl_4 and Amsco 123-15. From 0.3 *M* NaDBP* solutions, 0.1 and 1 *M* in NaOH, equal volumes of CCl_4 extracted 0.001% of the NaDBP*. Equal volumes of CCl_4 and Amsco 123-15 extracted less than 0.01% NaDBP* from 0.04 *M* NaDBP* that was 0.1, 1, and 3 *M* in NaOH.

Third-Phase Formation by 5.0 *M* NaOH. In the solubility tests at 5 *M* NaOH and 0.05 *M* NaDBP*, a third phase formed that contained on the order of 80% of the NaDBP*. The third phase also formed when other solvents including dibutyl ether, benzene, hexane, hexone, nitrobenzene, and aniline were employed, but not in the case of 2-ethyl butyl alcohol. The amount of NaDBP* present had a pronounced effect on the amount of third phase formed and the per cent of NaDBP* going into the third phase. At 0.20 *M* DBP* in dibutyl ether, 95% of the DBP* went into the third phase, compared with 83, 41, and 4% from 0.05, 0.01, and 0.003 *M* DBP* concentrations, respectively. Increasing the concentration of DBP up to 1.0 *M* caused no third phase formation when 1.0 *M* NaOH was used.

Preparation of Phosphorus-32 Labeled $POCl_3$. Phosphorus-32 labeled $POCl_3$ has been prepared from $H_3P^{32}O_4$ by the action of phosgene on ferric phosphate[3] and by the reaction of Geuther[4,5,6]

$$H_3P^*O_4 + 3PCl_5 \longrightarrow 4P^*OCl_3 + 3HCl \ .$$

The reaction of Geuther has proved to be satisfactory for synthetic work in this laboratory.

Preparation of Di(2-ethyl hexyl)-Phosphinic Acid-P^{32}. The methods developed by Whaley[7] were modified for small-scale (15 mmoles) synthesis in which 1 molar equivalent of $P^{32}OCl_3$ and 1 molar equivalent of pyridine were reacted with 2 molar equivalents of

(1) W H Baldwin and C E Higgins, *Chem Quar Prog Rep March 31, 1952*, ORNL-1285, p 57

(2) W H Baldwin and C E Higgins, *The Preparation of Tri-n-Butyl Phosphate P^{32}*, ORNL-887, Feb 5, 1951, also *J Am Chem Soc* **74**, 2431 (1952)

(3) J E Gardiner and B A Kilby, *J Chem Soc*, 1769 (1950)

(4) A Geuther, *J fur Prakt Chem* **8**, 360 (1873)

(5) O Lindberg, *Ark Kemi Mineral Geol* **23A**, No 2 (1946)

(6) B Axelrod, *J Biol Chem* **176**, 295 (1948)

(7) Private communication from W M Whaley, consultant to Materials Chemistry Division

2-ethyl hexyl magnesium bromide to give a mixture of phosphonic and phosphinic acids. For separation, the acids were converted to chlorides with thionyl chloride, fractionated under reduced pressure, and the fractions were hydrolyzed with sodium hydroxide. The isolated di(2-ethyl hexyl)phosphinic acid, $R_2P(O)OH$, was a yellow liquid with an observed neutral equivalent of 296 (calculated 290) and a specific activity of 0.12 mc/mmole.

The solubility of the acid in water is 17 mg/liter. The acid and similar preparations will be used to observe the distribution between organic solvents and aqueous solutions. The distribution data will aid in the prediction of losses in waste streams when these acids are used for the extraction of uranium from low-grade ores.

STUDY OF THE ELECTRODEPOSITION OF RUTHENIUM FROM VERY DILUTE SOLUTIONS

M. H. Lietzke J. C. Griess, Jr

The study of the deposition behavior of ruthenium at low concentrations as reported in previous Chemistry Division quarterly reports has now been finished. A completion report, ORNL-1399, describing all the experimental data and a proposed deposition mechanism is now being written

ION-EXCHANGE STUDIES

The Osmotic Free Energy of Ion Exchangers (G. E. Boyd, B A. Soldano). Further isopiestic measurements were conducted during the past quarter to estimate the magnitude of the osmotic free energy in various salt-forms of a strong-base type of anion exchanger that has a polystyrene-divinyl benzene network (Dowex-1, nominal 0.5 and 6% DVB). The experimental technique and treatment of the data were the same as described in the preceding quarterly report.[8] The moisture-uptake isotherms shown in Fig. 13 were sigmoid in shape, as were those previously given for various salt-forms of the cation exchanger (Dowex-50, nominal 8% DVB). However, the absorption at relative pressures, p/p_0, of less than 0.1 was significantly smaller with the anion exchanger. This difference may result from the structurally bound exchange group in the anion exchanger being the nonpolar $-CH_2N(CH_3)_3$ group, whereas in the cation exchanger the bound group was the polar $-SO_3M$ group. Limited swelling was shown by the anion exchangers, as expected, and the amounts of water taken up from a saturated vapor were either the same as, or

(8) G E Boyd and B A Soldano, *Chem Quar Prog Rep June 30, 1952*, ORNL-1344 (in press)

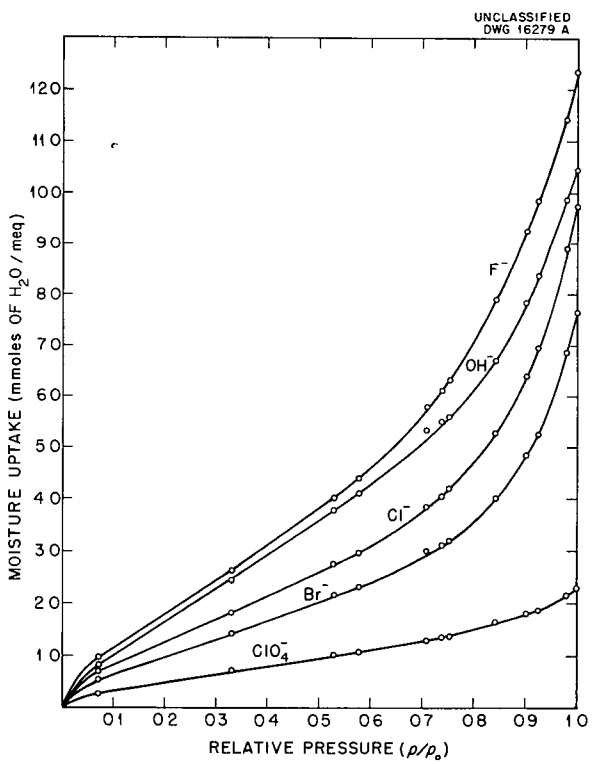

Fig. 13. Swelling-Water Isotherms for Halide Salt-Forms of Nominal 6% DVB-Dowex-1 Exchanger.

slightly greater than, for the cation exchanger. Interestingly enough, the fluoride salt imbibed more water at all relative pressures than the highly polar free-base form. The perchlorate salt seemed only weakly dissociated and showed but a very slight moisture uptake even at $p/p_0 = 1$. This behavior is consistent with the extremely high selectivity exhibited by the strong-base anion exchangers for perchlorate ions.

Pycnometric measurements of the dry and partly hydrated salt forms of the nominal 6% DVB Dowex-1 again showed that the exchanger volume was the sum of the dry volume plus the volume of water contained, as had been estimated from the per cent moisture by using unit density. Swelling pressures, π, in the variously hydrated salt-forms of the anion exchanger were computed as before and were plotted against the equivalental volume, V_e. Again (Fig. 14), a linear relation was obtained that permitted the equation of state,

$$V_e = 1.17\pi + 287 , \qquad (1)$$

to be written. For the nominal 8% DVB, Dowex-50 cation-exchanger, the equation was

$$V_e = 0.812\pi + 192 , \qquad (2)$$

from which it is seen that both the modulus of elasticity (coefficient of π) and the volume at zero pressure are larger for the more weakly cross-linked anion exchanger than for the strongly cross-linked exchanger. It is noteworthy again, as with the cation exchanger, that the swelling pressure in the anion exchanger is independent of the salt-form and depends only on the volume, that is, the pressure depends only on the extension of the hydrocarbon network of the exchanger It may be seen (Fig. 14) that the largest pressure is given by the fully hydrated fluoride salt, followed by the hydroxide, the chloride, and the bromide forms. The swelling pressure, even of the fully hydrated perchlorate salt form, was so small (<10 atm) that it was not possible to estimate it with any accuracy. A stable ion pair must be formed between the perchlorate anion and the cationic, quaternary, ammonium-exchange group.

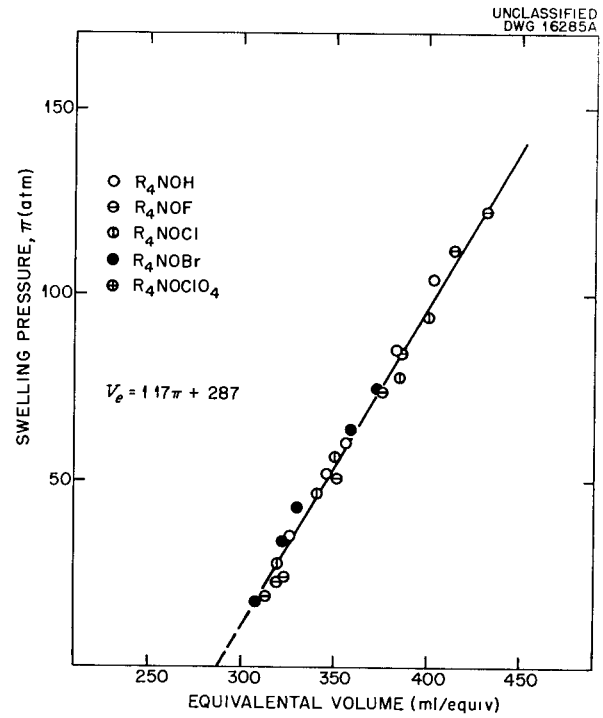

Fig. 14. Variation of Swelling Pressure with External Exchanger Volume for Several Salt-Forms of Nominal 6% DVB-Dowex-1 Exchanger.

It will be of interest in the future to extend the experiments to exchangers of widely differing cross-linking in order to determine whether a reduced equation of state of the form

$$\frac{V_e - V_0}{V_0} = K\pi$$

will hold, where K is the coefficient of expansivity (bulk modulus) and is possibly independent of cross-linking and V_0 is the zero pressure volume. An examination of the theories of

cross-linked polyelectrolytes will also be of interest to determine whether any of them will predict a linear equation of state.

Electrochemical Properties of Ion Exchange Materials (B. A. Soldano, G. E. Boyd). Radiation damage studies were continued on several cation- and anion-exchange membrane materials. In the more recent experiments, however, a pure gamma-ray source (1000-curie Co^{60} giving approximately 12,000 r/min at the sample position) was employed. Changes in ion-exchange capacity, swelling with addition of water, electric conductivity, and "counter-ion" transport number were measured as a function of radiation dose by means of the techniques described in the preceding quarterly report. Figure 15 compares the percentage changes in capacity for three different anion-exchange membranes with that for a cation exchanger. The anion-exchange membranes were in their chloride salt forms and the cation-exchanger was in the hydrogen form. Clearly, the cation-permeable membrane, which is a heterogeneous type that consists of pulverized exchanger bonded with a plastic, was considerably more stable to radiation than any of the anion membranes. Interestingly, the homogeneous-gel weak-base anion membrane, ARX-44, and the heterogeneous, strong-base, Rohm and Haas product A showed about the same stability towards gamma rays, whereas the homogeneous, strong-base, ARX-102 seemed notably more stable. With the heterogeneous membranes, it was not clear whether the capacity loss resulted from a true breaking away of the exchange groups from the exchanger network or whether the gamma radiation altered the plastic binder and permitted a mechanical loss of exchanger particles from the matrix.

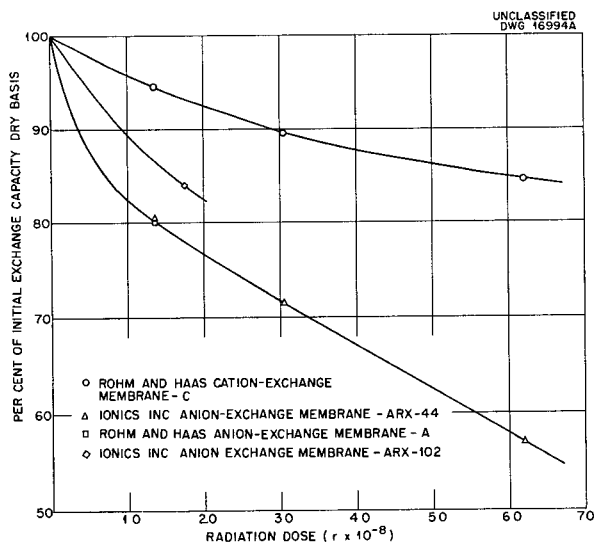

Fig. 15. Effect of Co^{60} Gamma Rays on Exchange Capacity of Ion-Exchange Membranes.

In addition to exchange capacity losses, measurements of the swelling-water uptake suggest that an alteration in the polymeric network may also occur. Although the capacity decreased with exposure to gamma rays, there was always an increase in the amount of water per equivalent of capacity (Fig. 16). There seemed, however, to be a tendency toward a constant water content after prolonged exposure. The exact cause for the moisture pickup is not entirely clear because the membranes were either backed with a foreign material or were heterogeneous. It is possible that the gamma radiation had one of two effects either it caused the ion-exchange portions to shrink, thereby pulling away from the supporting plastic or glass and producing microscopic cracks that readily filled with water, or the cross links in the exchanger were broken to an extent greater than the capacity loss, so that an increased swelling of the gel occurred. However, as far as gross effects are concerned, the homogeneous anion-exchanger material, ARX-44, was the least stable, whereas the heterogeneous cation and anion membranes (Rohm and Haas products C and A) showed almost the same, as well as the smallest, moisture increase.

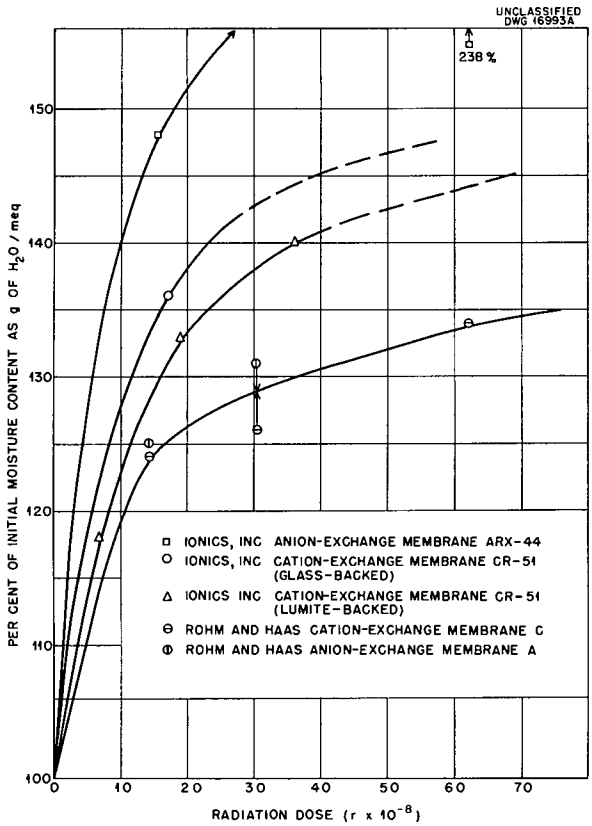

Fig. 16. Effect of Co^{60} Gamma Rays on the Moisture Content of Ion-Exchange Membranes.

There are not sufficient data to be sure that a true stability difference exists between the glass and Lumite-backed CR-51 membrane.

A summary of the changes induced in the electrical conductances by gamma radiations on the homogeneous or coherent cation membranes is given in Table 13, in the coherent anion membranes in Table 14, and in the heterogeneous cation and anion membranes in Table 15. With all membranes but two, the specific conductance decreased with increased radiation dose. The slight conductivity maximum observed with the one Lumite-backed cation membrane may be a consequence of radiation effects on the Lumite, because the glass-backed CR-51 showed no such effect. It may be concluded that moderate gamma-radiation dosages cause only small electric-conductance changes in the coherent cation and anion membranes. With the heterogeneous membranes, however, the conductance changes were much greater, with the cation membrane there was a 50% decrease, whereas the anion membrane showed a nearly tenfold

TABLE 13. EFFECTS OF Co^{60} GAMMA RAYS ON COHERENT TYPE OF CATION-EXCHANGE MEMBRANES*

RADIATION DOSE (r x 10^{-8})	EXCHANGE CAPACITY (meq/g of dry membrane)	MOISTURE (g of H_2O/g of dry membrane)	SPECIFIC CONDUCTIVITY** (ohm^{-1} cm^{-1} x 10^3)	MEMBRANE THICKNESS (mm)
Ionics CR-51, Lumite-backed				
0	1 67	0 534	9 94	0 9195
0 673	1 67	0 629	11 5	0 9855
1 885	1.62 (?)	0 710	11 0	0 990
3 61	1 24	0 748	9 92	1 003
Ionics CR-51, Glass-backed				
0	1 79	0 602	11 2	0 978
1 726	1 34	0 820	10 9	0 612
Ionics Modified CR-51, Lumite-backed				
0	2 14	0 409	7 77	1 186
1 726	1 89	0 444	7.30	1 036

*Strong-acid, sodium-form

**Specific conductivities not corrected for resistance of inert backing

decrease (Table 15). It is of incidental interest to note (Tables 13 and 14) that the cation body showed a smaller capacity than the anion exchanger but had a large initial moisture equivalent. This suggests that the anion exchanger may be somewhat more cross-linked. Initially, the apparent capacities and equivalental moisture contents of the heterogeneous cation and anion membranes (Table 15) were nearly the same. This, combined with the fact that the true capacity of the anion exchange material is smaller than the cation material, suggests the ratio of exchanger to plastic binder was larger in the cation exchanger. In the one case where a direct comparison between the conductivities for the homogeneous

TABLE 14. EFFECTS OF Co^{60} GAMMA RAYS ON COHERENT TYPE OF ANION-EXCHANGE MEMBRANES*

RADIATION DOSE ($r \times 10^{-8}$)	EXCHANGE CAPACITY (meq/g of dry membrane)	MOISTURE (g of H_2O/g of dry membrane)	SPECIFIC CONDUCTIVITY** (ohm^{-1} $cm^{-1} \times 10^3$)	MEMBRANE THICKNESS (mm)
Weak-base, Ionics ARX-44, Lumite-backed				
0	2 48	0 258	6 90	0 556
1.363	2 00	0 442	7 82	0 709
3 05			7 54	0.625
6.2	1 40	0 708	5 92	0.599
Strong-base, Ionics ARX-102, Glass-backed				
0	3 75	0 250	15 88	0 577
1 726	3 15	0 229	9 04	0 529

*Chloride-form.

**Specific conductivity not corrected for resistance of inert backing

TABLE 15. EFFECTS OF Co^{60} GAMMA RAYS ON HETEROGENEOUS TYPE OF ION-EXCHANGE MEMBRANES

RADIATION DOSE ($r \times 10^{-8}$)	EXCHANGE CAPACITY (meq/g of dry membrane)	MOISTURE (g of H_2O/g of dry membrane)	SPECIFIC CONDUCTIVITY (ohm^{-1} $cm^{-1} \times 10^3$)	MEMBRANE THICKNESS (mm)
Rohm and Haas product C strong-acid cation exchanger, hydrogen form				
0	3 05	$0\ 236_5$	13 1	0 660
1 363	2 88	0 296	12 6	0.696
3.05	2 73	$0\ 298_8$	$11\ 4_5$	0 683
6 20	2.58	0 317	7 86	0.683
Rohm and Haas product A strong-base anion exchanger, chloride form				
0	2 34	0 235	1 53	0 710
1.36_3	1 88	0 293	0 87	0 706
3 05	1 77	0 313	$0\ 67_6$	$0\ 689_6$
6 20			0 168 (?)	$0\ 680_7$

and heterogeneous materials can be made (Ionics ARX-102 with Rohm and Haas product A), it can be seen that the cation exchanger possessed a specific conductance about ten times greater than that of the ion exchanger.

In addition to conductance, permselectivity is an electrochemical property that is of importance to membrane performance. A quantitative measure of this property is afforded by cell emf measurements in which the membrane separates two solutions of the same salt at different concentrations. As outlined in the previous quarterly report, the cation transference number, t_+, for a cation exchanger is given by

$$t_+ = \frac{E}{E_0},$$

where E is the measured cell potential and E_0 the ideal potential given by

$$E_0 = \frac{2RT}{F} \ln \frac{a_I}{a_{II}}.$$

With anion exchange membranes, the formula is

$$t_- = \frac{E}{2E_0} + 0.5.$$

Measurements of the dependence of the anionic, t_{Cl^-}, transference number in an anion-exchange membrane on the external concentration of NaCl and on the gamma radiation dosage are summarized in Table 16. As with the cation exchanger, the "counter-ion" transference number (Na^+ with Cr-51 and Cl^- with Rohm and Haas product A) decreases with increasing external concentration (first row, Table 16). Further, for a fixed external concentration, t_{Cl^-} falls with increased exposure of the anion-permeable membrane to Co^{60} gamma rays, except at the lowest concentration, where a slight increase was observed. A decrease in permselectivity is to be expected because of the capacity loss occasioned by the irradiations. Also, any breaking of cross-links in the polymer network of the exchanger would cause a lowered permselectivity because of increased swelling. In view of these factors and the observed (Table 15) large decreases in specific conductivity with radiation dose, the slight, although apparently real, increased permselectivity observed at the lowest external concentrations is all the more unexpected.

The effects of increasing amounts of gamma radiation on both cation- and anion-exchange membranes may be summarized (1) the exchange capacity per unit weight of dry membrane uniformly decreases, (2) the moisture content uniformly increases, (3) the electric conductivity either remains almost constant (coherent membranes) or decreases markedly (heterogeneous membranes), (4) the permselectivity decreases only slightly, such decrease

TABLE 16. EFFECT OF Co^{60} GAMMA RAYS ON PERMSELECTIVITY OF STRONG-BASE, HETEROGENEOUS TYPE OF ANION-EXCHANGE MEMBRANE*

RADIATION DOSE (r x 10^{-8})	EXCHANGE CAPACITY (meq/g of dry membrane)	CHLORIDE-ION TRANSFERENCE NUMBER, t_-		
		1/128 to 1/64 *N*	1/8 to 1/4 *N*	1 to 2 *N*
0	2 34	0 965	0 958	0 790
1 36	1 88	0 965	0 954	0 790
3 05	1 77	0 973	0 947	0 766
6 20		0 981	0.919	0 731

*Rohm and Haas product A, chloride form

appears to be an insensitive function of membrane damage. For practical applications, electric conductivity is of greatest importance because of electric power consumption and membrane-heating considerations. Both the absolute magnitude and changes in the conductance need to be considered, particularly if high current density operations are to be conducted.

Self-Diffusion of Sodium Ion in Linear Sodium Polystyrenesulfonate Solutions (B. A. Soldano, G. E. Boyd, J. W. Cobble). In the earlier extensive work on ionic self-diffusion in variously cross-linked cation and anion exchangers, it was observed that the self-diffusion coefficients uniformly increased with decreasing polymer network cross-linking. It was not possible, because of the limitations in the technique employed, to obtain numerical values for polystyrene exchangers cross-linked with less than 1% divinylbenzene. Nevertheless, it was of interest to determine whether the self-diffusion coefficients would continue to increase as the polyelectrolyte became more dilute and whether they would finally tend toward values characteristic of ordinary strong, 1 1, electrolytes.

Accordingly, the apparent self-diffusion of sodium ion in aqueous solutions of sodium polystyrenesulfonate of varying concentrations was measured by using a sintered-glass-diaphragm diffusion cell (Northrup-McBain) and 2.6 y Na^{22} as the radiotracer. Linear polyelectrolyte solutions of the same concentration were placed in both cell compartments, one solution was marked with a trace of radiosodium, and then observations were made on the rate of appearance of radioactivity in the compartment containing the initially inactive solution. Diffusion coefficients were computed from

$$D = \frac{1}{Kt} \log \frac{C_1 + \frac{V_2}{V_1} C_2}{C_1 - C_2},$$

where C_1 = activity per unit volume in compartment No. 1, C_2 = activity per unit volume in compartment No. 2, V_2/V_1 is the ratio of volumes in the compartments, K = cell constant, and t is the time of diffusion in seconds. Apparent self-diffusion coefficients observed for three concentrations of sodium polystyrenesulfonate are presented in Table 17.

TABLE 17. SELF-DIFFUSION OF Na^{22} ION IN AQUEOUS SODIUM POLYSTYRENE SULFONATE SOLUTIONS AT 25°C

CONCENTRATIONS (eq/l × 10^4)	$D \times 10^5$ (cm^2/sec)
6.3	1.45 (?)
31.4	0.93
157.0	0.75

Except for the value at the lowest concentration, the self-diffusion coefficients with the linear polyelectrolyte are roughly one-half of those for NaCl solutions of the same concentrations. On the other hand, the value for the sodium polystyrenesulfonate at the highest concentration is slightly less than twice that reported[9] for sodium polyacyrlate at almost the same normality. The unexpectedly large value for the self-diffusion at concentrations of less than 10^{-3} N may be a consequence of surface diffusion effects that occur in the capillaries of the sintered-glass diaphragm of the diffusion cell. Further work, both in the more dilute ranges and in the concentration ranges that overlap those found with the cation exchangers, will be conducted. A correction of the diffusion data for the sodium polystyrenesulfonate solutions for viscosity effects will tend to bring the values in Table 17 somewhat closer to those for sodium chloride. In the work at extreme

[9] J R Huizenga, P F Grieger, and F T Wall, *J Am Chem Soc* **72**, 4228 (1950)

dilution, great care must be exercised to avoid contaminating the polyelectrolyte solution with ordinary sodium salts, such as NaCl

Donnan Partition Coefficients at Low External Electrolyte Concentrations (B. A. Soldano, G. E. Boyd). It is generally recognized that when an ion exchanger is immersed in an aqueous electrolyte solution, a small amount of the solution penetrates the gel phase of the ion exchanger and there is a definite partition of electrolyte between the exchanger and external solution at equilibrium. In addition, the concentration of electrolyte in the more highly cross-linked exchangers is always less than that in the external aqueous phase. Such behavior is in qualitative agreement with the hypothesis that a Gibbs-Donnan equilibrium exists. The thermodynamic theory for the equilibrium further requires that as the outside electrolyte concentration decreases, the Donnan partition coefficient, defined by $\lambda = (MX)_r/(MX)_w$, also decrease and become vanishingly small as the external concentration approaches zero. This necessary behavior is observed[10] experimentally, except at the lowest external concentrations. The molality at which appreciable deviations from the theory occur varies with the exchanger cross-linking. For a nominal 8% divinylbenzene cross-linked cation exchanger (Dowex-50 type), λ becomes constant for concentrations below 1 *N*, whereas with a 1% product, λ becomes constant below 0.1 *N*. Some investigators have considered this phenomenon to be a real effect, λ has even been reported to increase and thus have cast doubt on the whole concept of a membrane equilibrium. Other investigators have stated that the deviations from theory probably result from inadequate experimental procedures used in evaluating λ. One item that gives considerable difficulty is the efficient removal of all the external solution from the surface of the exchanger. With dilute external solutions, even a very thin film of solution adhering to the exchanger may be sufficient to introduce appreciable error

To further study and perhaps resolve this crucial issue, an alternative method that does not involve a liquid-phase separation was used to establish the equilibrium A volatile electrolyte solute (HBr) was used, and an attempt was made to establish the Donnan partition of this species through the vapor phase. A conventional isopiestic technique was employed when hydrogen-form cation exchanger (8% DVB Dowex-50) was equilibrated with aqueous HBr solutions containing radiobromide (36 h Br^{82}). In one experiment, a 0.406 *N* HBr solution was allowed to come to isopiestic equilibrium with the initially bromide-free cation exchanger for a period of two weeks, after which the uptake of bromide activity was measured. A λ value of only 3.45×10^{-5} was observed. Since this magnitude was unexpectedly small, a second experiment was performed by using a 5 *N* HBr solution. The value of λ in this instance was 1.29×10^{-3}, which is far below the directly determined value of 0.15 obtained by using the older technique. Since longer times of vapor equilibration did not appreciably increase the uptake of HBr by the exchanger, it was concluded that the rate of attainment of isopiestic equilibrium with a solute species, such as HBr, was far too slow to permit an evaluation of Donnan partition coefficients This behavior is in contrast to the rapid attainment of isopiestic equilibrium observed in the transfer of solvent (H_2O) molecules between electrolyte solutions and ion exchangers Further efforts to evaluate λ in the low external concentration range will be conducted through the use of ion exchangers of small surface-to-volume ratio

(10) G E Boyd and Q V Larson, *Chem Quar Prog Rep Dec 31, 1951*, ORNL-1260, p 74, Fig 17

CHEMICAL PHYSICS

RADIO-FREQUENCY SPECTROSCOPY

R. Livingston H. Zeldes
B. Benjamin

Iodine Problem Work has continued on the microwave study of methyl iodide for determining the nuclear moments of I^{131}. A Stark modulation spectrometer was installed by J. T. Cox, a graduate student from Duke University, in order to determine whether the improved operation at higher gas pressures would eliminate the need for preparing high-purity methyl iodide. A test experiment was conducted with I^{129}, and the results indicated that additional chemical purification will be needed. Only a few of the stronger CH_3I^{129} lines were seen, and rapid exchange with CH_3I^{127} that was adsorbed on the walls of the Stark cell limited the working time to a few hours. The original video spectrometer will be installed again, and the approach will center on additional chemical work. Operations in the hot laboratory were temporarily suspended because of a serious contamination problem from an adjoining room. Cox has returned to Duke University, and the video spectrometer will be installed after additional chemical work has been completed.

The main chemical problem has been to synthesize a pure iodide starting material from several micrograms of I^{131}. A solvent-extraction process, in which the iodine is extracted into CCl_4 and back-extracted into dilute hydrazine hydrate solution, has been investigated. Tests have shown that there is some reaction of the CCl_4 with the hydrazine, which contributes greatly to the weight of the final product. A search is under way for a suitable extracting liquid. Benzene has also proved unsatisfactory, and present tests are being conducted on cyclohexane.

Quadrupole Spectroscopy The Cl^{35} line width and frequency have been studied as a function of temperature in solid ethylene dichloride. The new cryostat and chart recording equipment were used. This substance shows a lambda point in the specific heat curve at about -100°C, and proton resonance studies[1] indicated that the transition is associated with motions of the hydrogen in the lattice. Subsequent crystallographic data[2] indicated that, indeed, the carbon atoms were disordered above the transition temperature, whereas the chlorine atoms remained in fixed lattice positions. From the model presented, considerable motion of the C-Cl bond would be expected in warming through the lambda point, and this might cause a noticeable drop in the quadrupole coupling because of the averaging of the field gradient tensor over the motion. The line width undergoes a very pronounced broadening in the region near -175°C and continues to broaden so rapidly on warming that it is soon lost. For this reason, it has not been possible to observe the line up to the temperature of the lambda point. The data are summarized in Table 18. The width is the full width between flexes on the absorption curve, which was recorded as a second derivative.

The change of frequency with temperature is considered normal. One possible explanation for the line-width transition is that the thermal relaxation time has become extremely short (about 10^{-4} sec). This interpretation will require further study.

The quadruple apparatus has been moved to the new laboratory and is now back in operating condition.

---

(1) H S Gutowsky and G E Pake, *J Chem Phys* **18**, 162 (1950)

(2) M E Milberg and W N Lipscomb, *Acta Cryst* **4**, 369 (1951)

TABLE 18. LINE WIDTH AND FREQUENCY FOR Cl^{35} IN ETHYLENE CHLORIDE

TEMPERATURE (°C)	FREQUENCY (mc)	WIDTH (kc)
-253	34.442	*
-195.8	34 362	2.9
-182.7	34.329	4.6
-178.4	34.318	6.6
-176.0	34.308	12
-175.7	34.308	10
-175.2	34.308	10
-174.75	34.305	11
-174.3	34.304	10
-173.7	34.299	13
-173 2	34.299	15

*Width not directly measured at this temperature, but appeared to have essentially the same width as at -196°C

NEUTRON DIFFRACTION STUDIES

H. A. Levy S. W. Peterson

Crystal Structures of the Modification of Ammonium Bromide and Ammonium Iodide with the Sodium Chloride Type Structure. A neutron diffraction study of the crystal structure of high-temperature cubic ammonium bromide was recently described.[3] It was reported that, in the high-temperature modification (phase I), the ammonium ions do not undergo free or nearly free rotation and that a model in which the ammonium ion rotates about a single threefold axis, oriented parallel to a fourfold axis of the crystal, gave satisfactory agreement with the neutron diffraction data. In this model, one hydrogen atom makes a close approach (2.42 Å) to a bromide ion, the six orientations per ammonium ion that satisfy this condition are occupied at random.

At the suggestion of V. Schomaker, two other models have been examined in which two and three hydrogen atoms make equivalent minimal approaches of length 2.44 Å and 2.48 Å to bromide ions. Neutron diffraction data from ammonium iodide at room temperature have been obtained also, these patterns show close similarity to those from the bromide in phase I. In each model, N is placed in positions[4] 4(*a*) and the anion in positions 4(*b*) of space group O_h^5. The hydrogen positions were as shown in Table 19.

The parameter *b* in the table, the ratio of the N-D distance to the unit cell edge, corresponded to N-D = 1 03 Å. Separate temperature factors were assigned to each atomic species. The

[3] H A Levy and S W Peterson, *Chem Quar Prog Rep March 31, 1952*, ORNL-1285, p 58

[4] The notation is that of the International Tables for the Determination of Crystal Structure

TABLE 19. HYDROGEN POSITIONS FOR THE SEVERAL MODELS OF NaCl TYPE OF MODIFICATION NH_4Br and NH_4I

MODEL	HYDROGEN POSITIONS
Freely rotating	16 D uniformly on 4 spheres around 4(*a*)
Single approach	4 D in 24(*e*), $x = b$ 12 D uniformly distributed around 6 circles centered at 6(*e*), $x = b/3$
Double approach	8 D in 96(*j*), $y_1 = b \cos 9°44'$, $z_1 = b \sin 9°44'$ 8 D in 96(*k*), $x_2 = (b/\sqrt{2}) \cos 54°44'$, $z_2 = b \sin 54°44'$
Triple approach	12 D in 96(*k*), $x_1 = b/3\sqrt{3}$, $z_1 = 5\ b/3\sqrt{3}$ 4 D in 32(*f*), $x_2 = b/\sqrt{3}$

single-approach model corresponds to free rotation about a single threefold axis of the ion, oriented along a fourfold axis of the crystal as previously reported.[3] The models are illustrated in Fig. 17.

The results of these studies are summarized in Tables 20 and 21. For both substances, the free-rotating-ion model is in disagreement with the observed data, whereas the remaining three models achieve nearly equivalent agreement that is satisfactory within experimental error. A number of other models for the bromide structure, in which no close approach of D to Br is achieved, was previously found to be in disagreement with the data.[3]

TABLE 20. NEUTRON DIFFRACTION DATA FROM ND_4Br AT 250°C

INDEXES	$\|F\|$ (obs)	F (calc)*			
		Single Approach	Double Approach	Triple Approach	Free Rotation
111	6 7 ± 0 1	6 69	6 70	6 68	6 64
200	11 1 ± 0 1	10 82	10.84	10 85	10 48
220	6 8 ± 0 1	7 00	7 05	7 03	6.86
311	0 7 ± 0 35	0 91	1 14	1 17	0 72
222	4 0 ± 0 33	4 49	4 41	4 34	4 68
400	5 0 ± 0 16	4 88	5 04	5 08	3 75
331	1 0 ± 0 5	-0 93	-0.97	-0 99	0 61
420	3 8 ± 0 2	3 67	3 75	3 77	3 28
422	2 9 ± 0 3	2 69	2 58	2 54	3 11
620	3 0 ± 0 45	3 82	3 95	3 92	

*For all models, B_D = 4, B_N = B_{Br} = 3, for free rotation, N-D = 1 05 Å, for the others 1 03 Å

TABLE 21. NEUTRON DIFFRACTION DATA FROM ND_4I AT ROOM TEMPERATURE

INDEXES	$\|F\|$ (obs)	F (calc)*			
		Single Approach	Double Approach	Triple Approach	Free Rotation
111	7 8 ± 0 1	7 73	7 71	7 79	7 76
200	11 2 ± 0 1	10 92	10 93	10 93	10 79
220	7 2 ± 0 1	7 45	7 43	7 42	7 52
311	2 0 ± 0 2	2 11	2 12	2.11	1 97
222	4 0 ± 0 3	4 99	4.87	4 81	5 50
400	5 8 ± 0 2	5 26	5 40	5 47	4 30
331	1 2 ± 0 6	-0 41	-0 47	-0 53	-0 01
420	3 8 ± 0 2	4 15	4 07	4 11	3 69

*For all models, B_D = 3, B_N = 1 7, B_I = 1, N-D = 1 03 Å

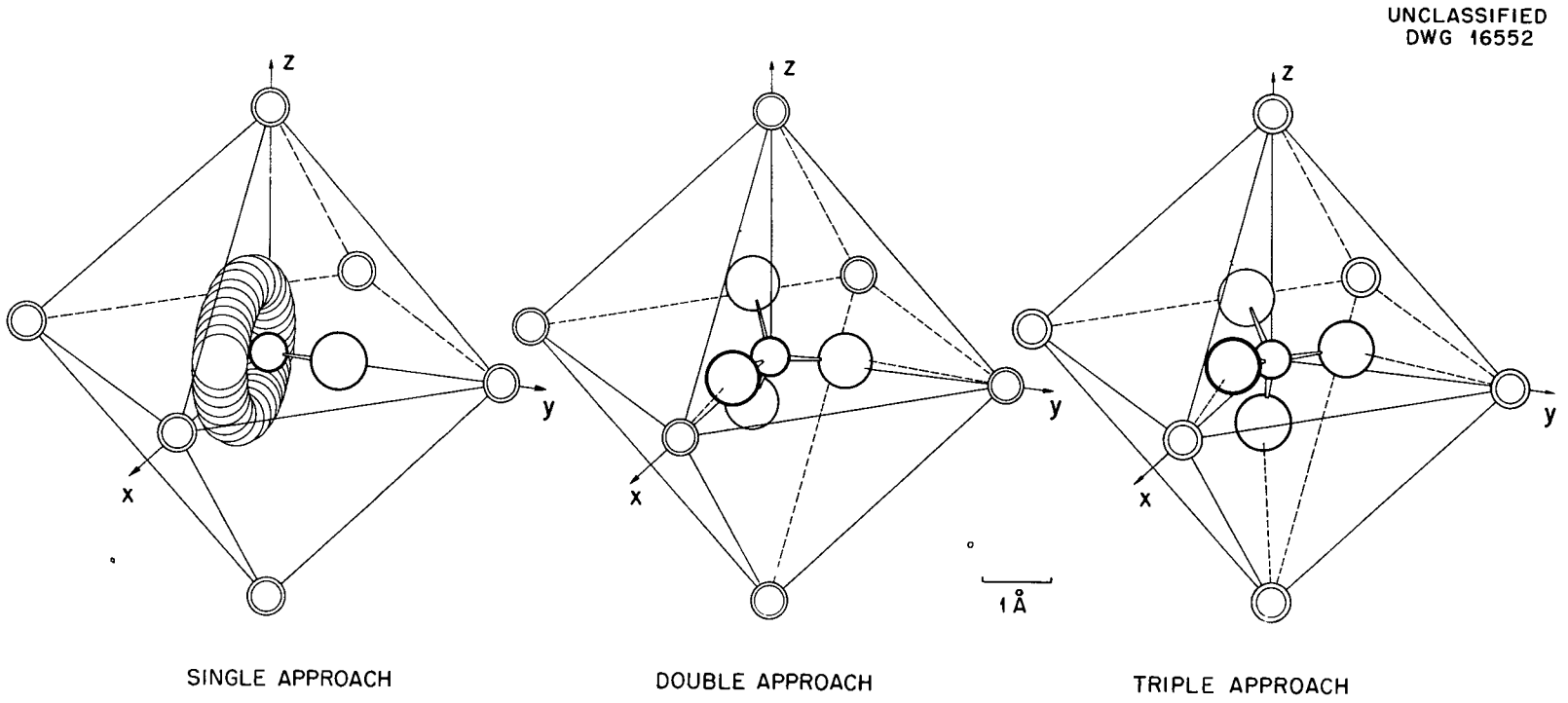

Fig. 17. Coordination of Ammonium Ion in Acceptable Models of NH_4Br, Phase I. In each case there is shown one orientation of the 6, 12, and 8, respectively, occupied at random. Circles represent approximate thermal motion of the nuclei.

Stevenson, Landers, and Cole[5] have interpreted heat-capacity measurements on NH_4I and mixed crystalline $KI-NH_4I$ (which possesses the same skeletal structure) to indicate ammonium ion rotation. Ammonium ion rotation was indicated in $KI-NH_4I$ even at temperatures near 15°K. Their observations are twofold (1) the heat capacity of NH_4I in phase I is 3.8 cal/mole degree lower than that in phase II at the transition temperature of -17.6°C, and (2) the heat capacity of the mixed crystal is higher than that of KI or NH_4I at temperatures between 14 and 100°K. The first observation was recognized as suggestive of, but not demanding, rotation, since this heat capacity difference cannot be attributed entirely to a change in that associated with rotatory motion of the ammonium ion. The second observation indicates that a spectrum of energy levels exists with spacings comparable to 14°K. This was taken by Stephenson and coworkers to indicate one or more degrees of freedom that are rotational in nature. In fact, a closely spaced spectrum of energy levels could well result from any of the models found to be in agreement with the neutron data in the double- and triple-approach models by virtue of the multiple potential minima resulting from the superposition of tetrahedral and cubic symmetries, and in the single-approach model also from single-axis rotation. A qualitative interpretation of heat capacities therefore does not favor any one of these models over the others.[6]

A study of the infrared absorption spectrum of NH_4I and ND_4I in phase I has been made by Plumb and Hornig.[7] Their interpretation led them to a single-axis rotation model, identical to our single-approach model.

The extension of the neutron diffraction study to single crystals of NH_4I and $KI-NH_4I$ is planned. The more numerous data obtained by this method from NH_4I and low temperature data from $KI-NH_4I$ should make it possible to determine the details of the phase I structure more closely.

Theoretical Study of the Ammonium Ion Potential in Phase I Ammonium Halide (V. Schomaker). The form of the ammonium-ion potential expected from electrostatic considerations is being investigated. At present only fourth-degree harmonic terms have been considered, a number of statements can be made to this approximation.

1. The triple-approach model represents a stable minimum.
2. The double-approach model represents a saddle point only slightly less stable.
3. The single-approach model also represents a saddle point and is still less stable.
4. Axial rotation in the single-approach model is substantially free. This is true to approximations including tenth-degree harmonic terms. This observation has also been made by Plumb.[7]
5. Potential maxima occur when the symmetry elements of the tetrahedron match those of the cube, for example, model 1 of a previous report,[3] in which the approaches of hydrogen to anion are maximized.

The preliminary results are in agreement with the absence of free rotation in these materials. They also suggest that the single-approach model is unlikely as such. Depending on the magnitudes of the potential differences involved, either the triple-approach model alone, a combination of triple and double approach, or a combination of all three would be expected. The combination of all three would, to some extent, resemble two degrees of rotational freedom.

---

(5) C C Stephenson, L A Landers, and A G Cole, *J Chem Phys* **20**, 1044 (1952)

(6) Discussions of this matter with V Schomaker are gratefully acknowledged

(7) Private communication from R C Plumb

RADIATION CHEMISTRY

NUCLEATION OF BUBBLES IN SUPERHEATED SOLUTIONS BY FISSION RECOILS

J. A. Ghormley C. J. Hochanadel
A. C. Stewart

A knowledge of the conditions under which fission recoil tracks can serve as nuclei for bubbles in superheated solutions is essential in predicting the behavior of homogeneous boiling reactors. Nuclei formed by the fission recoils could, under some conditions, contribute to stable operation of reactors. However, too many nuclei might cause the liquid to foam and thereby could limit the power obtainable.

Glaser[1] has recently reported bubble nucleation in superheated ether by gamma rays. In the present work, superheated ether was irradiated with 50-kv x rays and fast neutrons, and bubble nucleation by both types of radiation has been observed.

Sealed silica ampoules, which had previously been used in a study of water decomposition produced by fission recoils,[2] were available for some preliminary experiments to determine the conditions under which bubbles could be nucleated by fission recoils in superheated solutions. The ampoules contained enriched uranyl sulfate (44 g of uranium per liter) and, as a result of irradiation, hydrogen and oxygen gas at total pressures of 122 to 290 cm of Hg. The ampoules were made of capillary tubing, about 2 mm ID, with one end drawn down to about 0.4 mm ID for a length of about 4 cm. The original purpose of the drawn-down capillary end was to permit measurement of gas pressure in the ampoule from the boiling temperature, which was determined from the temperature necessary to maintain a small vapor phase. With only liquid phase present, the tip could be greatly superheated before a vapor phase formed that rapidly forced liquid out of the tip.

In a typical ampoule (No. 6) with a normal boiling temperature of 142.4°C, solution in the capillary tip could be heated repeatedly to 198 to 200°C before ebullition occurred. When the tip of the ampoule was placed in the glycerine bath at temperatures exceeding 200°C, ebullition always occurred within a few seconds.

To determine the effect of fission recoils, a neutron source was brought near the heated glycerin bath and the tip of the ampoule immersed. In 21 observations with bath temperatures between 190 and 197°C, the average time before ebullition was 9.2 seconds. In 26 observations at 154 to 161°C, the average time was still only 10.9 seconds. No bubbles were observed to form at temperatures below 153°C, even when the solution was held between 149 and 152.5°C for a period of 24 hr with the neutron source present.

The small difference between the average time before ebullition at different temperatures could be attributed to the difference in the volume of liquid in the capillary heated to the required temperature and the time required to reach the necessary 153°C.

No measurement has been made of the neutron flux, therefore the number of fissions occurring in the solution is not known. The average time required for bubble formation is independent of temperature over a wide range. This indicates that the probability of bubble nucleation by fissions does not change with temperature, and it seems reasonable that this could be true only if the probability is unity. Therefore it is concluded that every

(1) D A Glaser, *Phys Rev* **87**, 665 (1952)

(2) J W Boyle, W F Kieffer, C J Hochanadel, T J Sworski, and J A Ghormley, "Radiation Chemistry of Aqueous Reactor Solutions," submitted for publication in *Journal of Reactor Science and Technology*

fission produces a bubble when the temperature of the superheated uranyl sulfate solution exceeds a definite lower limit. The probability of bubble formation drops rapidly at lower temperatures. The data for the four ampoules are summarized in Table 22. The data indicate, as would be expected, that the superheating possible in neutron-irradiated uranyl sulfate solutions, expressed in terms of temperature, drops with increasing temperature. Further experiments are planned to determine conditions of bubble nucleation at higher temperatures and pressures.

OXIDATION OF URANIUM(IV) BY GAMMA RAYS

C. J. Hochanadel

Some preliminary experiments have been made to determine the effects of several variables on the gamma-ray oxidation of dilute uranium(IV) solutions in sulfuric acid. Typical dose-concentration curves are shown in Fig. 18 for solutions at pH 1.0 that were irradiated in a system that had a free gas space approximately equal to the liquid volume. Uranium(IV) is oxidized completely and an equivalent amount of hydrogen is formed. Curves A and B show that, for initially evacuated 10^{-3} *M* and 10^{-2} *M* solutions, the oxidation rate decreases with increasing dose and the rate is little affected by the concentration of uranium(IV). Curve A indicates that varying the initial ratio of uranium(IV) to uranium(VI) from 10 to 1 in degassed, 10^{-3} *M* uranium(IV) solutions has no effect on uranium(IV) oxidation rate. Curve C, obtained for 10^{-3} *M* uranium(IV) solutions initially containing approximately 6×10^{-4} moles of H_2 per liter, indicates that hydrogen retards the oxidation of uranium(IV). This may result from competition for OH radicals according to the reaction

$$H_2 + OH \longrightarrow H_2O + H \,, \qquad (1)$$

with possible reduction of uranium(V) by hydrogen atoms. The initial yield in all these solutions is 1.6 to 1.8 ions oxidized per 100 ev. Peroxide was not present in any of the solutions

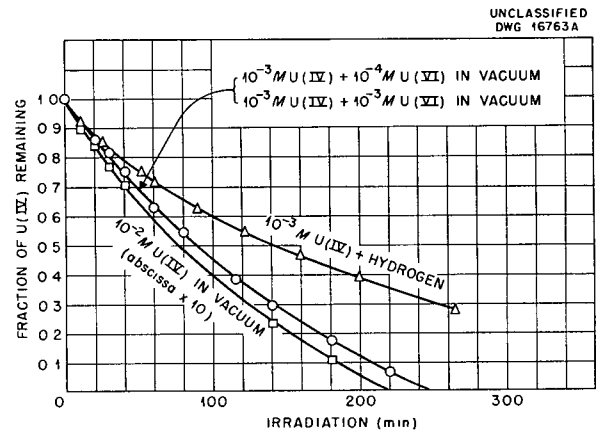

Fig. 18. Gamma-ray Oxidation of Uranium(IV) Solutions with 2.1×10^{17} ev/ml/min at pH 1.0.

TABLE 22. BUBBLE NUCLEATION IN SUPERHEATED URANYL SULFATE SOLUTION BY FISSION RECOILS

AMPOULE NO	NORMAL BOILING TEMPERATURE, T_B (°C)	GAS PRESSURE P_B (cm Hg)	MINIMUM FISSION NUCLEATION TEMPERATURE, T_N	VAPOR PRESSURE AT NUCLEATION TEMPERATURE, P_N	$T_N - T_B$	$P_N - P_B$
2	113 8	122	136 6	246	22 8	124
5	129 4	199	145 0	312	15 6	113
4	134 2	230	148 1	339	13 9	109
6	142 4	290	153 0	387	10 6	97

at the termination of irradiation, as indicated by the lack of continued oxidation of uranium(IV) after irradiation. Although it is probable that some H_2O_2 was produced during irradiation, it would have been removed by the reaction

$$H_2O_2 + H \longrightarrow H_2O + OH \quad . \qquad (2)$$

The addition of H_2O_2 to the uranium(IV) solution prior to irradiation increased the oxidation resulting from radiation. The measurement is complicated by the normal oxidation of uranium(IV) by the H_2O_2. After correcting for this reaction, the radiation yield was approximately double the yield obtained in vacuum. This increase probably results from the conversion of H atoms to OH radicals through reaction 2.

Added oxygen greatly accelerates the gamma-ray oxidation rate. Measurements are complicated by a slow thermal oxidation of uranium(IV) by O_2 and also by the build-up of H_2O_2 in solution during irradiation.

The normal reaction of H_2O_2 with uranium(IV) is much faster at a higher pH. When oxygen-saturated solutions at pH 0.1, 1.0, and 2.0 were irradiated until the oxidation was nearly completed and then analyzed immediately, yields of 5.8 to 7.8 uranium(IV) ions oxidized per 100 ev were obtained. At the higher pH, most of the peroxide had time to react with uranium(IV) during irradiation, and the yield 7.8 is near the maximum yield. At the low pH, very little H_2O_2 reacted with uranium(IV) during irradiation. On further irradiation after complete uranium(IV) oxidation, H_2O_2 built up at a rate comparable to that for H_2O_2 production in acid solution with no uranyl ion present ($G \sim 1.4$ H_2O_2 molecules per 100 ev).

GAMMA-RAY EFFECTS IN ICE

A. C. Stewart J. A. Ghormley

Initial yields for H_2O_2 production in gamma-irradiated ice that contained dissolved oxygen at -196 to 0°C have been reported previously.[3] Extrapolation of the data for this temperature range indicates a steady decrease in peroxide formation to zero at -273°C (0°K). Ice, prepared from helium-saturated and oxygen-saturated water, has been irradiated at temperatures from -269°C (4°K) to -196°C, and the H_2O_2 yield has been found to be approximately constant in this temperature range. The yield is approximately the same with helium or oxygen present in the ice.

The hydrogen, hydrogen peroxide, and oxygen concentrations found in gas-free ice that had been irradiated at -196°C for periods up to 47 hr at 13,000 r/min are shown in Fig. 19. A steady-state concentration of products had not been reached, even at the longest irradiation, although the yield at this point is much lower than the initial yield. After irradiations of 1 hr or longer, at least 85% of the total oxidized product was hydrogen peroxide, as determined by molybdate-catalyzed oxidation of iodide immediately after ice had melted and at several time intervals later. As would be expected for ordinary hydrogen

[3] A C Stewart and J A Ghormley, *Chem Quar Prog Rep March 31, 1952*, ORNL-1285, p 65

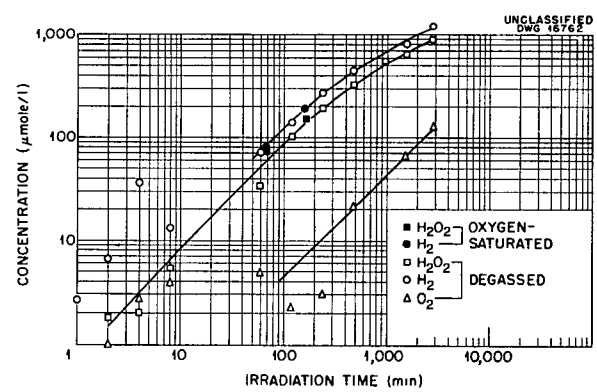

Fig. 19. Products Found in Oxygen-saturated and Degassed Water After Irradiation as Ice at -196°C with Co^{60} Gamma Rays at an Intensity of 7.0 × 10^{17} ev/g/min (~ 13,000 r/min).

peroxide, no decomposition was detectable in 30 minutes.

To determine the effect of dissolved oxygen in ice irradiated at -196°C, two samples of oxygen-saturated water were irradiated as ice at -196°C for 67 and 160 minutes. The yields of hydrogen and hydrogen peroxide were comparable with yields obtained for similar irradiations of ice prepared from degassed water, as shown in Fig. 19. From these data, the conclusion is that little, if any, reaction occurs between molecular oxygen and the primary products produced by the radiation at -196°C.

It is postulated that at higher temperatures additional hydrogen peroxide is formed by reactions involving the oxygen present. It is assumed that the necessary activation energy for some step in the process is provided only at temperatures above -196°C. The previously observed low steady-state concentrations of products after irradiations at -78°C are consistent with the idea that reactions of the primary decomposition products with the normally stable molecules H_2, H_2O_2, and O_2 in the irradiated ice are possible at temperatures above -196°C.

At -78°C, a low steady state (~7 μmoles of H_2O_2 per liter) was reached in degassed or helium-saturated ice in less than 1 hr at 13,000 r/min, but a higher steady state (~30 μmoles of H_2O_2 per liter) was found in helium-saturated water containing 0.01 *M* of KBr, irradiated as ice at -78°C. This seems to indicate that products are recombining at -78°C and that this recombination is slower in the presence of bromide, in accord with the known inhibition of back-reaction in water by bromide ion.

Yields of hydrogen and hydrogen peroxide in oxygen-saturated solutions over a wide temperature range will be determined to test the validity of the ideas presented.

GAMMA IRRADIATION OF AQUEOUS BENZENE SOLUTIONS

T. J. Sworski

The optical density at 290 mμ of alkaline phenol solutions containing hydrogen peroxide increases with time. In the method previously described[4] for the determination of phenol, the optical density at 290 mμ of the alkaline solution must be followed as a function of time of alkalinity and extrapolated to zero time. This extrapolation corrects for interference caused by hydrogen peroxide.

Figure 20 shows the formation of phenol and hydrogen peroxide in oxygen-saturated aqueous benzene solutions irradiated with cobalt gammas. For those solutions irradiated for periods longer than 30 min, the optical density at 290 mμ of the alkaline phenol solutions decreased with time. It is assumed that some interfering substance is formed in the presence of hydrogen peroxide. This was verified by a study

[4] T J Sworski, *Chem Quar Prog Rep June 30, 1951*, ORNL-1116, p 75

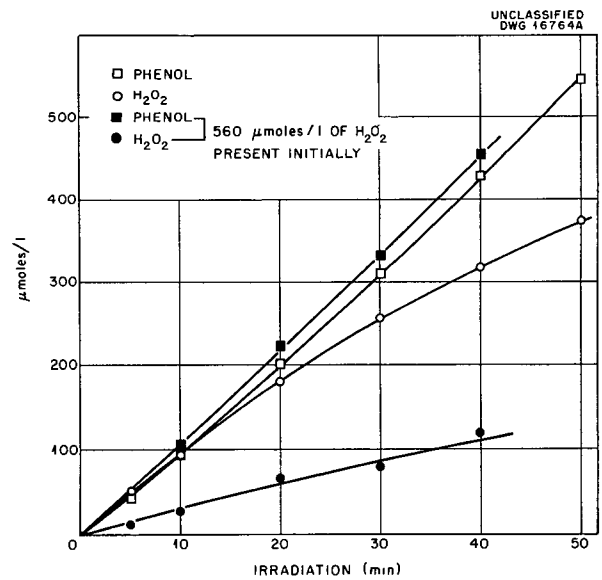

Fig. 20. Phenol and Hydrogen Peroxide Formation by Co^{60} Gamma Rays in Oxygen-saturated Aqueous Benzene Solutions at 2.03×10^{20} ev/l·min^{-1}.

of the effect of hydrogen peroxide initially present at a concentration of 560 μmoles/liter. As shown in Fig. 20, the initial yield of phenol apparently increased. This is not real, since the interference in phenol determinations is now present even for samples irradiated for short periods (5 min).

REDUCTION OF CERIUM(IV) BY GAMMA RADIATION

T. J. Sworski

It has been shown in a previous quarterly report[5] that, following the complete reduction of ceric sulfate in air-saturated 0.8 *N* sulfuric acid solution, the initial yield for hydrogen peroxide formation is identical to that observed in air-saturated 0.8 *N* sulfuric acid and stoichiometrically equivalent to the yield for cerium(IV) reduction. In the light of this observation, the mechanism of cerium(IV) reduction is under investigation.

Two discussions of the mechanism of cerium(IV) reduction have recently appeared. Haissinsky, Lefort, and Le Bail[6] have suggested that cerium(IV) reduction is due to the reaction of OH with cerium(IV). On the other hand, Hardwick[7] has suggested that cerium(IV) reduction is due to the reaction of cerium(IV) with either H or HO_2, thus explaining the absence of any observed oxygen effect. Hardwick also reported that hydrogen doubles the yield of cerium(IV) reduction by the reaction

$$H_2 + OH \longrightarrow H_2O + H$$

and concluded that OH recombination in solution to form hydrogen peroxide does not occur.

Although the yield for cerium(IV) reduction in air-saturated solutions is independent of pH,[7] Fig. 21 shows the pH dependency observed for the reduction of cerium(IV) in solutions containing a mixture of H_2 and O_2. The initial yield for the hydrogen-enhanced cerium(IV) reduction has a pH dependency similar to that reported[8] for the yield of hydrogen peroxide in water containing a mixture of H_2 and O_2. This indicates that cerium(IV) reduction in solutions containing oxygen may take place through the intermediate formation of hydrogen peroxide and not by reaction with HO_2 or with OH.

Preliminary experiments indicate the presence of an oxygen effect in cerium(IV) reduction. Since oxygen is a product accompanying cerium(IV) reduction, the oxygen concentration was minimized by vigorous sweeping of the solutions with helium while being exposed to gamma radiation of lower

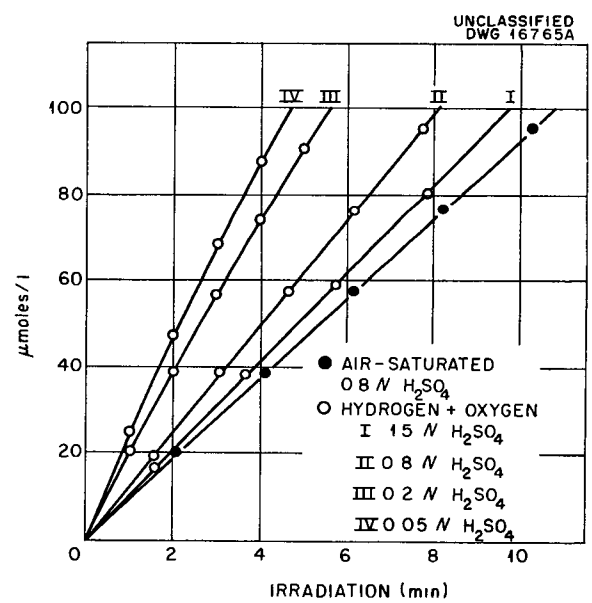

Fig. 21. Effect of Hydrogen on the Reduction of 10^{-4} *M* Cerium(IV) Sulfate in Aqueous Solutions by Co^{60}.

(5) T J Sworski, *Chem Quar Prog Rep March 31, 1952*, ORNL-1285, p 66

(6) M Haissinsky, M Lefort, and H LeBail, *J Chim Phys* **48**, 209 (1951)

(7) T J Hardwick, *Can J Chem* **30**, 23 (1952)

(8) T J Sworski, *Chem Quar Prog Rep June 30, 1952*, ORNL-1344, (in press)

intensity than used in studies of oxygenated solutions. Under these conditions, the rate of cerium(IV) reduction increased 17%, 27%, and 61% above that in air-saturated solutions. Although this is in disagreement with the results of Hardwick,[7] it is in agreement with the observations of the Los Alamos group,[9] who report an increased initial rate in thoroughly degassed solutions with an air space present. It thus seems that oxygen, through formation of HO_2, prevents reduction of cerium(IV) by H.

[9] Private communication, H P Hammond, Los Alamos

INSTRUMENTATION

CHEMISTRY DIVISION

C. J Borkowski F. Porter
E. Fairstein J. K. East
R. Stone

The circuit development of a new linear amplifier was completed during the last quarter The design appears to be successful in that it has about 10 to 20 times the overload capacity of the A-1 amplifier and can tolerate about 10 times its counting rate for a given energy-resolution degradation. A pilot model will be constructed to determine how well the instrument functions under actual operating conditions. The design characteristics were described in an earlier quarterly report.

The circuit for a scintillation-counter-regulated high-voltage supply that uses an r-f oscillator for the voltage source was developed. This circuit has a number of advantages over the earlier design (1) the coil used in the oscillator is very simple and of noncritical design, (2) the high voltage does not appear at the terminals of the oscillator tube, with the result that a low-power receiving type of tube can be used, and (3) the operating efficiency is quite high, resulting in low heat dissipation. Unfortunately, the nature of the design is such that it is not economical for use in a self-contained unit However, it is economical for use in an amplifier-high-voltage-supply combination where a low-voltage supply already exists.

The alpha-energy analyzer began to give trouble after three years of continuous operation. Most of the difficulty was caused by the argon filling gas stocked by the Laboratory. The last month was spent in changing the instrument in a way that would prevent a future recurrence of the trouble. The operation of the analyzer was greatly improved in the process of change and is now giving better results than ever before.

A 404-A tube tester and ager was designed and built with the cooperation of the Instrument Department Until now, the Service group has not had an adequate means of conditioning 404-A tubes, which are used in quantity in scintillation spectrometers.

The multichannel analyzer that incorporates a Hathaway galvanometer has been testing using 10 channels. Excellent stability has been obtained with the system In order to increase the speed of the system so that the amplitude of 1000 pulses/sec can be measured accurately, a pulse with both positive and negative polarity will have to be fed into the transformer that drives the galvanometer. In this way the shift of the baseline, which is now present, will be eliminated.

A method of simulating scintillation pulses is being developed that uses a Hathaway galvanometer and a light-integrating sphere to diffuse the

light over a photomultiplier photocathode. It is hoped that some of the factors that govern the energy resolution of photomultipliers will be determined by the use of the constant source of light flashes.

REACTOR CHEMISTRY

SOLUBILITY OF UO_3 IN AQUEOUS UO_2SO_4 AND UO_2F_2 AT 175 AND 250°C

E. V. Jones W. L. Marshall
J. S. Gill C. H. Secoy

Investigations of UO_3 solubility in UO_2SO_4 solutions at 250°C, which have been reported in part for UO_2SO_4,[1] have been continued and expanded to include solubilities in aqueous UO_2F_2. The technique of filtering a solution from excess solid phase at temperatures above 100°C was described previously.[1]

UO_3-UO_2SO_4-H_2O System. Data for the solubility of UO_3 in UO_2SO_4 at 175°C and the acidities of such solutions are given in Table 23. The solubility of UO_3, the solubility ratio, and the acidity have been plotted individually against uranium concentration and are shown in Figs. 22, 23, and 24, respectively. Curves representing data at 250°C, which were presented in the last quarterly report, are included. This investigation still has not clarified the behavior in the low-concentration region, that is, below 0.1 *M*. The question is whether the equilibrium ratio, U to SO_4, drops below 1.00 as concentration is lowered. If the ratio does fall below 1.00, then the data would best be represented by the system UO_3-H_2SO_4-H_2O. On this basis, there is no valid reason why the ratio of U to SO_4 must

(1) J. S. Gill, E. V. Jones, and W. L. Marshall, *HRP Quar. Prog. Rep. June 30, 1952*, ORNL-1318, p. 143.

TABLE 23. SOLUBILITY OF UO_3 IN UO_2SO_4-H_2O SOLUTIONS AT 175°C

Molarities based on room temperature densities

TOTAL MOLARITY URANIUM	MOLARITY SO_4	SOLUBILITY EXCESS MOLARITY UO_3	TOTAL MOLE RATIO UO_3 TO SO_4	pH (at 25°C)	HOURS OF MIXING AT 175°C
0.119	0.100	0.019	1.19	3.25	72
0.292	0.239	0.053	1.22	3.30	72
0.594	0.471	0.123	1.26	3.25	72
0.890	0.680	0.210	1.31	3.20	72
1.217	0.948	0.269	1.28	3.20	96
1.528	1.178	0.350	1.30	2.73	72
1.790	1.360	0.430	1.31	2.80	68
2.508	1.934	0.574	1.30	3.80(?)	72
2.986	2.397	0.589	1.25	2.30	72
4.020	2.964	1.056	1.36	2.20	192
4.370	3.370	1.000	1.30	1.70	120
4.440	3.380	1.060	1.31	1.90	192

-1432
9/52

remain equal to or greater than 1.00. Also, for a given sulfate concentration, the ratio should decrease with temperature because of increased hydrolysis of the uranyl ion. During the next quarter an effort will be made to clarify this low concentration region.

The solid phase at 250°C was previously reported[1] as $UO_3 \cdot \frac{1}{2}H_2O$. This phase has been further identified by x-ray diffraction as a hydrate of UO_3.

UO_3-UO_2F_2-H_2O System. Experimental data for the UO_3-UO_2F_2-H_2O system at 175 and 250°C are given in Table 24 and are shown in Figs. 25, 26, and 27. The data at 250°C are erratic and are included as preliminary data only. In most of the experiments on the fluoride system at 250°C, corrosion of the titanium filter bombs and some reduction of uranium was noted, but this attack was not evident at 175°C.

The ratio of U to 2F at 250°C appears to decrease below 1.00 at low concentrations, therefore the system probably could be represented best as UO_3-HF-H_2O.

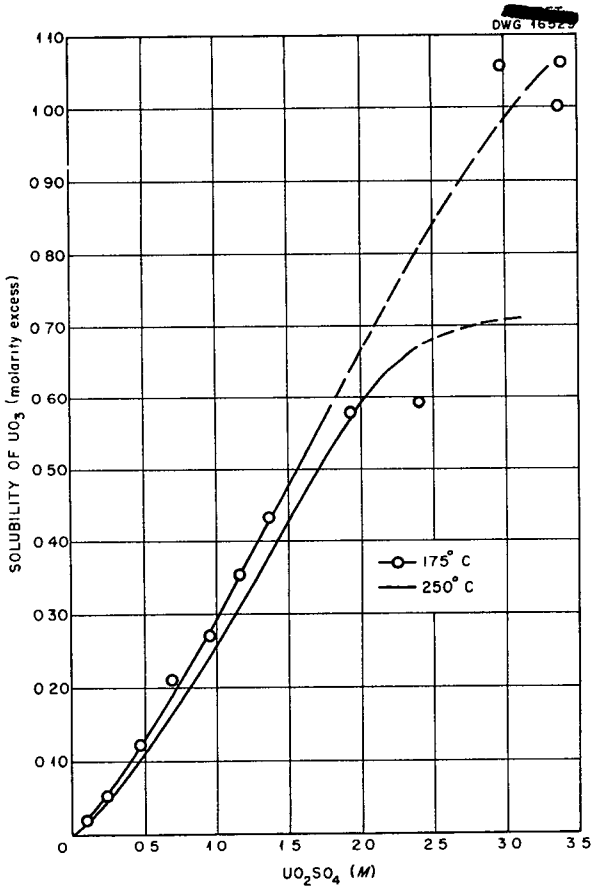

Fig. 22. The Solubility of UO_3 in UO_2SO_4-H_2O Solutions at 175°C.

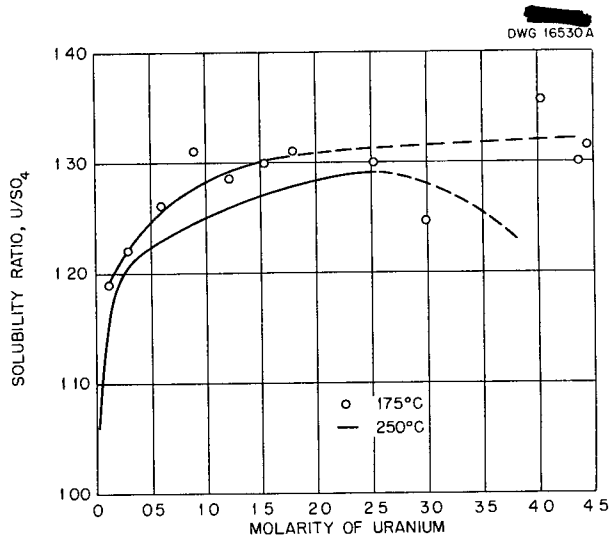

Fig. 23. The Solubility Ratio, U to SO_4, in UO_2SO_4-H_2O Solutions at 175°C.

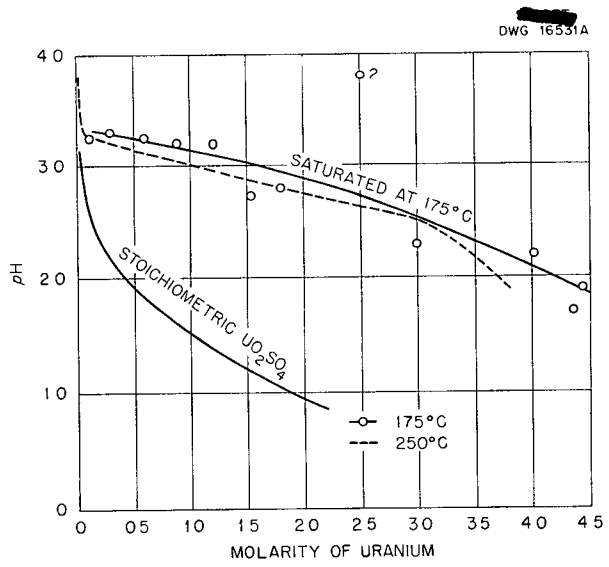

Fig. 24. pH Curves for Saturated Solutions of UO_3 in Uranyl Sulfate Solutions pH readings at room temperature.

TABLE 24. SOLUBILITY OF UO_3 IN UO_2F_2-H_2O SOLUTIONS AT 175 AND 250°C

Molarities based on room-temperature densities

TOTAL MOLARITY URANIUM	MOLARITY UO_2F_2	SOLUBILITY EXCESS MOLARITY UO_3	TOTAL MOLE RATIO UO_3 TO UO_2F_2	pH (at 25°C)	HOURS OF MIXING
At 175°C					
0 0483	0 04775	0 00055	1 012	4 65	96
0 1740	0 1685	0 0055	1 033	4 40	96
0.230	0 225	0 0050	1 022	4 30	90
0 954	0 8675	0 0865	1 100	3 90	96
1 964	1 692	0 272	1 161	3 57	96
2 478	2 150	0 328	1 153	3 37	96
3 066	2 409	0 657	1 273	3 20	180
4 121	3 416	0 705	1 206	2 70	180
4.200	3 315	0 885	1 267	2 60	120
At 250°C					
0 169	0 185	−0 016	0 914	2 92	
0.732	0 745	−0 013	0 979	3 50	
1.06	0 993	0 067	1 07	3 90	
1 58	1 40	0 18	1 13	3 60	
1 89	1 71	0 18	1 11	3 49	
3 02	2 69	0 33	1 12	3 90	
3 29	2 82	0 47	1 17	3 25	
3 43	2 95	0 48	1 16	3 10	
2.73*	2.45	0 28	1 11	3 70	
2.42**	2 12	0 30	1 14	3 40	

*Run made in a Teflon liner

**Three drops of 30% H_2O_2 added.

EXTENSION OF THE STUDY OF THE TWO-LIQUID-PHASE REGION OF THE SYSTEM UO_2SO_4-H_2SO_4-H_2O

H. W. Wright W. L. Marshall
C. H. Secoy

The effect of free sulfuric acid on the coexistence curve of the two-liquid-phase region of the uranyl sulfate-water system at acid concentrations up to about 0.63 *M* was described previously.[2,3,4,5] The acid was found to decrease the scope

(2) C H Secoy, *Chem Quar Prog Rep Aug 1948*, ORNL-176, p 58

(3) C H Secoy, *Chem Quar Prog Rep Dec 31, 1949*, ORNL-607, p 33

(4) W L Marshall, J S Gill, C H Secoy, *Chem Quar Prog Rep June 30, 1950*, ORNL-795, p 22

(5) R E Leed and C H Secoy, *Chem Quar Prog Rep Sept 30, 1950*, ORNL-870, p 29

-1432
9/52

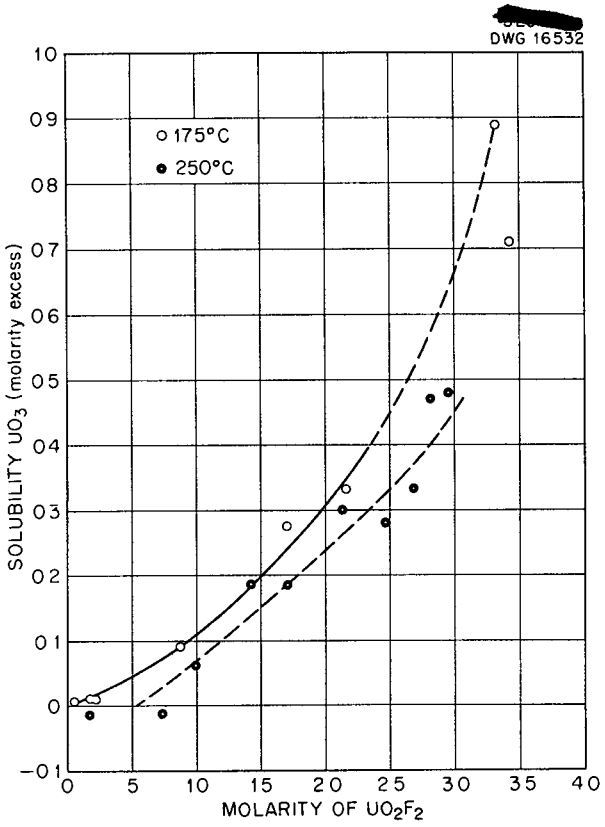

Fig. 25. The Solubility of UO_3 in UO_2F_2-H_2O Solutions at 175 and 250°C.

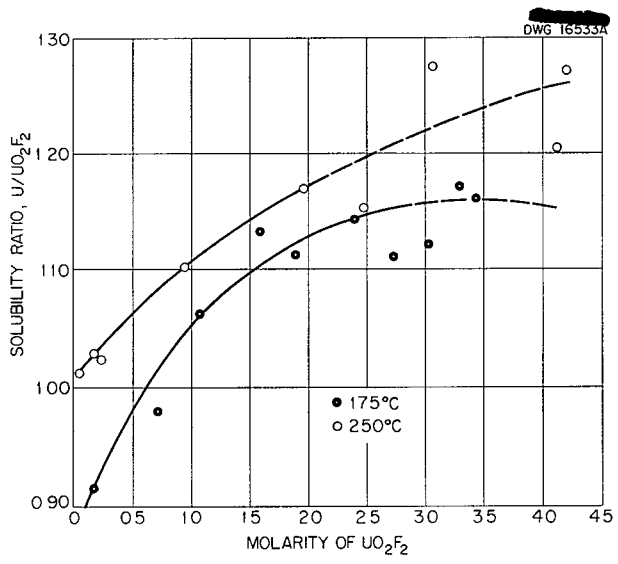

Fig. 26. The Solubility Ratio U to UO_2F_2 in UO_3-UO_2F_2-H_2O Solutions at 175 and 250°C.

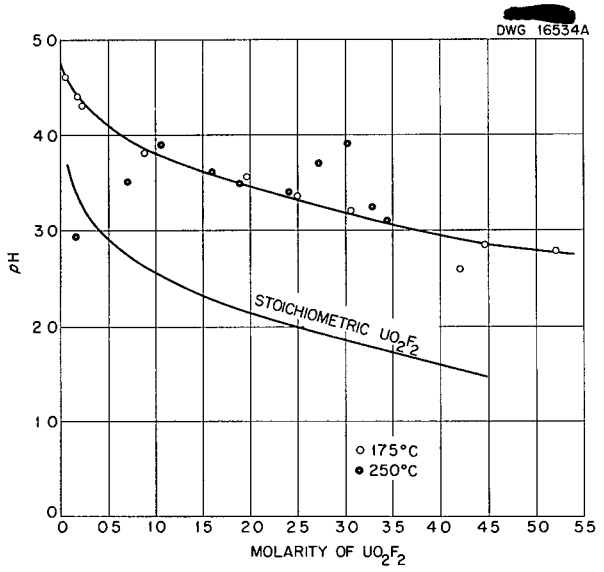

Fig. 27. pH Curves for UO_2F_2 Solutions Saturated with UO_3 at 175 and 250°C. pH readings at room temperature.

of the region (increase miscibility) and to shift the minimum critical solution point to higher temperatures. The addition of sulfuric acid elevates the critical temperature not only because of the acid present but also because of the increased solubility of uranyl sulfate in the supercritical fluid.

The experimental techniques of earlier investigators had two major failings. One was the laborious and time-consuming job of tube preparation, coupled with the long cooling time required before the heating element could be reloaded for subsequent runs. Another limitation was the inability (or perhaps the impossibility) to prepare silica tubes with sufficient strength to withstand the high pressures developed, out of 66 prepared tubes, 46 blew up before data could be obtained.[5]

Both the tube failures and the tube preparation time factor were solved by resorting to commercially available capillary silica tubing, 1-mm base,

1-mm wall thickness. When half filled with water, these tubes withstood temperatures in excess of 740°C and could be prepared in several minutes. The other limitations were overcome by the use of a redesigned heating element (Fig. 28).

The redesigned element consists of a cylindrical, heat conducting block C (Al and graphite have been used) 30 cm in length and 5 cm in diameter. A hole 8 mm in diameter was drilled through the longitudinal axis. The glass (or silica) sleeve D fits into this hole, which acts as a housing for the sample tube and the iron-constantan thermocouple, the sample enters from one end and the thermocouple from the other. A window E, 50 by 8 mm, cut normal to the sample hole, allows visual observation of the sample. Evenly spaced grooves F were machined over the block to hold the heating wire. Sleeve B covers the entire block. Sleeves B and D act as insulators and reduce air movement through the slotted areas. The entire heating element rests in a cradle (not shown in the diagram).

The buzzer A is a simple bell buzzer adapted with an alligator clamp in place of a striker. It is mounted on the adjustable arm that holds the sample in position and effects mixing of the sample by automatic, alternate on-off buzzing.

A shield mounted between the observer and the heating element

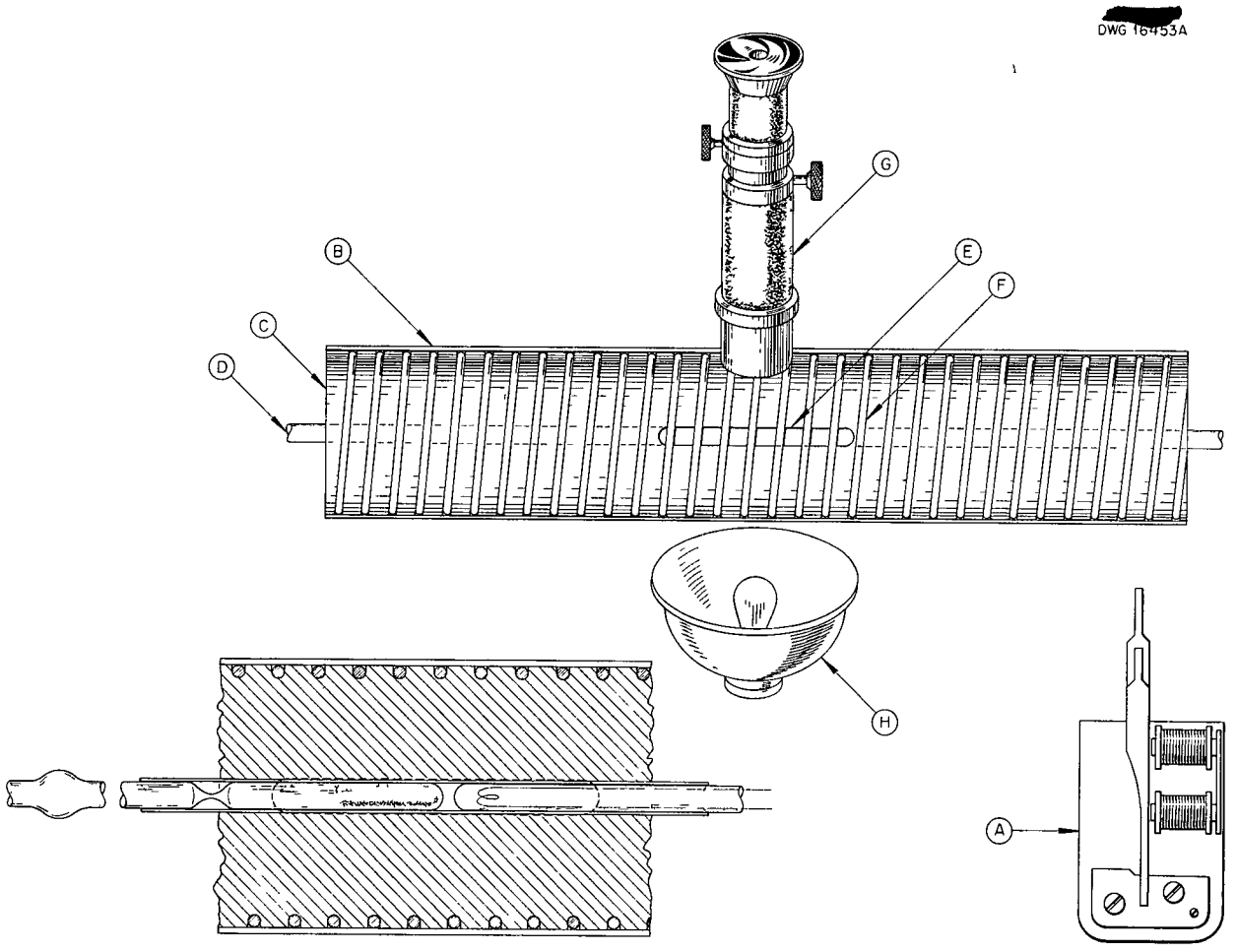

Fig. 28. Apparatus for Phase-Transition Studies on Semimicro Scale.

-1432
9/52

affords complete protection to the observer from explosions. The telescope G, along with the light source H, located on the opposite side of the window, allows minute changes within the sample to be observed before they are discernible to the naked eye.

Temperature control is maintained with the use of a conventional Variac and is measured with an iron-constantan thermocouple and conventional instruments.

The use of this new apparatus offers the following advantages

1. a smaller sample than previously used,
2. greatly increased temperature range,
3. time economy in tube preparation,
4. ease of temperature control,
5. evenness of heating, which reduces temperature gradients throughout the sample,
6. ability to remove and reload samples at high temperatures without the heretofore necessary wait while the heating element cooled,
7. ease of substitution of entire heating unit,
8. reduction of tube explosion hazard,
9. increased visual perception obtainable with the telescope,
10. adaptability of the apparatus to high-temperature visual observations of other systems.

A 10-ml UO_2SO_4 solution of approximately 30 wt % uranium with an SO_4-to-U ratio of 1.000 was prepared. A small sample was withdrawn, and the remaining solution was diluted to volume Again a sample was withdrawn, and the remaining solution was diluted with water. By this procedure, a series of solutions was obtained that varied in uranium concentration but had a constant SO_4-to-U ratio. In similar fashion, five other series were prepared with SO_4-to-U ratios ranging up to 2.955.

Once the SO_4-to-U ratio was established by analysis of the more concentrated solutions, only the uranium concentration of the more dilute samples was measured, since it is evident that the SO_4 concentration follows that of uranium.

Tubes containing each dilution of each series were prepared in similar fashion, with each tube containing approximately the same volume of solution. The samples were heated in the unit described above, and the temperature at which the second liquid phase appeared and disappeared was recorded (Table 25) and the data were plotted (Fig. 29).

These data can be applied directly to a selection of reactor fuel media. In other words, the two-liquid-phase boundaries can be determined for uranium concentrations up to 30% and for any constant ratio of SO_4 to U from 0.83[6] to 2.9.

The system UO_3-H_2SO_4-H_2O is comparable to UO_3-H_3PO_4-H_2O as a fuel media for homogeneous reactors operating between about 300 and over 500 °C. Bidwell, Thamer, and Hammond[7] are studying the phosphate system at Los Alamos, and some work has been done at ORNL.[8] However, there are some distinct differences between the two systems with regard to reactor fuels. First, the ratio of PO_4 to U required for phase stability from 25 to above 300°C is between 5.0 and 9.0. These ratios are greater than those required for the sulfate system to reach the upper temperatures. Accordingly, the sulfate system might exhibit less corrosion than the phosphate system on container surfaces. Second, the cross section of sulfur is 0.49 barn compared with 0.15 barn for phosphorus. However, this difference is decreased by the lower

(6) E V Jones, *op cit*, ORNL-1318, p 147

(7) R M Bidwell, B J Thamer, R P Hammond, Private communication

(8) J S Gill, H W Wright, W L Marshall, *HRP Quar Prog Rep Aug 15, 1951*, ORNL-1121

-1432
9/52

amount of sulfate necessary to stabilize a solution of the same uranium concentration.

CONDUCTIVITY MEASUREMENTS OF AQUEOUS SOLUTIONS OF URANYL SULFATE AND URANYL FLUORIDE

R. D. Brown W. L. Marshall
W. B. Bunger C. H. Secoy

Investigations of the electrical conductivity of uranyl sulfate and uranyl fluoride in aqueous solution as a function of temperature and concentration have been terminated this quarter. The work will be presented in a completion report. The following is an abstract of the report.

The conductance of uranyl sulfate in aqueous solution has been studied at 0, 25, 50, 90, 125, and 200°C in concentrations ranging from 10^{-4} to 7.25 *N*. Uranyl fluoride has been

TABLE 25 APPEARANCE TEMPERATURE OF TWO LIQUID PHASES IN UO_2SO_4-H_2SO_4-H_2O

CONSTANT RATIO SERIES	URANIUM (wt %)	TWO-LIQUID-PHASE APPEARANCE TEMPERATURE (°C)	CONSTANT RATIO SERIES	URANIUM (wt %)	TWO-LIQUID-PHASE APPEARANCE TEMPERATURE (°C)
CR-I SO_4/U = 1 121			CR-IV SO_4/U = 2 481		
1	29 65	312	1	25 92	
2	21 59	303	2	17 40	Above 530
3	16 01	300	3	11 82	387
4	10 98	299 5	4	7 42	370
5	6 65	301	5	4 04	360
6	4 23	308	6	2 40	356
7	2 20	317	7	1 44	355
8	1 03	327	8	0 75	358
9	0 47	338	9	0 33	364
CR-II SO_4/U = 1 428			CR-V SO_4/U = 2 955		
1	27 85	355	1	22 60	
2	20 49	337	2	17 00	Above 530
3	14 35	326	3	9 98	Above 525
4	10 29	322	4	5 11	372
5	7 28	320	5	2 83	363
6	5 22	321	6	1 23	360
7	3 29	324	7	0 43	364
8	2 27	326	8	0 17	370
9	1 40				
10	0 84	340			
CR-III SO_4/U = 1 883			CR-VI SO_4/U = 1 000		
1	27 02	Above 525	1	30 11	287
2	18 15	379	2	20 07	285
3	12 06	353	3	13 75	286
4	7 70		4	7 89	288
5	4 50	339	5	3 60	298
6	2 61	339	6	1 87	308
7	1 51	342	7	0 99	320
8	0 54	351			

-1432
9/52

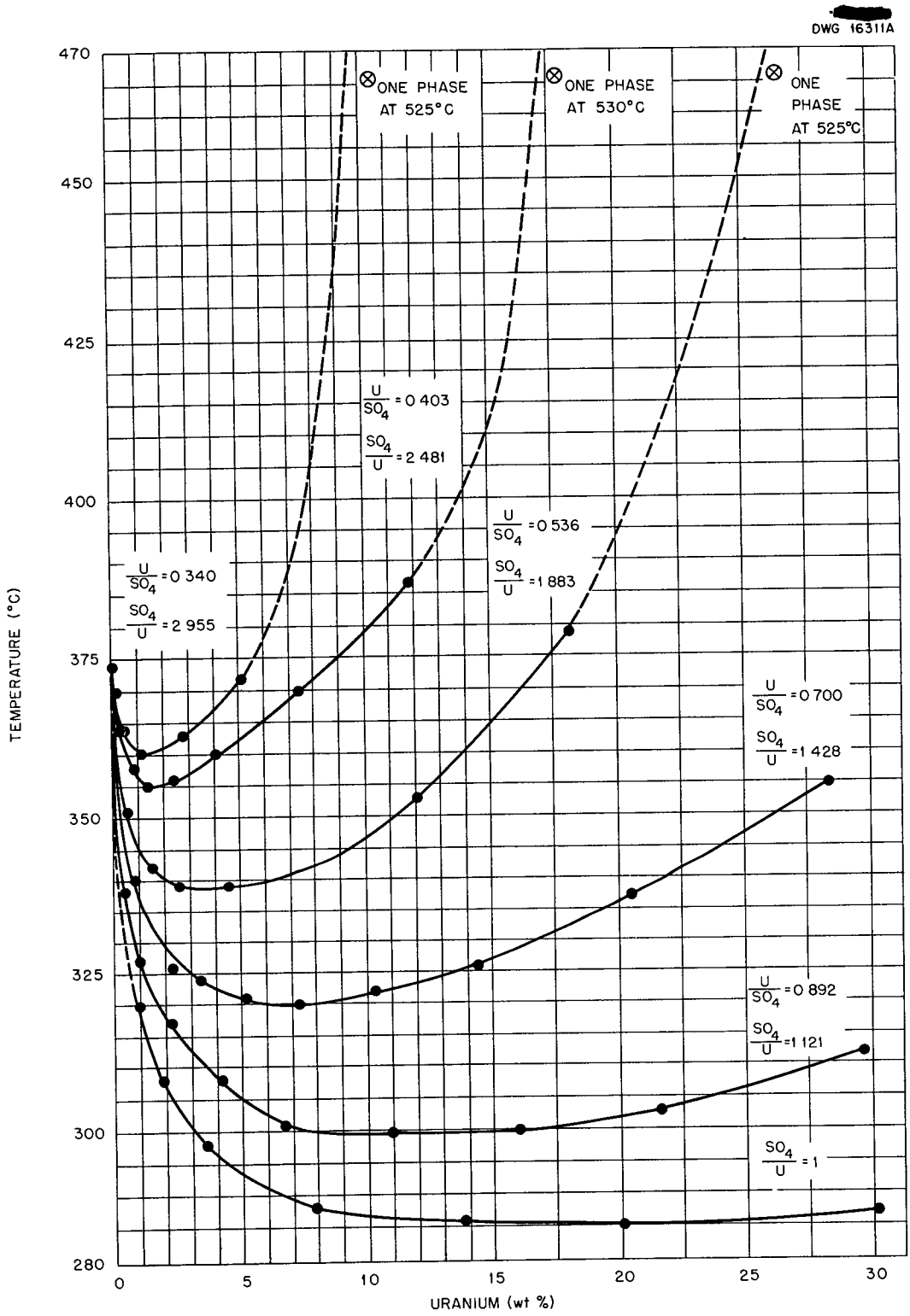

Fig. 29. Coexistence Curves for Two Liquid Phases in the System, UO_2SO_4-H_2SO_4-H_2O. Constant mole ratio of U to SO_4.

studied at 0, 25, 50, and 90°C over a similar concentration range. All the data and experimental details are given in previous quarterly reports of this series and will not be repeated.

Uranyl Sulfate-Water. The only previous work of this nature is that of Dittrich[9] and of Jones[10] on UO_2SO_4-H_2O at 25°C. There is a wide disagreement between the two sets of experimental data. The present results confirm the work of Dittrich.

A plot of equivalent conductance, Λ, vs. $\sqrt{c}$, where c is concentration in equivalents per liter, shows that UO_2SO_4 behaves as a weak electrolyte in aqueous solution. As usual with weak electrolytes, the resulting curves approach the conductance axis asymptotically, therefore it is not possible to obtain a satisfactory value of the equivalent conductance at infinite dilution. Accordingly, a more definitive treatment than the application of the Onsager equation was sought.

There are several methods by which the equivalent conductance of a weak electrolyte at infinite dilution and the dissociation constant, K, may be determined, if it is assumed that simple dissociation occurs. One such method is that of Kraus and Bray,[11] which is based on Ostwald's dilution law. This method, however, is incompatible with present-day theory of interionic attraction, although it will yield results in keeping with those obtained by more rigorous methods when applied to weak electrolytes.

The most promising methods are those of Davies,[12] of Kraus and Fuoss,[13] and of Shedlovsky.[14]

In all these methods it is recognized that the Ostwald dilution law is not exact, even in concentration ranges as low as 10^{-4} N because of the effect of long-range interionic attraction on activities and conductance. When the methods are applied to weak electrolytes, it must be taken into account that the electrolyte is not completely ionized. Thus, the Onsager equation,

$$\Lambda = \Lambda_0 - \mathcal{S}_{(\Lambda)} \sqrt{c} ,$$

where $\mathcal{S}_{(\Lambda)}$ is the limiting slope, is modified to consider α, the degree of dissociation, as follows[14]

$$\Lambda = \alpha(\Lambda_0 - \mathcal{S}\sqrt{\alpha c}) ,$$

where

$$\alpha = \frac{\Lambda}{\Lambda_0\left(1 - \frac{\mathcal{S}\sqrt{\alpha c}}{\Lambda_0}\right)},$$

which, in the limit, reduces to Λ/Λ_0.

Both Kraus and Fuoss[13] and Shedlovsky[14] have evaluated functions and tabulated data for the determination of α from Λ, Λ_0, and c. Use of the methods requires a previous knowledge of Λ_0 if an accurate analysis of conductance data is to be made. In this work, approximate values of Λ_0 were obtained from the method of Kraus and Bray[11] and were used to obtain an initial value of the degree of dissociation, α. The mean ionic activity coefficient, $f_{\pm}$, was evaluated at each concentration by means of the Debye-Huckel equation,

$$\log f_{\pm} = -A\sqrt{\tfrac{1}{2}c_i z_i^2} ,$$

The function of Fuoss, $F_{(z)}$, and the activity coefficient were introduced into the Ostwald equation to give

$$\frac{F_{(z)}}{\Lambda} = \frac{1}{\Lambda_0} + \frac{\Lambda c f_{\pm}^2}{F_{(z)} K (\Lambda_0)^2} .$$

A plot of $F_{(z)}/\Lambda$ vs. $\Lambda c f_{\pm}^2/F_{(z)}$ yields a final value of Λ_0. The dissociation constant, K, may be determined from the

(9) C Dittrich, *Z Physik Chem* **29**, 449 (1899)

(10) H C Jones, *Carnegie Institution of Washington*, Publication No 170 (1912)

(11) K. A Kraus and W C Bray, *J Am Chem Soc* **35**, 1315 (1913)

(12) C W Davies, *The Conductivity of Solutions*, 2nd ed , p 101, Wiley, New York, 1933

(13) R M Fuoss and K A Kraus, *J Am Chem Soc* **55**, 476 (1933)

(14) T Shedlovsky, *J Franklin Inst* **225**, 739 (1938)

-1432
9/52

slope of the resulting curve or calculated from the relation,

$$K = \frac{f_{\neq}^{2} \alpha^{2} c}{1 - \alpha}.$$

Results of the application of the foregoing method to these conductance data at 0, 25, 50, and 90°C, together with calculated values of $\Delta H°$, $\Delta F°$, and $\Delta S°$, are given in Table 26.

The treatment of conductance data for UO_2SO_4 in the manner described is obviously open to question. For one thing, in using this method, the dissociation of UO_2SO_4 into UO_2^{++} and SO_4^{--} ions is assumed in calculating both the degree of dissociation and $f_{\neq}$, the mean activity coefficient. It is also assumed that there is little, if any hydrolysis, whereas there is ample evidence to the contrary. Since the acidity was known and a hydrolysis pattern involving UO_2SO_4, UO_2^{++}, SO_4^{--}, $U_2O_5^{++}$, H^+, HSO_4^-, and H_2O was assumed, a hydrolysis correction (from the method of Owens and Gurry[15]) was applied to the conductance data. At 25°C, this method leads to a value of $\Lambda_0 \simeq 132\ 0$ for UO_2SO_4. This appears to be a more reasonable value than 210 ohms^{-1} cm^2 given in Table 26. The average K at 25°C, calculated from corrected conductances, was of the order 7.37×10^{-4}, as compared with the 2.94×10^{-4} determined from data not corrected for hydrolysis.

An interesting feature of the conductance data is the effect of temperature change. According to Walden's generalization, $\eta\Lambda$ = constant. In effect, for a completely dissociated electrolyte the conductance should be a function of the viscosity of a nonconducting solvent. For a UO_2SO_4 aqueous solution, however, a plot of $(\eta_0\Lambda)_t/(\eta_0\Lambda)_{0°C}$ (normalized) vs. t°C gives a curve (Fig 30) with a negative slope, indicating that fewer ions are present to carry the current at the more elevated temperatures than at lower temperatures. This indicates that there is an increase in association due, perhaps, to the decreased dielectric strength of the solvent at the higher temperatures

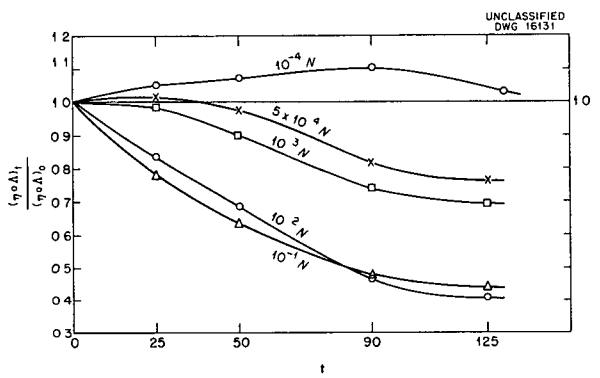

Fig. 30. Conductivity of UO_2SO_4 as a Function of t° and η

(15) B B Owen and R W Gurry, *J Am Chem Soc* **60**, 3074 (1938)

TABLE 26. THERMODYNAMIC DATA FOR UO_2SO_4 DISSOCIATION IN AQUEOUS SOLUTION

Equivalent Conductance at Infinite Dilution

TEMPERATURE (°C)	Λ_0 (ohms^{-1} cm^{-1})	$K \times 10^4$	$\Delta H°$ (cal/mole)	$\Delta F°$ (cal/mole)	$\Delta S°$ (e u)
0	96	4.20	-7000	+4220	-34.0
25	210	2.94	-7000	+4870	-40.0
50	360	1.64	-7000	+5580	-39.1
90	1000	0.356	-7000	+7570	-40.3

Uranyl Fluoride-Water. Dean[16] has measured the conductivity of UO_2F_2 in H_2O at 25°C in concentrations of 0.125 *N* and above. The present results in this temperature and concentration range are in excellent agreement with Dean.

It is evident from experimental data given previously that UO_2F_2 in aqueous solution is a very weak electrolyte. It is much less conductive than an equivalent solution of UO_2SO_4, in fact, a comparison shows that UO_2F_2 solution is approximately as conductive at 90°C as UO_2SO_4 is at 0°C. The per cent increase in conductance over the range 0 to 90°C is much greater for UO_2F_2 than for UO_2SO_4. This increase, however, is approximately what would be expected from the decrease in the viscosity of the solvent, Fig. 31 is a plot of

$$\frac{(\eta_0 \Lambda)_t}{(\eta_0 \Lambda)_{0°C}}$$

(normalized) vs. *t*. On this basis, it would appear that there has been little or no increase in ionization in going from 0 to 90°C, or if the UO_2F_2 exists as a dimer,[17] it may be concluded that there has been little change in its concentration.

(16) G R Dean, *Metallurgical Project Report*, CC-2092, Sept 11, 1944

(17) J S Johnson and K A Kraus, *J Am Chem Soc* **74**, 4436 (1952)

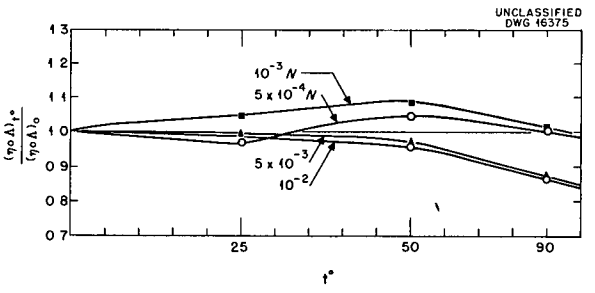

Fig. 31. Conductivity of UO_2F_2 as a Function of $t°$ and η.

The data for the conductance of UO_2F_2 have not given comprehensible results when the methods of Kraus and Bray[11] were used to derive a value for Λ_0 at the various temperatures. It is true that a plot of ΛC vs. $1/\Lambda$ yields certain values at 0, 25, and 50°C, but the method fails when applied at 90°C - the plot gives a meaningless intercept for $1/\Lambda$.

Fruitful results have not been obtained by the application of the method of Kraus and Fuoss[13] or by correction for hydrolysis.

VAPOR PRESSURES OF AQUEOUS URANYL SULFATE SOLUTIONS

H. O. Day, Jr. W. L. Marshall
C. H. Secoy

Vapor pressure data for some solutions of uranyl sulfate were reported in a previous HRP report.[18] The experimental values were obtained by using a differential manometer with dibutylphthalate as the manometer fluid. The experimental technique has remained the same, except for the use of *m*-diphenylbenzene as a manometer fluid. In the latest run, considerable difficulty was encountered in attaining equilibrium. The data are reported in Table 27.

Uncertainty in concentration units is ±0 0004_5 in molality and ±0.000008 in mole fraction. The values are reported to five and seven decimal places, respectively, to show concentration changes resulting from increased quantities of water in the vapor phase.

Examination of the data reported here and previously[18] reveals all too clearly the presence of experimental errors. Before activity coefficients can be calculated, not only must more data be obtained, but experimental errors must be further reduced.

(18) H O Day, Jr, *op cit*, ORNL-1318, p 138

-1432
9/52

TABLE 27. VAPOR PRESSURE OF AQUEOUS URANYL SULFATE SOLUTIONS

TEMPERATURE (°C)	MOLALITY OF UO_2SO_4	MOLE FRACTION OF UO_2SO_4	ΔP(mm Hg)
25	1.14482	0.0202083	0.464
30	1.14485	0.0202088	0.615
35	1.14488	0.0202093	0.804
40	1.14492	0.0202100	1.047
45	1.14496	0.0202107	1.342
50	1.14502	0.0202117	1.703
60	1.14516	0.0202142	2 659(?)
70	1.14536	0.0202176	3.844
80	1.14565	0.0202226	5.620
90	1.14607	0.0202299	7.859(?)

CONDUCTOMETRIC METHOD FOR STUDYING THE KINETICS OF PEROXIDE DECOMPOSITION IN URANYL SULFATE SOLUTIONS

M. D. Silverman H. F. McDuffie
G. M. Watson C. H. Secoy

A kinetic study of the decomposition of hydrogen peroxide in uranyl sulfate solution was undertaken because the peroxide concentration appears to be a limit to the power level of an aqueous homogeneous reactor.

When hydrogen peroxide is introduced into a uranyl sulfate solution, there is an immediate reaction according to

$$UO_2^{++} + H_2O_2 \rightleftharpoons UO_4 \text{ (aqueous)} + 2H^+ . \quad (1)$$

The hydrogen peroxide reacts quantitatively. This can be demonstrated by the change in hydrogen ion concentration being consistent with the amount of peroxide added, according to the stoichiometry, whether or not the solubility of uranyl peroxide is exceeded. If the solubility of uranyl peroxide is exceeded, another equilibrium,

$$UO_4 \text{ (aq.)} \rightleftharpoons UO_4 \text{ (s)} , \quad (2)$$

must be taken into account. The experiments were planned so that precipitation was avoided.

A chemical titration method was used for the earlier studies on the kinetics of peroxide decomposition as a function of temperature.[19] However, the precision of the method is limited at higher temperatures mainly by experimental difficulties. Because the chemical method of analysis is only precise at low temperatures and consumes part of the reaction mixture, it was thought advisable to develop a method for measuring *in situ* An instrumental method is obviously indicated for this purpose.

A conductometric method was developed to measure the rate of peroxide decomposition in the system. For the purpose of discussion, an oversimplified mechanism can be presented

[19] *Chem Quar Prog Rep June 30, 1952*, ORNL-1344 (in press)

whereby peroxide is decomposed by either

$$UO_4\ (aq.) + 2H^+ \longrightarrow UO_2^{++} + H_2O + \tfrac{1}{2}O_2\ , \qquad (3)$$

or

$$H_2O_2 \longrightarrow H_2O + \tfrac{1}{2}O_2\ , \qquad (4)$$

or by both. If reactions 3 and 4 are the rate-determining steps of the processes and if reaction 1 proceeds far to the right, then a conductance method for peroxide decomposition should approximate the chemical or titration method, provided a linear relationship exists between conductance and hydrogen-ion concentration. Chemical titration does not distinguish between H_2O_2 and UO_4 but determines both additively. On the other hand, conductance changes depend only on the disappearance of UO_4. Dilute solutions (~8 g of uranium per liter) were used in order to avoid buffering and non-linear effects.

Only the major points are covered here, since a more complete and detailed treatment of the conductometric method will be given in a forthcoming report.[20]

The data were obtained at 100°C in approximately 0.034 *M* uranyl sulfate solutions. For each experiment, hydrogen peroxide was added to provide an initial concentration of approximately 0.004 to 0.008 *M* peroxide.

The conductometric data, along with those obtained by the chemical method, are given in Table 28. The conductometric data have usually been analyzed by Guggenheim plots,[19] which offer the advantage of avoiding end-effects. It should be noted that tenfold variations in the rates of decomposition were reproduced conductometrically with an average variation of 6% from the corresponding results obtained by chemical titration. The conductance results uniformly gave the faster rates, no doubt because of the cooling of the chemical samples before the reaction could be quenched.

The conductometric method satisfies several requirements. First, it is reproducible and consistent with chemical titration. Second, it is adaptable to remote control and automatic recording and thus appears capable of following fast reactions. It has been tried on a semimicro basis, and microscale runs appear feasible. Finally, since the method is instrumental and can be carried out *in situ*, it does not consume or contaminate solutions.

It is apparent from the data presented that a high-frequency method

[20] M D Silverman, *Peroxide Decomposition in Aqueous Reactor Solutions*, ORNL-1400 (to be published)

TABLE 28. CORRELATION OF RATES OF PEROXIDE DECOMPOSITION IN URANYL SULFATE SOLUTIONS AS DETERMINED BY TITRATION AND BY CONDUCTANCE AT 100°C

DETERMINATION NO	PERIODS OF HALF LIFE (sec)		
	Titration	Conductance	Difference (%)
I	345	315	8.7
II	173	164	5.2
III	98	95	3.1
IV	95	92	3.3
V	33	30	9.1
			Avg 6

-1432 9/52

that is sensitive to changes in hydrogen-ion concentration would be even more desirable, since it would eliminate the use of electrodes. Progress along this line is now being pursued.

The conductometric method has been used for catalytic studies of various ionic species, both corrosion and fission products, that are expected to be present in the HRE. The results of these studies and their effect on the power level are summarized elsewhere.[20,21]

ALTERNATE FUEL MEDIA AND POSSIBLE CORROSION INHIBITORS

H. O. Day
J. S. Gill
E. V. Jones
W. L. Marshall
C. H. Secoy
H. W. Wright

It is well known that uranyl fluoride forms double salts easily because uranyl fluoride is, coordinately, unsaturated. J. S. Johnson and K. A. Kraus have also shown that pure UO_2F_2 in aqueous solutions at ordinary temperatures forms a dimer $(UO_2F_2)_2$. These facts lead to the supposition that by addition of other compounds to uranyl fluoride solutions the uranyl ion might become so strongly complexed that a very definite inhibition of the corrosion of type 347 stainless steel might be obtained when the steel is exposed to the solution. The work performed so far on this investigation is of an exploratory nature.

Possible additives that might cause complexing, and at least cause an increase in pH, are metallic hydroxides of strongly basic nature and the fluoride salts of such bases. For these additions of $M(OH)_x$ and MF_x to be of value, the following criteria must be met

1. Significant quantities of the additives must go into solution with the uranyl fluoride and remain in solution at elevated temperatures (at least 250°C). Although it would not be necessary that the additives completely dissolve at room temperature, since they are completely soluble at 250°C, it would be advantageous if they were soluble over the entire temperature range. A corollary to the quantity of additive that dissolves is the resulting increase of pH. Assuming that corrosion inhibition is aided by an increase in pH, then the higher the pH the better, if phase instability does not occur.

2. The cross section (neutron capture) of the metal hydroxide or fluoride should be small, and the smaller the better.

3. The added compound must materially inhibit the corrosion of type 347 stainless steel by the solution.

The last criterion is obviously the most important one, for even if the first two are completely satisfied, the whole object of the addition of the extra compounds is lost if the third criterion is not fulfilled.

The systems being studied experimentally and those for which studies are contemplated can be written in the general form M_xO-UO_3-HF-H_2O, insofar as the original components are concerned. These systems are tabulated in the following, together with the cross section of the element M as taken from a 1949 General Electric Chart of the Nuclides. Lithium has been included because Li^7 might become available if Li additives are successful as corrosion inhibitors.

SYSTEM	CROSS SECTION OF M
Li_2O-UO_3-HF-H_2O	67
Na_2O-UO_3-HF-H_2O	0.48
K_2O-UO_3-HF-H_2O	2.0
Rb_2O-UO_3-HF-H_2O	0.7
MgO-UO_3-HF-H_2O	0.07
CaO-UO_3-HF-H_2O	0.42

(21) *HRP Quar Prog Rep Oct 1, 1952*, ORNL-1424 (in press)

ZrO_2-UO_3-HF-H_2O	0.40
Bi_2O_3-UO_3-HF-H_2O	0.015
SnO_2-UO_3-HF-H_2O	0.6
ZnO-UO_3-HF-H_2O	1.0

Static Corrosion Tests. It can be readily seen that the investigation from the viewpoint of phase relationships of so many four-component systems over a large temperature range would be a very formidable undertaking. Since the main consideration is the behavior of these solutions toward type 347 stainless steel, some static corrosion tests have been made to serve as a guide. These tests were made in an attempt to decide which of the systems of additives looked promising and thereby warranted more complete investigation of phase behavior. It is realized that if a static corrosion test looked promising, this behavior cannot be extrapolated to dynamic systems. However, if the static test result is poor, then the dynamic test would surely be poor also, and thus some M_xO-UO_3-HF-H_2O systems could be eliminated from further consideration.

The experimental technique and detailed results obtained may be found in the HRP report.[22] The results may be summarized as follows

1. Pure aqueous UO_2F_2 solutions with a small amount of oxygen attack type 347 stainless steel. This fact has long been known.

2. UO_2F_2 solutions with LiOH and practically no oxygen attack type 347 stainless steel but not so violently or so rapidly as UO_2F_2 and a small amount of oxygen. UO_2F_2 with other additives would probably behave similarly.

3. With small amounts of oxygen and additives such as LiOH, NaOH, NaF, etc., corrosion under static conditions is definitely inhibited. It is not known whether this inhibition is of sufficient strength to be of value for the HRP as far as dynamic behavior is concerned.

4. The optimum system or optimum concentration of any particular system for inhibiting corrosion is not known. Also, the optimum oxygen concentration for the particular system and concentration is not known.

Dynamic Corrosion Tests Solutions of additives have been tested and are under further tests in the dynamic test loops in operation at the Y-12 site. The results are, as yet, fragmentary and will be reported by the Corrosion Study groups under the direction of E. G. Bohlmann.

Conductometric and Acidimetric Titrations In an attempt to determine possible molecular species existing in the solutions, conductometric titrations were run. The theory would be that if a strongly stable species existed and such species showed a composition attainable by titration, a significant break should occur in the titration curve at that particular composition. Sodium fluoride, KF, and LiOH were used to titrate UO_2F_2 solutions of varying concentration. The results are given in the current HRP quarterly report.[22]

In all conductometric titration curves there were some questionable breaks in the continuity. The only sharp break was one shown by two conductometric titrations of the UO_2F_2-NaF-H_2O system and occurred at NaF-to-UO_2F_2 ratio of 1 to 3 in both a 0.61 and 0.83 *M* uranium solution.

Solubility and Phase Behavior in the M_xO-UO_3-HF-H_2O System The data obtained thus far are given in detail in the current HRP quarterly report.[22]

As a general statement, it should be pointed out that if corrosion inhibition proves to be of practical significance, not only should the complete phase behavior data of the best system be obtained, but other phase data as well. These data would

(22) H O Day, *et al*, *op cit*, ORNL-1424, (in press)

-1432 9/52

be the behavior of the fission products and plutonium produced in the UO_2F_2 solution containing additives. If Cu^{++} is used as a homogeneous gas-recombination catalyst, the behavior of Cu^{++} in the M_xO-UO_3-HF-H_2O system should be investigated to be sure that Cu^{++} is not precipitated from the solution under operating conditions.

Kinetics of the Formation of UO_4 Caused by the Addition of H_2O_2 The information concerning the kinetics of UO_4 precipitation from UO_2F_2 solutions containing various additives is only of a qualitative nature. However, a mention appears to be worthwhile, since the behavior is somewhat unusual as compared with UO_4 formation in pure UO_2F_2 solution. When H_2O_2 (3%) is added to solutions of pure UO_2F_2 varying from 0.168 to 1.26 *M*, an immediate precipitation of UO_4 occurs. Since the reaction is

$$UO_2^{++} + H_2O_2 \rightleftharpoons UO_4 + 2H^+ ,$$

a higher pH would tend to aid the formation of UO_4. However, upon adding H_2O_2 to UO_2F_2 solutions containing additives in various concentrations, a considerable period of time elapses before precipitation occurs. This induction period varies but is usually about 15 seconds. For NaF solutions of a high Na-to-U ratio, the period is much greater. This behavior could possibly be cited as some evidence that the UO_2^{++} ion is complexed by the various additives. In the case of the NaF solution, the precipitate may not be UO_4 but substances such as $NaUO_4F \cdot 5H_2O$.[23]

HRP RADIATION CHEMISTRY

C. H. Secoy

J. W. Boyle	A. W. Smith
E. L. Compere	H. H. Stone
W. E. Hill	F. H. Sweeton
H. F. McDuffie	L. F. Woo
D. M. Richardson	W. C. Yee

The work of the HRP Radiation Chemistry group has been reported in detail,[24] therefore only a summary will be presented here.

A 14-week irradiation of a uranyl sulfate solution in a type 347 stainless steel bomb has been completed and has yielded data concerning the corrosion of the container and the stability of the solution. The average corrosion rate, as measured by either the consumption of oxygen or by solution analysis for nickel ion, is approximately 1.4 mpy in contrast to a rate of less than 0.03 mpy found in similar unirradiated tests. It therefore appears that reactor radiation increases the static corrosion rate of uranyl sulfate solution containing 40 g of uranium per liter on type 347 stainless steel at 250°C by a significant amount.

During the course of the experiment, the rate of gas production decreased uniformly. Evidence indicates that this was caused by precipitation of uranium by interaction of the solution with corrosion products and not by reduction of the uranium.

One experiment with a uranyl sulfate solution in a titanium bomb has been completed, two others are yet in progress, and a fourth was terminated after only two days of irradiation because of instrument failure. On the evidence presented by the one complete experiment, titanium appears far superior to type 347 stainless steel as a corrosion-resistant container for uranyl sulfate solution.

Work on the kinetics of catalytic recombinations of hydrogen and oxygen has continued. Experiments with copper sulfate in distilled water show that the reaction rate, although first order in copper concentration at low concentrations, is not first order in copper concentration at high concentrations. It is believed that the first-order

(23) J J Katz and E Rabinovich, *The Chemistry of Uranium*, p 573, National Nuclear Energy Series VIII-5, McGraw-Hill, New York, 1951

(24) *Op cit*, ORNL-1424 (in press)

-1432
9/52

law would hold if activity were used instead of concentration.

The specific rate constant for copper as a 0.01 *M* cupric fluoride solution in 0.17 *M* uranyl fluoride has been found to be about one-half that of copper in a similar copper sulfate-uranyl sulfate solution. The difference is believed to be due to the difference in complexing power between the sulfate and fluoride.

Studies of suspended heterogeneous catalysts of the platinum family have continued. Improved methods for preparing catalysts have been developed, deposition of catalyst on the walls of the containers has been eliminated, improved techniques for obtaining adequate shaking have been devised, and, as a result, more reproducible data have been obtained. Of the single catalysts tested, palladium appears to be the most interesting from the point of high activity combined with resistance to poisoning. Apparatus for in-reactor studies of recombination is being prepared for use in hole 60 of the ORNL graphite reactor.